Symmetries investigation through PEP high sensitivity tests

K. Piscicchia
LNF (INFN), Centro Ricerche Enrico Fermi

on behalf of the VIP-2 collaboration

Nuclear Physics Mid Term Plan in Italy - LNGS session, 11/10/2022, LNGS (L'Aquila)

Two classes of PEP violation models -> two classes of experiments

Local QFT - Greenberg & Mohapatra (Quon Model), Ignatiev, Kuzmin, Rahal, Campa … <u>are subjected to</u> Messiah-Greenberg superselection rule: transition probability between two symmetry states is zero

introduce new fermions (current) in a pre-existing identical fermion system and check for PEP-violating atomic transitions **VIP-2 Open Systems**
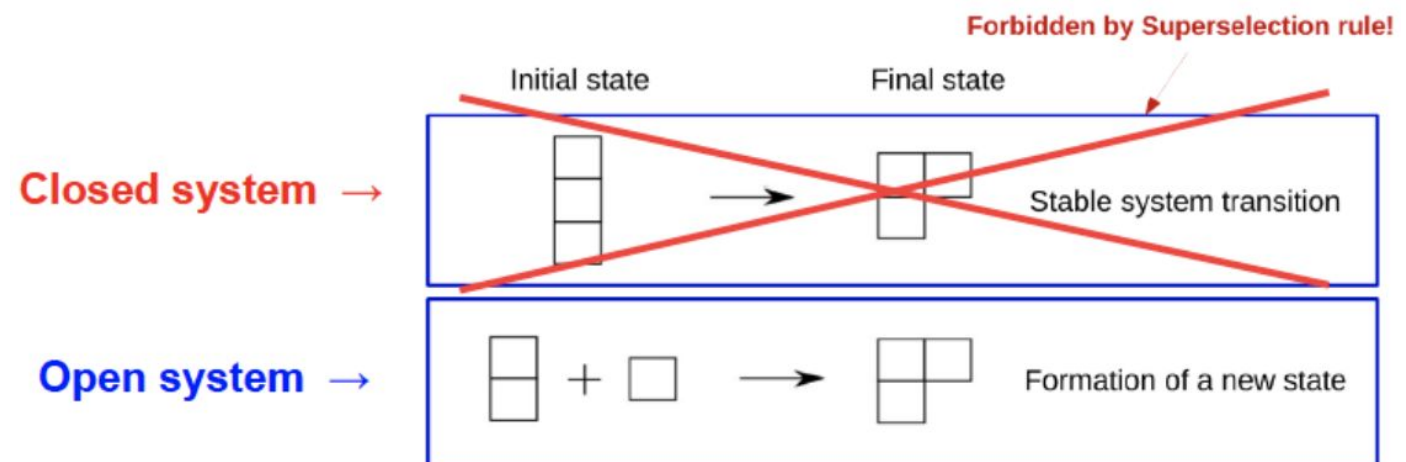
Non-commutative Quantum Gravity, CPT deformation … - Marcianò, Addazzi, Balachandran, Mavromatos …

- <u>are not subjected to Messiah-Greenberg</u> superselection rule
- PEP violation probability: *a)* depends on the transition energy *b)* depends on the energy scale of new-physics emergence *c)* is subject to not isotropic corrections
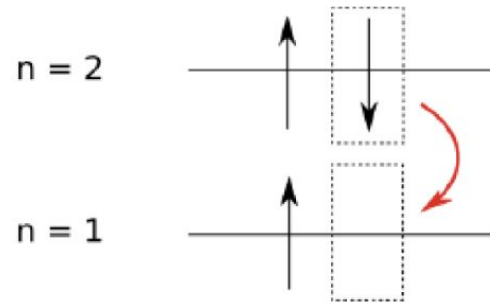
VIP-2 Closed Systems - High Purity Ge detectors, set of ultra-radiopure targets to check $\delta^2(E)$ with a systematic scan over Z, tests of directionality.

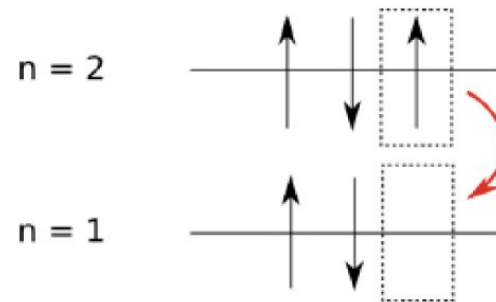# *Experimental signature of a PEPV transition*

In both **VIP-2 Open & Closed Systems** we search for electrons transitions to the fundamental level, already filled by 2 electrons, **e.g. in Cu target:**
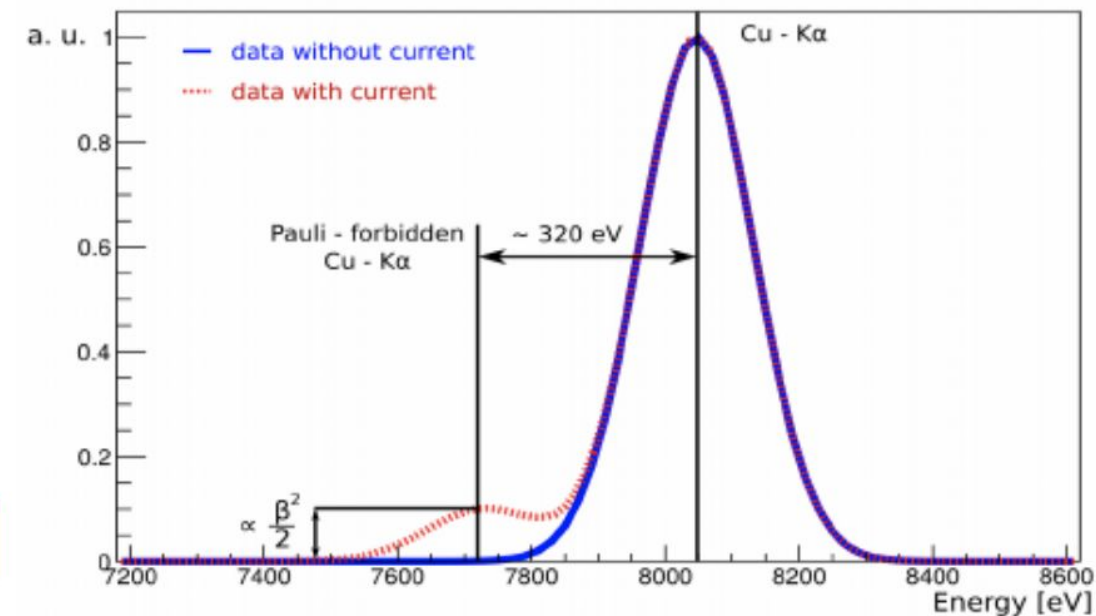
Allowed transition
$2p \rightarrow 1s$ (Kα)

$n = 2$

$n = 1$

~ 8.05 keV in Cu

Pauli-forbidden transition
$2p \rightarrow 1s$ (Kα)

$n = 2$

$n = 1$

~ 7.7 keV in Cu

— data without current
····· data with current

Cu - Kα

Pauli - forbidden
Cu - Kα ~ 320 eV
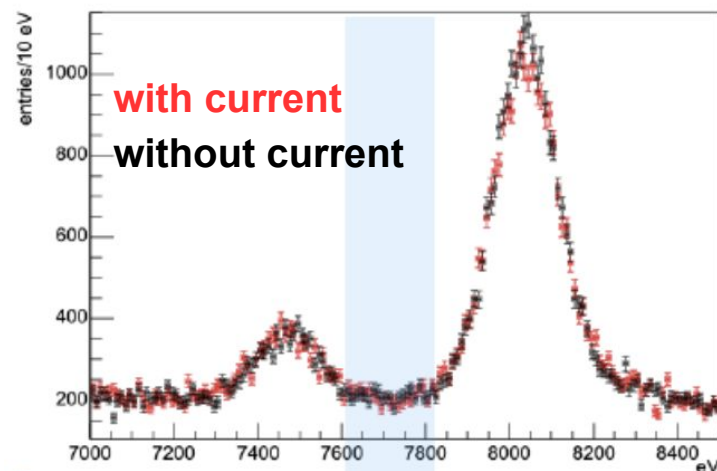
$\propto \dfrac{\beta^2}{2}$

Paul Indelicato (Ecole Normale Supérieure et Université Pierre et Marie Curie)
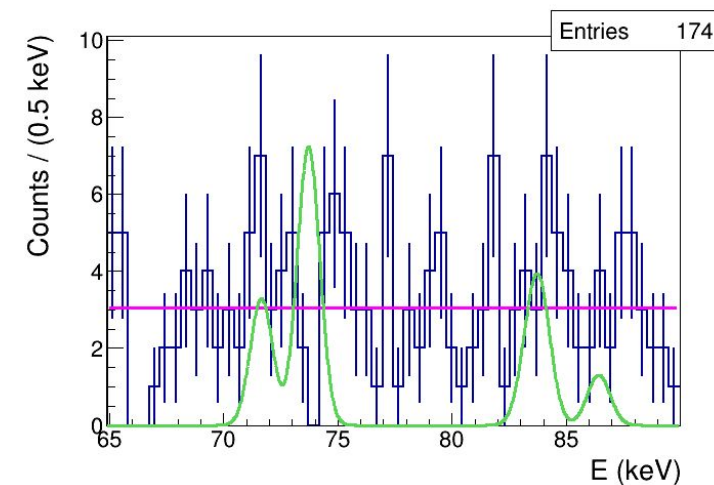**Multiconfiguration Dirac-Fock approach**
Accounts for the shielding of the two inner electrons

Background in VIP-2 Open Systems :
provided by data acquisition without current

with current
without current

$t^{wc} = 27110263$ s $= 314$ days
$t^{woc} = 26916404$ s $= 311$ days

Background in VIP-2 Closed Systems :
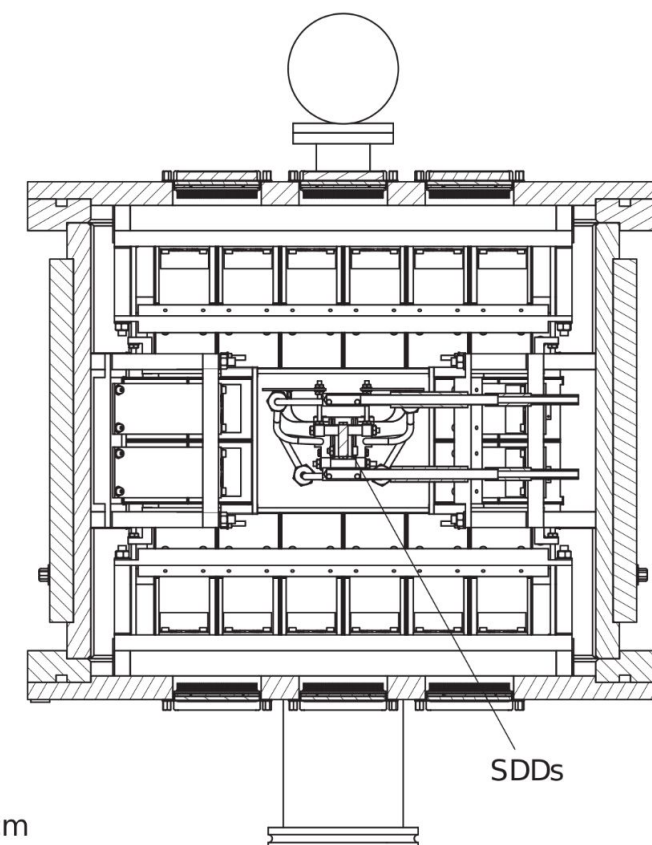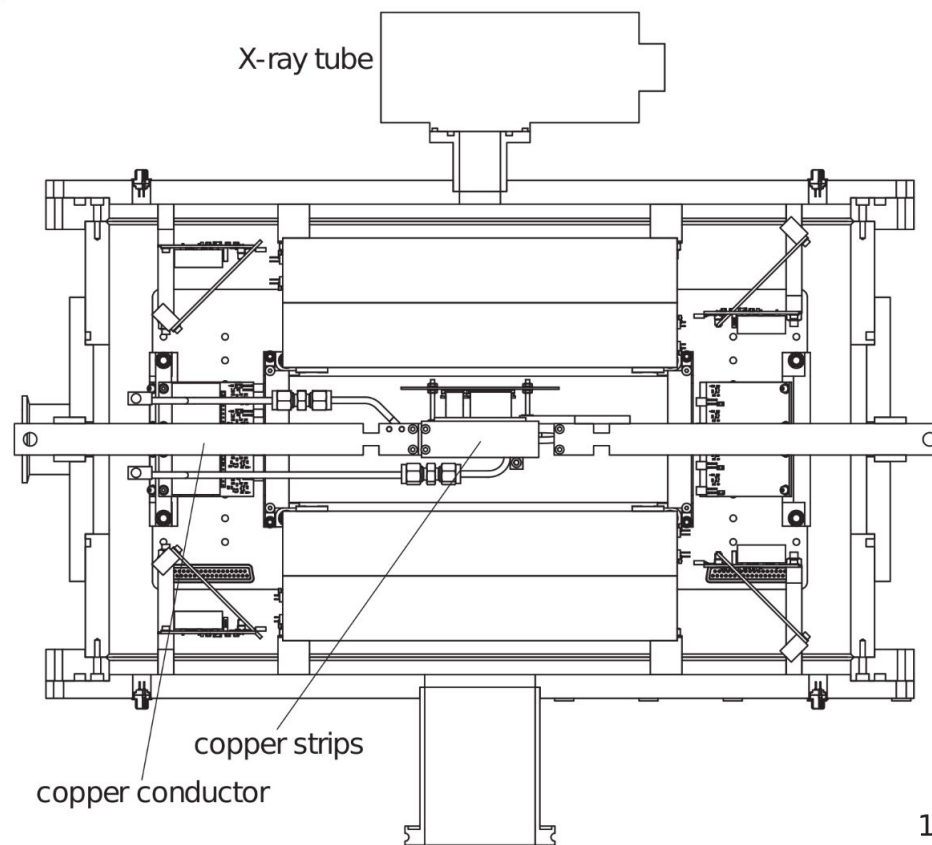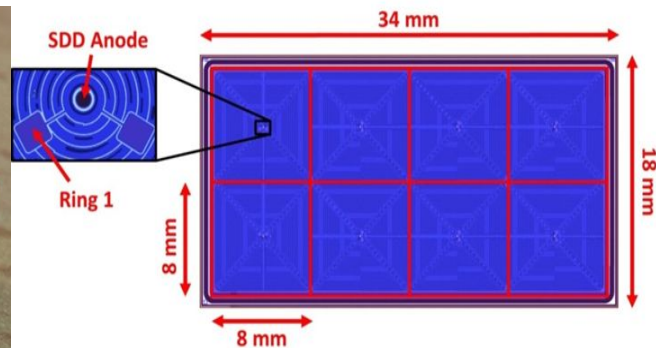**accurate characterization of the detector**

Entries   174

acquisition time
6.1×10^6 s $70 \sim$ d

VIP-2 Open Systems -

- **SDD detectors (high resolution 190 eV FWHM at 8 keV)**
- **4 arrays of 2x4 SDDs, liquid Argon closed circuit cooling**
- **2 strip shaped Cu targets (cooled by closed chiller circuit -> with 100A circulating current 1 $^{\circ}$K heating in the SDDs)**

The statistical model accounts for uncertainties on the parameters of the signal and background shapes, and scale factor of the current on/off spectra:
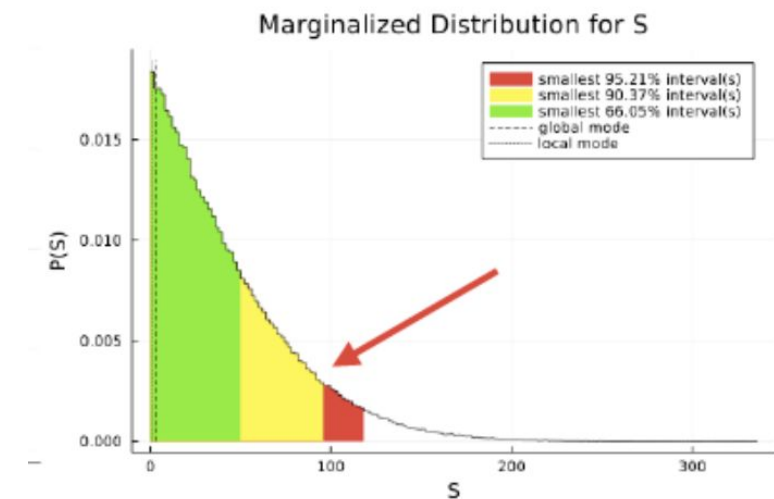
the two spectra are simultaneously analysed by constructing the joint likelihood:

$$\mathcal{L}\left(\mathscr{D}^{wc}, \mathscr{D}^{woc} | \boldsymbol{\theta}, \boldsymbol{y}, \mathscr{S}\right) = \text{Poiss}\left(\mathscr{D}^{wc} | \mathscr{F}^{wc}\left(\boldsymbol{\theta}, \boldsymbol{y}, \mathscr{S}\right)\right) \times \text{Poiss}\left(\mathscr{D}^{woc} | \mathscr{F}^{woc}\left(\boldsymbol{\theta}, \boldsymbol{y} \times \mathscr{R}\right)\right)$$

θ is the vector of spectral shape parameters, y of yields, $\mathscr{R}$ is the ratio of the acquisition times and $\mathscr{L}$ is the signal yield. Spectra are described by the functions $\mathscr{F}$.

the posterior p.d.f. of the signal yield provides an upper limit on $\beta^2/2$

$$p\left(\mathscr{S} | \mathscr{D}^{wc}, \mathscr{D}^{woc}\right) = \int p\left(\boldsymbol{\theta}, \boldsymbol{y}, \mathscr{S} | \mathscr{D}^{wc}, \mathscr{D}^{woc}\right) d\boldsymbol{\theta} d\boldsymbol{y}$$

Upper limit β^2/2 vs time

VIP-2 Internal
All available data
625 days of data taking

CLs: 4.32 10^-31
Target: 4.7 10^-31
Bayes: 4.14 10^-31

BEST CONSTRAINT EVER RESPECTING MG

Analysis validated by means of frequentist CLs exclusion method, exploiting Neyman construction for a robust evaluation of the CLs.
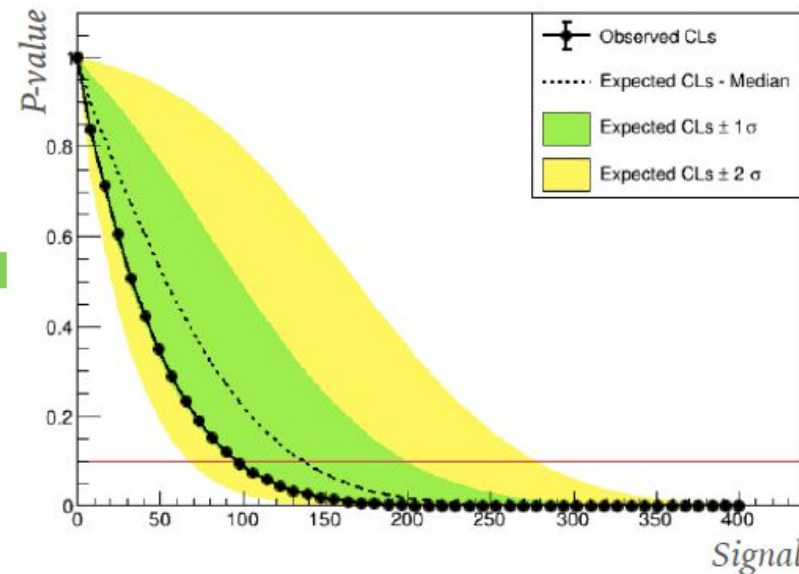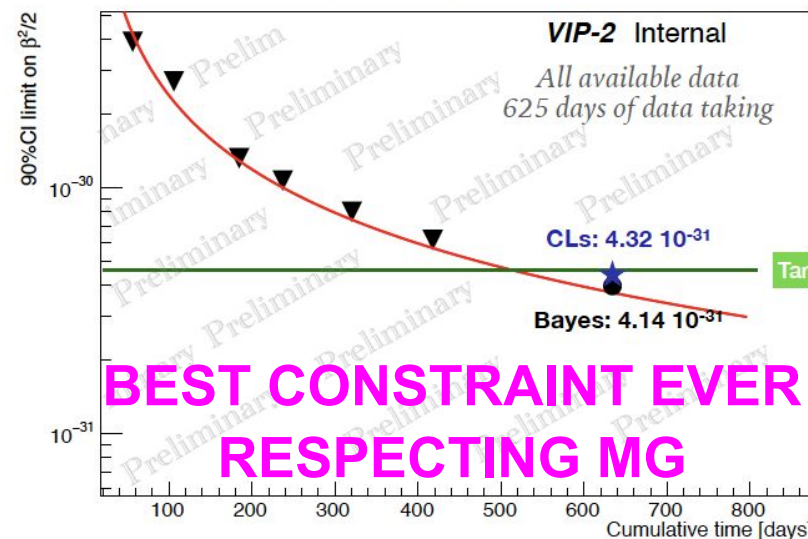
PUBLICATIONS this year:

- **Symmetry 2022, 14(5), 893**
- **Phys.Scripta 97 (2022) 8, 084001**
- **Il NUOVO CIMENTO 45 C (2022) 103**

total statistics paper
under finalization

VIP-2 Closed Systems - present status and results

High Purity Ge detector based setup:

- high purity co-axial p-type germanium detector (HPGe), diameter of 8.0 cm, length of 8.0 cm, surrounded by an inactive layer of lithium-doped germanium of 0.075 mm.
- The target material is composed of three cylindrical sections of radio-pure Roman lead, completely surrounding the detector.
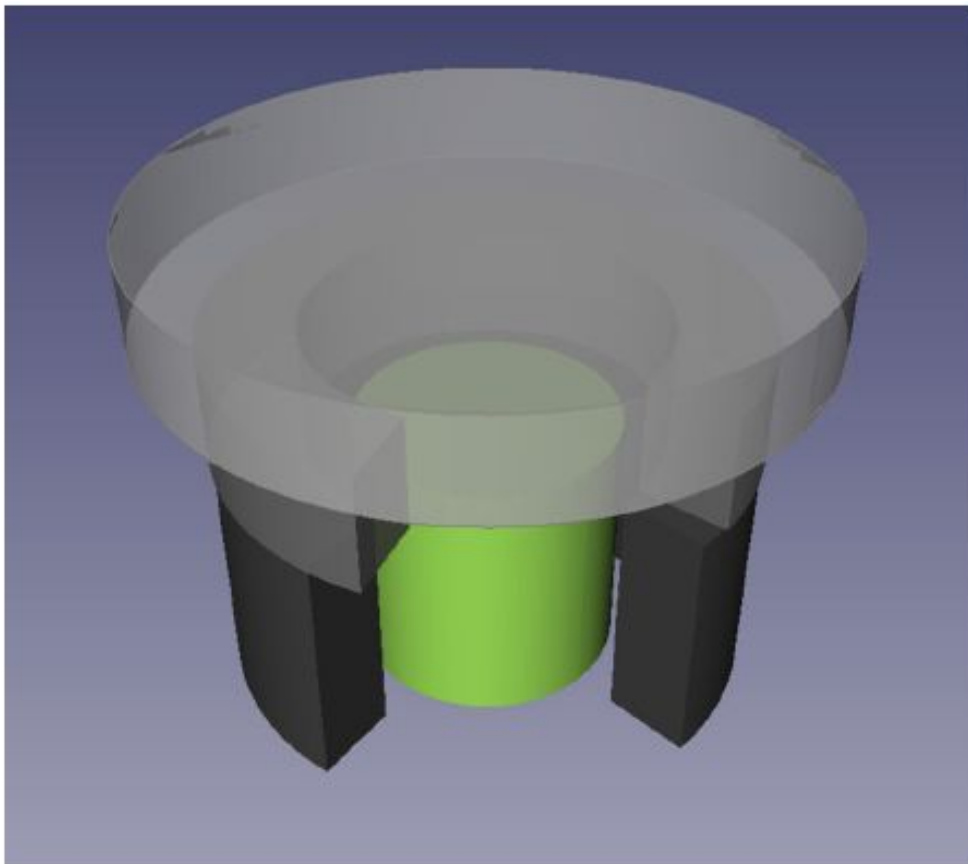
- Passive shielding: inner - electrolytic copper, outer - lead

- 10B-polyethylene plates reduce the neutron flux towards the detector

- shield + cryostat enclosed in air tight steel housing flushed with nitrogen to avoid contact with external air (and thus radon).

K. P. et al., Eur. Phys. J. C (2020) 80: 508
https://doi.org/10.1140/epjc/s10052-020-8040-5

Fig. 1 Schematic representation of the Ge crystal (in green) and the surrounding lead target cylindrical sections (in grey)

- **First analysis which accounts for the predicted energy dependence** of the PEP violation probability. Expected rate of Kalpha1 transitions:

$$\Gamma_{K_{\alpha1}} = \frac{\delta^2(E_{K_{\alpha1}})}{\tau_{K_{\alpha1}}} \cdot \frac{BR_{K_{\alpha1}}}{BR_{K_{\alpha1}} + BR_{K_{\alpha2}}} \cdot 6 \cdot N_{atom} \cdot \epsilon(E_{K_{\alpha1}}).$$

$$f_S(E,k) = \frac{1}{N} \cdot \sum_{K=1}^{N_K} \Gamma_K \frac{1}{\sqrt{2\pi\sigma_K^2}} \cdot e^{-\frac{(E-E_K)^2}{2\sigma_K^2}}$$
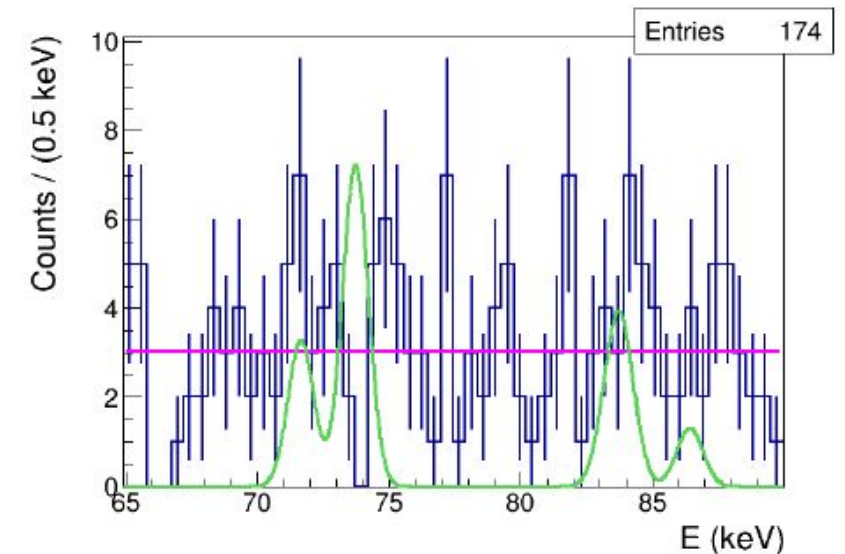

FIG. 1. The measured X-ray spectrum, in the region of the K_α and K_β standard and violating transitions in Pb, is shown in blue; the magenta line represents the fit of the background distribution. The green line corresponds to the shape of the expected signal distribution (with arbitrary normalization) for the A_3 analysis and the M_3 parametrization.
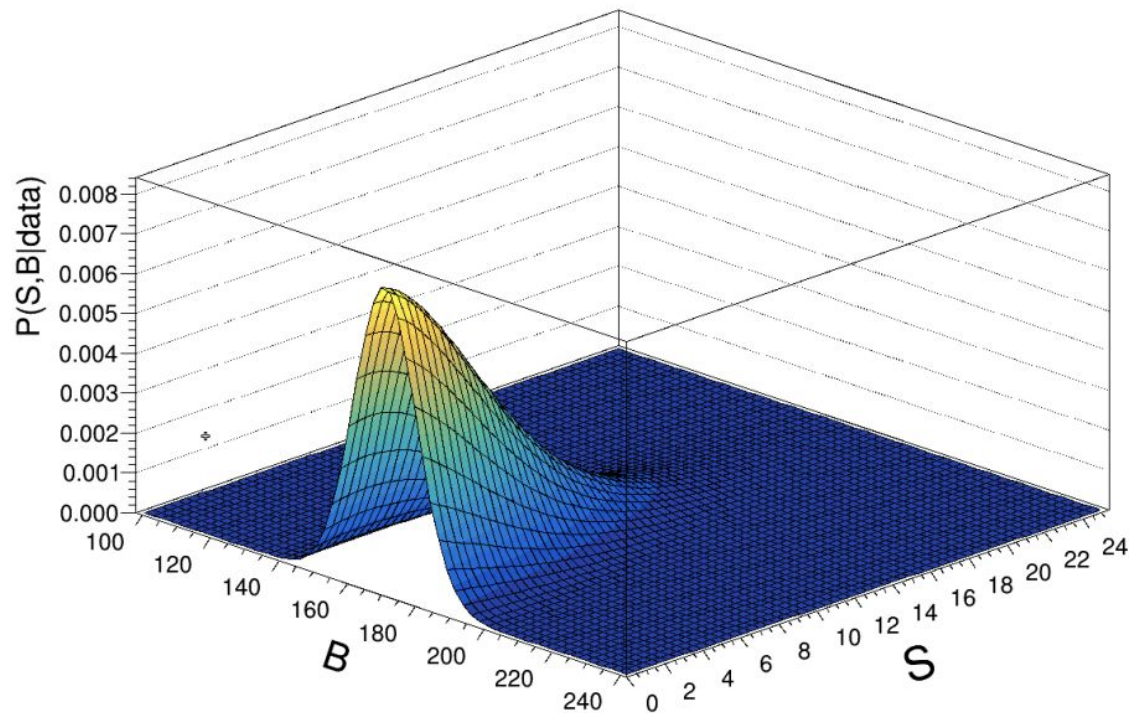

FIG. 2. Joint *pdf* $P(S, B|data)$ of the expected number of total signal and background counts corresponding to $\theta_{0i} \neq 0$.

90% Probability limits on the NC scale
BEST CONSTRAINT EVER

θ_{0i}	$\bar{S}$	lower limit on Λ (Planck scales)
$\theta_{0i} = 0$	13.2990	$6.9 \cdot 10^{-2}$
$\theta_{0i} \neq 0$	18.1515	$2.6 \cdot 10^2$

K. P., Addazi, Marcianò, Curceanu, Napolitano et al.,
Phys. Rev. Lett. 129, 131301 (2022)

Gantt chart

class of experimental test	experimental setup	2022	2023	2024	2025	2026	2027	2028	2029	2030	2031
Open Systems	VIP-2 Open Systems	DT	DT								
	VIP-3 Open Systems	SR	SR	DT	DT	DT					
	layered 1mm thick SDDs					SDDs R	SDDs D + SD	SR	DT	DT	DT
	VIP-GATOR	TM	SR + DT	SU + DT	SU + DT						
Closed Systems	BEGe setup	SR	DT	DT	SU + DT	SU + DT					
	New setup anysotropy				R&D	R&D	SR	DT	DT	DT	

Legend	
DT	data taking
SR	setup realization
TM	test measurement
SU	setup upgrade
R&D	research & development
R	research
SD	setup design
D	development

VIP Open Systems
future plans

Future directions

Theory side

T1 Explore symmetries for PEP-violations on Open Systems

Loop Quantum Gravity, Non-local Completion of Gravity Theories, Gauge Formulations of Gravity Theories etc…

T2 Extend falsification of quantum gravity models

Loop Quantum Gravity, Non-local Completion of Gravity Theories, Gauge Formulations of Gravity Theories etc…

T3 Generalized Uncertainty Principle as a class of universality

M-Theory, String Theory, Non-local Completion of Gravity Theories, Gauge Formulations of Gravity Theories etc…

T4 CPT violation and quantum decoherence, and the role of gravity

M-Theory, String Theory, Stochastic Quantization of Gravity, Dynamical Triangulation etc…

T5 Inhomogeneity and anisotropy of the geometry ground state

M-Theory, String Theory, Loop Quantum Gravity, Non-local Completion of Gravity Theories, etc…

VIP Open Systems future plans - VIP-3

L. Okun, Possible violation of the Pauli principle in atoms. JETP Lett. 1987, 46, 529532: **"it is specifically the fundamental nature of the Pauli principle which would make such tests, over the entire periodic table, of special interest"**

↓

VIP-3 Open systems: **Scan the PEP violation probability as a function of Z**

paper IN PRINT on APPA

New avantgarde 1mm thick SDD detectors **in production in collaboration with FBK & Politecnico di Milano**
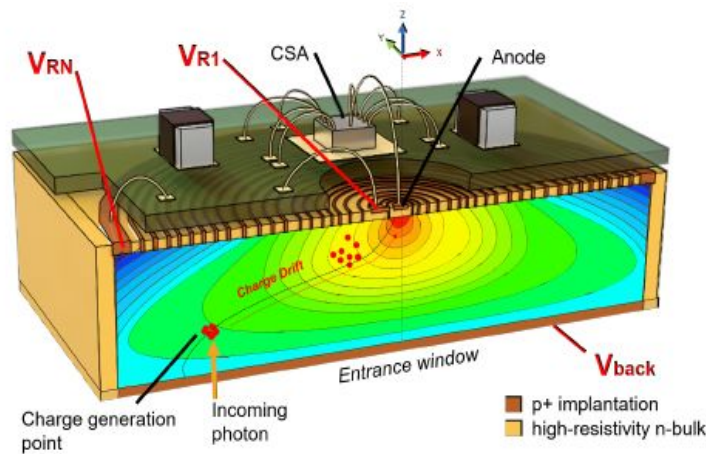
- Pixel dimensions: 7.9 mm × 7.9 mm
- Extended width of last drift ring (improve collection at the border of the active area)
- Increased number of GRs (control lateral depletion in thick sensors)
- Total chip dimensions: 35.6 mm × 19.8 mm -> ~ 2 mm wider than previous chip
- Introduced focusing electrode on the window (reduce charge sharing)
- Single connection to polarize all the pixel windows
- Single connection to polarize focusing electrode
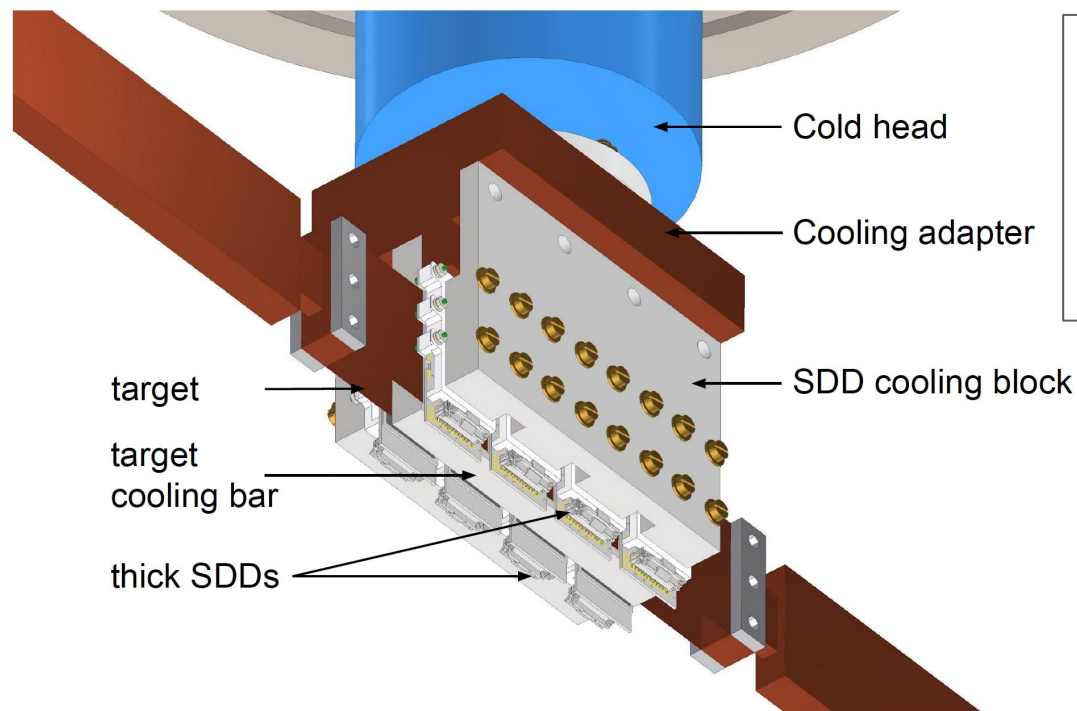- Improved robustness of bonding pads
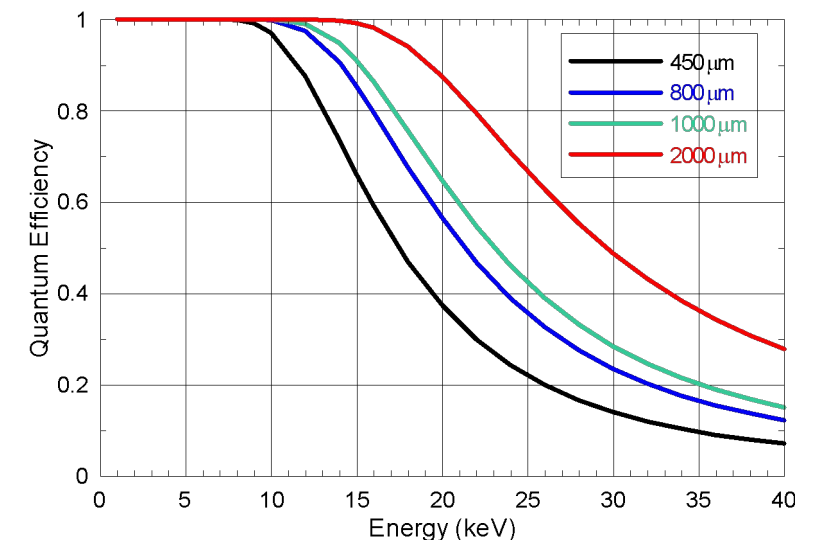
Proved increment of a factor 2 in efficiency at 20 keV keeping fixed E resolution (with respect present technological limits for 450µm)

↓

scan of $\beta^2/2$ for electrons in higher Z materials (Ag, Sn and Pd) with sensitivity comparable with VIP-2.

VIP-3 Open Systems - plan of activity

- **Completion 1mm SDD production, finalization of the new readout electronics & testing - within summer 2023.**
- **New calibration system, SDDs characterization (resolution, linear response and stability) - within autumn 2023.**
- **Thermal contact (cold-finger and SDDs detectors), new target cooling system, new vacuum chamber - within autumn 2023.**

VIP SETUP WITH "CROSS VACUUM CHAMBER"

Cold head

Cooling adapter

SDD cooling block

target

target cooling bar

thick SDDs

Total 8 thick SDD units
- 64 SDD cells
- each cell 64 mm^2
- active area 41 cm^2
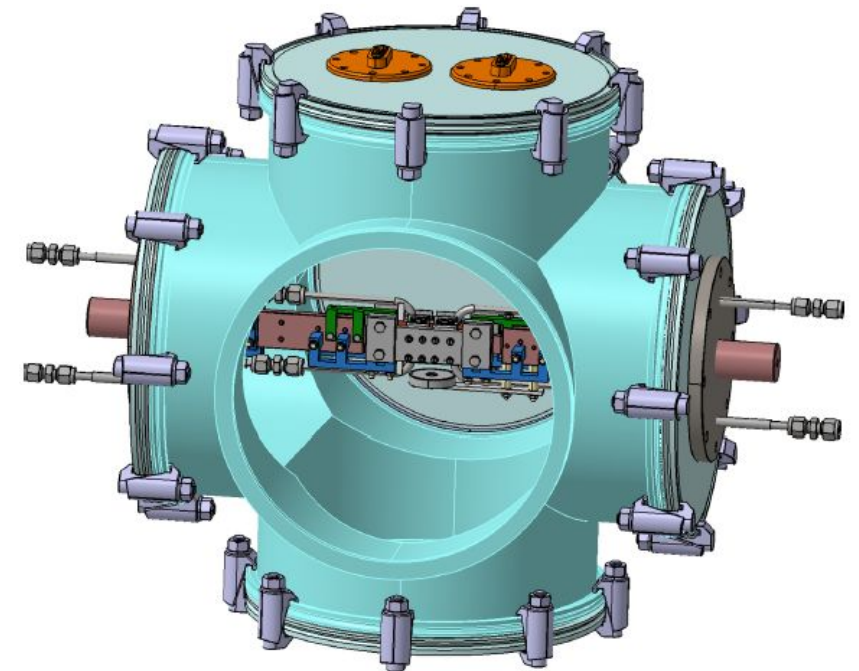
- **Assembly, testing, debugging, mounting the setup and upgraded shielding at LNGS - within end 2023**
- **Data taking alternating periods with current to periods without current and energy calibration, continuous maintenance of the barrack and of the setup - 2024-2026**
- **finalization of the whole acquired statistics data analysis - within 2027.**

Beyond VIP-3 - testing intermediate Z materials

In the period 2026:

- **Research on layered architecture of 1mm thick SDDs,**

- **energy resolution more than 2 times better than Ge detectors,**

- **scan of $\beta^2/2$ for electrons in materials with Z ~ 60 (e.g. Gadolinium) $K_{\alpha 1}$ transition energies in the range of 40 keV, with sensitivity comparable with VIP-2.**

During 2027-2028:

- **development layered architecture of 1mm thick SDDs,**
- **design of the improved experimental apparatus (new SDDs system cooling block, new vacuum flange connectors (more pins) to bring the signals out to the DAQ …)**

- **realization of the upgraded setup.**

In the period 2029-2031:

- **Data taking alternating periods with current to periods without current and energy calibration, continuous maintenance of the barrack and of the setup.**

VIP-GATOR collaboration - Open systems test for high Z elements

- **Unique opportunity to measure $\beta^2/2$ in Pb (Z = 82), Au ... respecting MG superselection, at energies currently not accessible with SDD detectors,**

Transitions in Pb	allow. (keV)	forb. (keV)
1s - 2p$_{3/2}$ K$_{\alpha 1}$	74.961	73.713
1s - 2p$_{1/2}$ K$_{\alpha 2}$	72.798	71.652
1s - 3p$_{3/2}$ K$_{\beta 1}$	84.939	83.856
1s - 4p$_{1/2(3/2)}$ K$_{\beta 2}$	87.320	86.418
1s - 3p$_{1/2}$ K$_{\beta 3}$	84.450	83.385

- **exploiting the facility GATOR (> 500 kEuro) high-performance low-background Ge spectrometer, in collaboration with ETH Zurich group (lead by Prof. Laura Baudis The Charpak-Ritz Prize 2022) Alexander Bismark, Michelle Galloway + 2PhD students.**

- **Low-background germanium counting facility for high-sensitivity γ-ray spectrometry**

- **Core: p-type coaxial high-purity germanium (HPGe) detector with 2.2 kg sensitive mass**

The Gator Detector
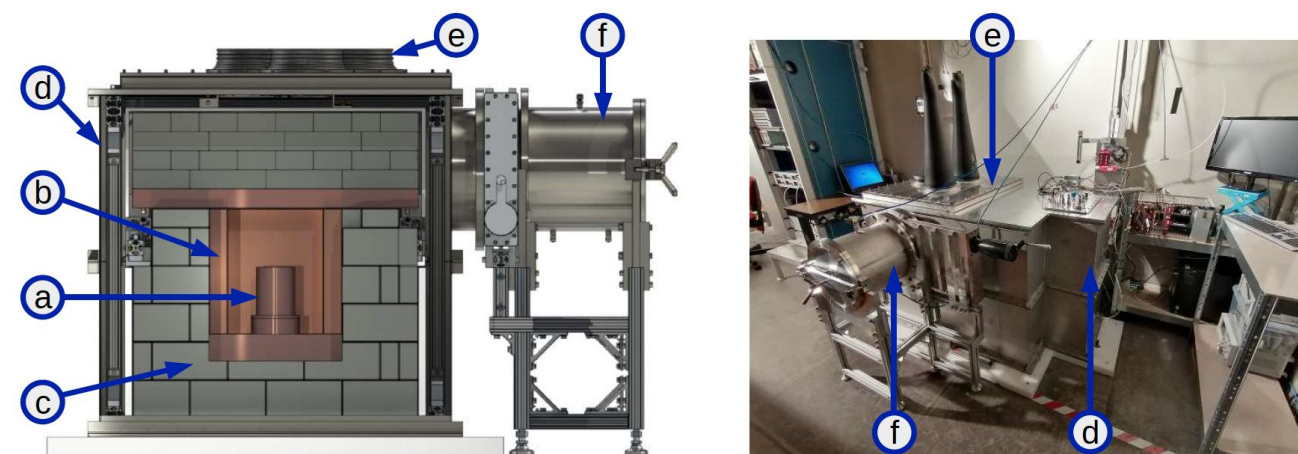
(a) HPGe detector inside Cu-OFE cryostat (cooled with LN$_2$ via copper coldfinger), (b) OFHC Cu cavity, (c) lead shield, polyethylene sheet, (d) airtight stainless steel enclosure (purged with GN$_2$), (e) glove ports, (f) sample load lock

VIP-GATOR collaboration - plan of activity

- Main contributions:
  - detector & shielding materials
  - environmental radon

- Integrated background rate in the energy region
  - 65-90 keV: (4.4 ± 0.3) d^{-1}kg^{-1}
  - 100-2700 keV: (82.0 ± 0.7) d^{-1}kg^{-1}

- Temporally stable within runs $(\chi^2/ndf \approx 1)$

test measurement in preparation **to be performed within 2022 for**:

- **background determination with Pb target**
- **low-energy calibration optimization**

Previous exploratory measurement Found.Phys. 42 (2012) 1015-1030

obtained limit:

$$\beta^2/2 < 1.5 \cdot 10^{-27}$$

expected improvement from the

VIP - GATOR collaboration (I = 400 A)

dedicated measurement 2 o.m. at least

VIP-GATOR collaboration - plan of activity

- **MC simulations** (efficiency, resolution, figure of merit) as a function of the target geometry/thickness **already performed** + prel. sym of power dissipation:
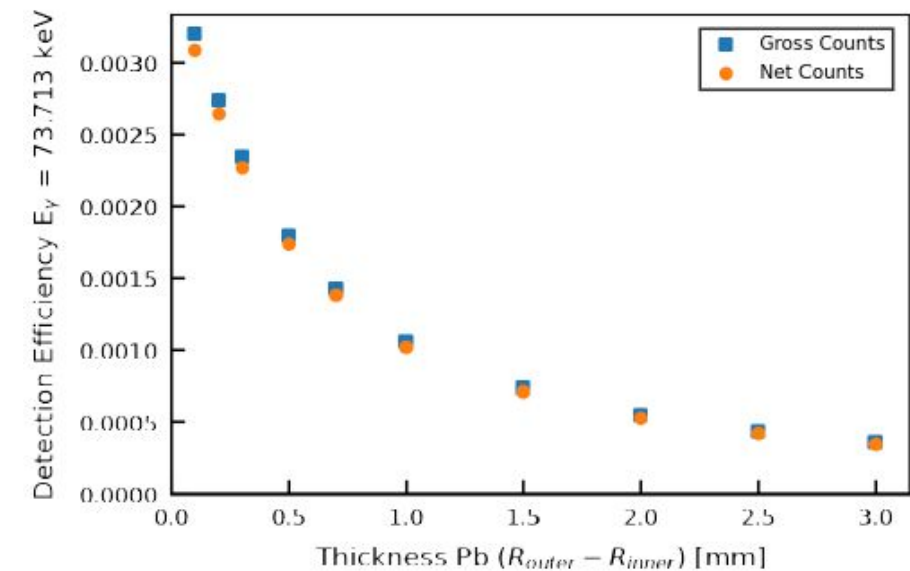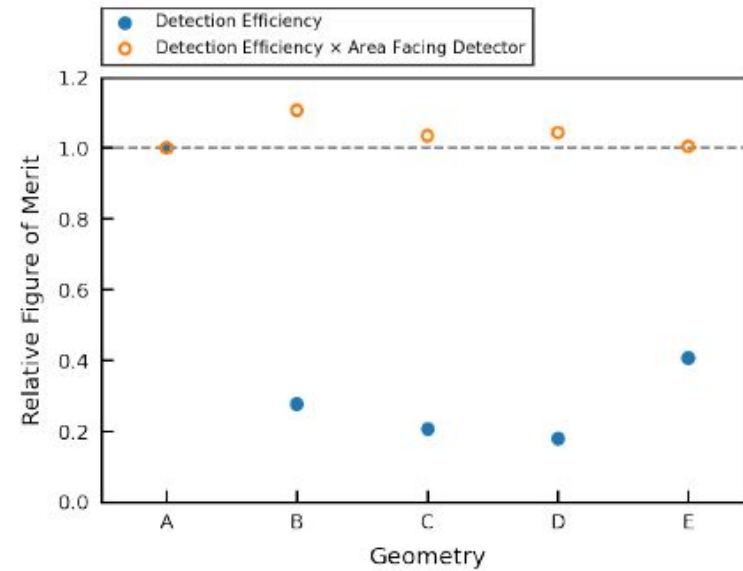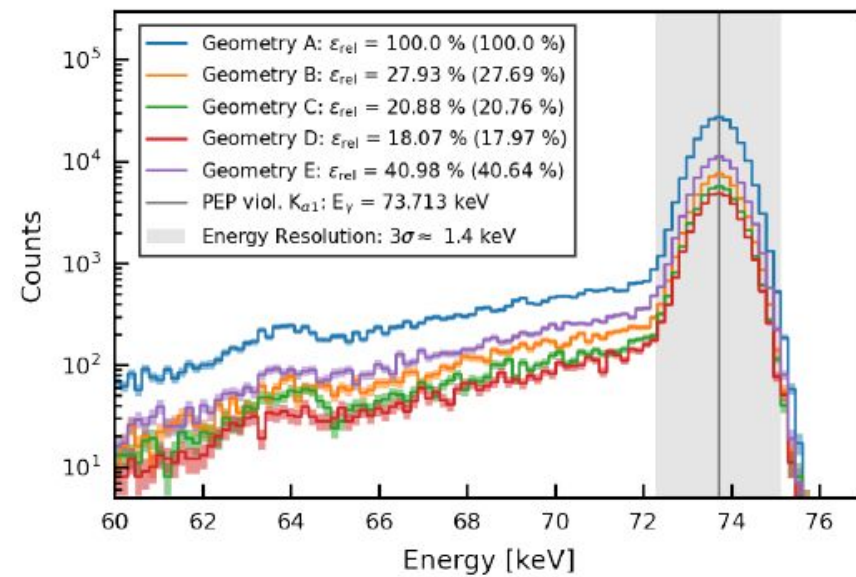
- **planned activity 2022**: test measurement, estimation heat-up for different cabling + connectors design,

- **planned activity 2023**:
  realization of the dedicated setup:
  - high radio-purity Pb target,
  - fed by a 400A DC power supply,
  - target and cabling cooling system and feed-through flange
    3/4 months data taking,
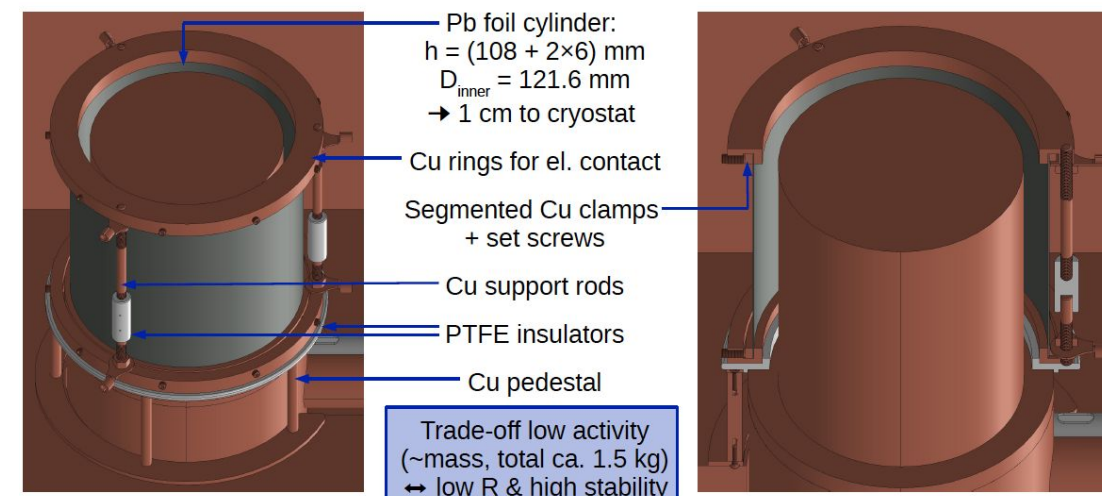
- **planned activity 2024/2025**: measurements with other high Z targets.

VIP Closed Systems
future plans

VIP Closed Systems future plans - BEGe setup

- **In order to improve 1 o.m. on the $\theta_{0i} = 0$ limit → improve on efficiency → use Ge as active material.**

Forb. transitions	BR	ϵ
$K_{\alpha 1}$	0.462 ± 0.009	$(5.39 \pm 0.11) \cdot 10^{-5}$

- **Difficulty: HPGe below 20 keV high background due to electronic noise,**

- **solution BEGe + Pulse Shape analysis: rejection of electronic noise, disentangle multi vs single hits events (photons from Ge vs photons from outside)**

Test setup realized, 2 data taking runs in 2021/2022
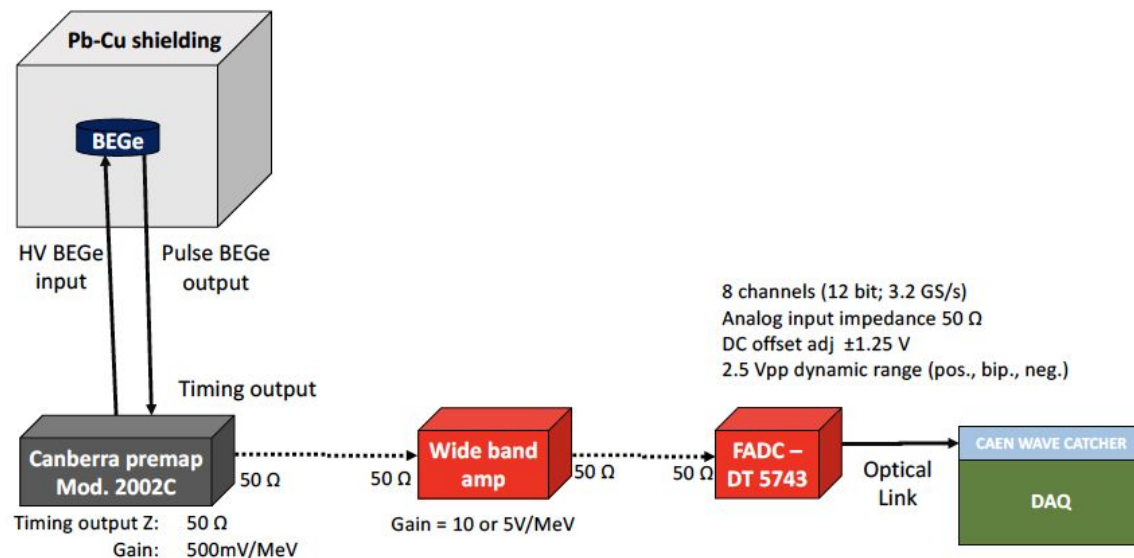
Block diagram of BEGe experimental apparatus

Connection of the Front-End electronic to the BEGe's Canberra preamplifier (Mod. 2002C), behind the liquid N2 dewar

- **data taking campaigns served for DAQ optimization -> increase amplitude for few keV photons: optical fibre Flash-ADC-Computer interface, wide band low noise amplifier, extremely-low noise digitizer/computer power supply,**

- **deep learning based pulse shape discrimination algorithm under development.**

Future directions

Theory side

T1 Explore symmetries for PEP-violations on Open Systems

Loop Quantum Gravity, Non-local Completion of Gravity Theories, Gauge Formulations of Gravity Theories etc…

T2 Extend falsification of quantum gravity models

Loop Quantum Gravity, Non-local Completion of Gravity Theories, Gauge Formulations of Gravity Theories etc…

T3 Generalized Uncertainty Principle as a class of universality

M-Theory, String Theory, Non-local Completion of Gravity Theories, Gauge Formulations of Gravity Theories etc…

T4 CPT violation and quantum decoherence, and the role of gravity

M-Theory, String Theory, Stochastic Quantization of Gravity, Dynamical Triangulation etc…

T5 Inhomogeneity and anisotropy of the geometry ground state

M-Theory, String Theory, Loop Quantum Gravity, Non-local Completion of Gravity Theories, etc…

VIP Closed Systems - plan of activity

Activity BEGe 2022-2024:   **T2, T3 & T4**

- **finalization of the BEGe setup based apparatus & finalization of the pulse shape discrimination algorithm,**

- **data taking + analysis in the context of NCQG, CPT violation and Generalized Uncertainty Principle theories.**

Activity BEGe 2025-2026:   **advanced**   **T2, T3 & T4**

- **data taking alternating various targets in accordance with energy dependence of the δ^2 in NCQG.**

New setup development 2025-2030:   **T5**

- **2 years R&D of a new setup dedicated to test angular modulation of the emitted spectrum and anisotropy predicted by the models on the PEPV amplitudes depending on the atomic structure, also by the introduction of a magnetic field,**
- **1 year realization and test of the upgraded setup,**
- **3 years of data taking**

Thank you

spares

Spin statistics theorem (Fierz 1939, Pauli 1940, Schwinger 1950)

Postulates: inhomogeneous Lorentz group,
locality,
microcausality,
vacuum is the state of lowest energy,
Hilbert space metric positive definite,
vacuum is not identically annihilated by a field $\longrightarrow$

(pseudo)scalar fields commute and spinor fields anticommute

Models of PEP violation:

Pioneering work of Fermi, Gentile, Green ...

Igniatiev and Kuzmin [A.Y. Ignatiev, V.A.Kuzmin, Proceedings of the Seminar, Tbilisi, USSR, 15-17 April 1986] (deformation of the standard Fermi oscillator)

$$a^+|0\rangle = |1\rangle \qquad a|0\rangle = 0$$
$$a^+|1\rangle = \beta|2\rangle \qquad a|1\rangle = |0\rangle$$
$$a^+|2\rangle = 0 \qquad a|2\rangle = \beta|1\rangle$$

Govorkov -> leads to states with negative norm [Phys. Lett. A 137(1-2), 7-10 (1989)]

Greenberg & Mohapatra, quon model [O.W. Greenberg, R.N. Mohapatra, Phys. Rev. Lett. 59(22), 2507-2510 (1987)]

$$a_k a_l^\dagger - q a_l^\dagger a_k = \delta_{k,l}$$

quon field theory is non-relativistic [A.B. Govorkov, Phys. A Statist. Mech. Appl. 203(3), 655-670 (1994)]

Rahal and Campa [V. Rahal, A. Campa, Thermodynamical implications of a violation of the pauli principle. Phys. Rev. A 38(7), 3728-3731 (1988)] global w.f. of the electrons is not exactly antisymmetric, PEP holds as long as the number of wrongly entangled pais is small.

Each model respects the MG superselection rule

VIP-2 tests the Pauli Exclusion Principle (PEP)
(spin-statistics) for electrons in a clean environment (LNGS) using a method which respects the

Messiah-Greenberg superselection rule :

Superpositions of states with different symmetry are not allowed →
transition probability between two symmetry states is ZERO

Forbidden by Superselection rule!

Initial state   Final state

Closed system →   Stable system transition

Open system →   Formation of a new state
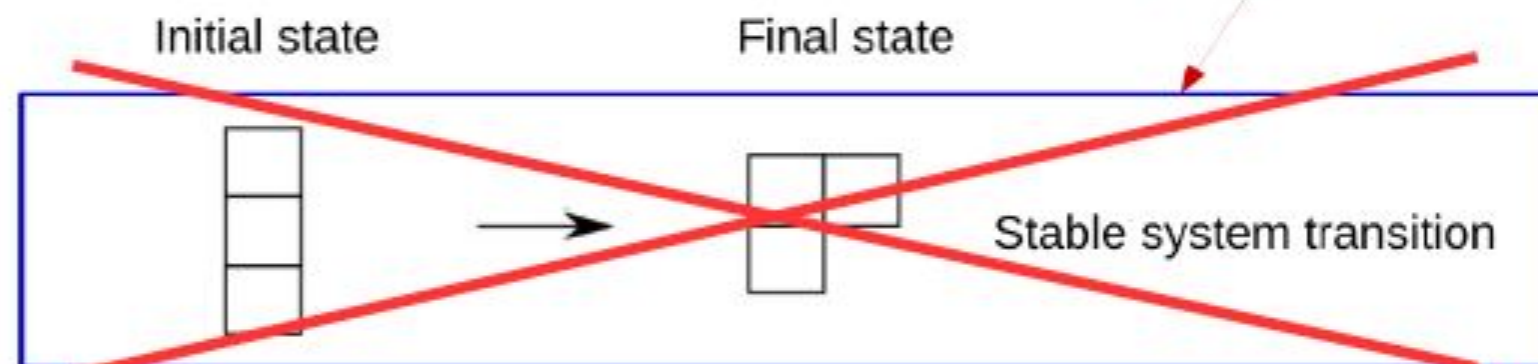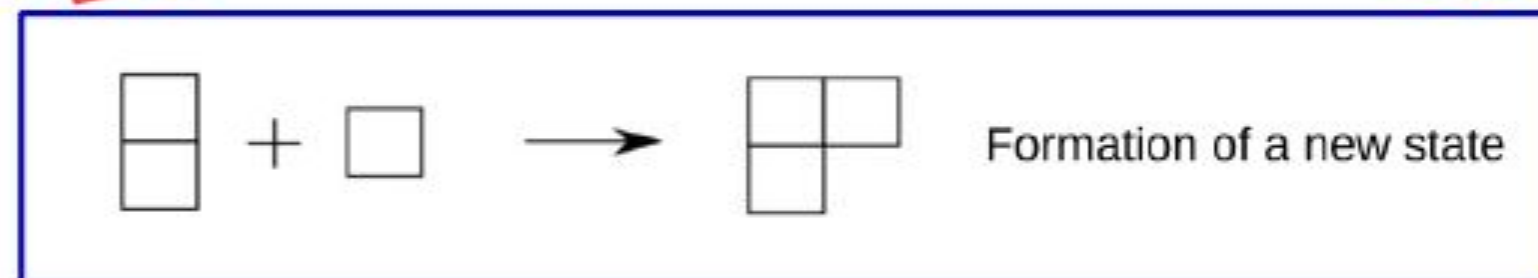
VIP sets the best limit on PEP violation for an elementary particle respecting the M-G superselection rule

5

VIP open systems - experimental method

Search for anomalous X-ray transitions performed by electrons introduced in a target _through a DC current (open system)_
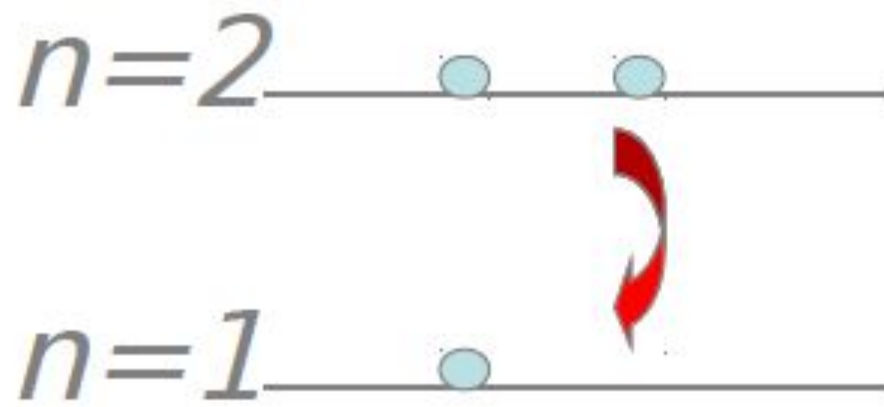
Normal 2p → 1s transition

~ 8.05 keV in Cu
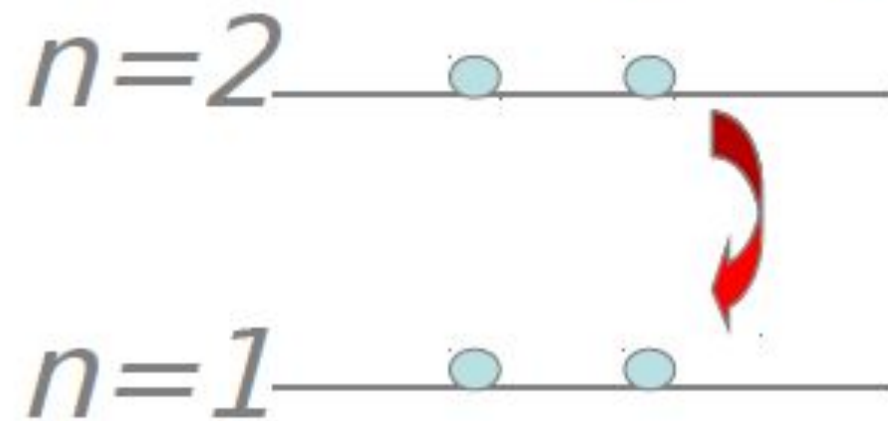
2p → 1s transition violating Pauli principle

~ 7.7 keV in Cu

Paul Indelicato (Ecole Normale Supérieure et Université Pierre et Marie Curie)
Multiconfiguration Dirac-Fock approach
Accounts for the shielding of the two inner electrons

The current-off spectrum provides the estimate of the background.

VIP open systems - experimental method

Greenberg, O. W. & Mohapatra, R. N., Phys Rev Lett 59, (1987).
E. Ramberg and G. A. Snow, Phys Lett B 238, 438–441(1990)

Search for anomalous electronic transitions in Cu
induced by a circulating current
introduced electrons interact with the valence electrons
search transition from 2p to 1s already filled by 2 electrons
alternated to X-ray background measurements without current
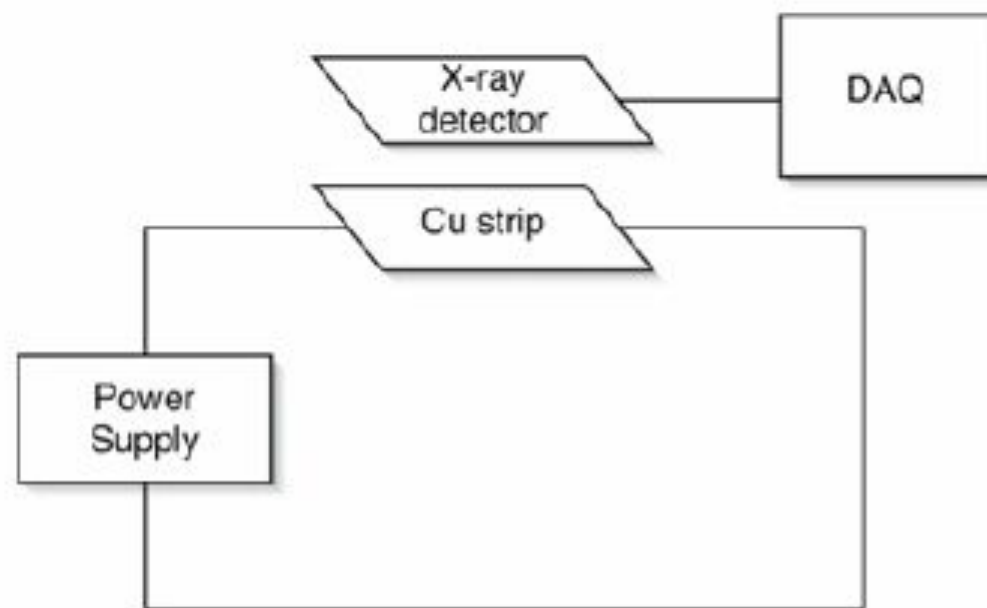
Undesired result :
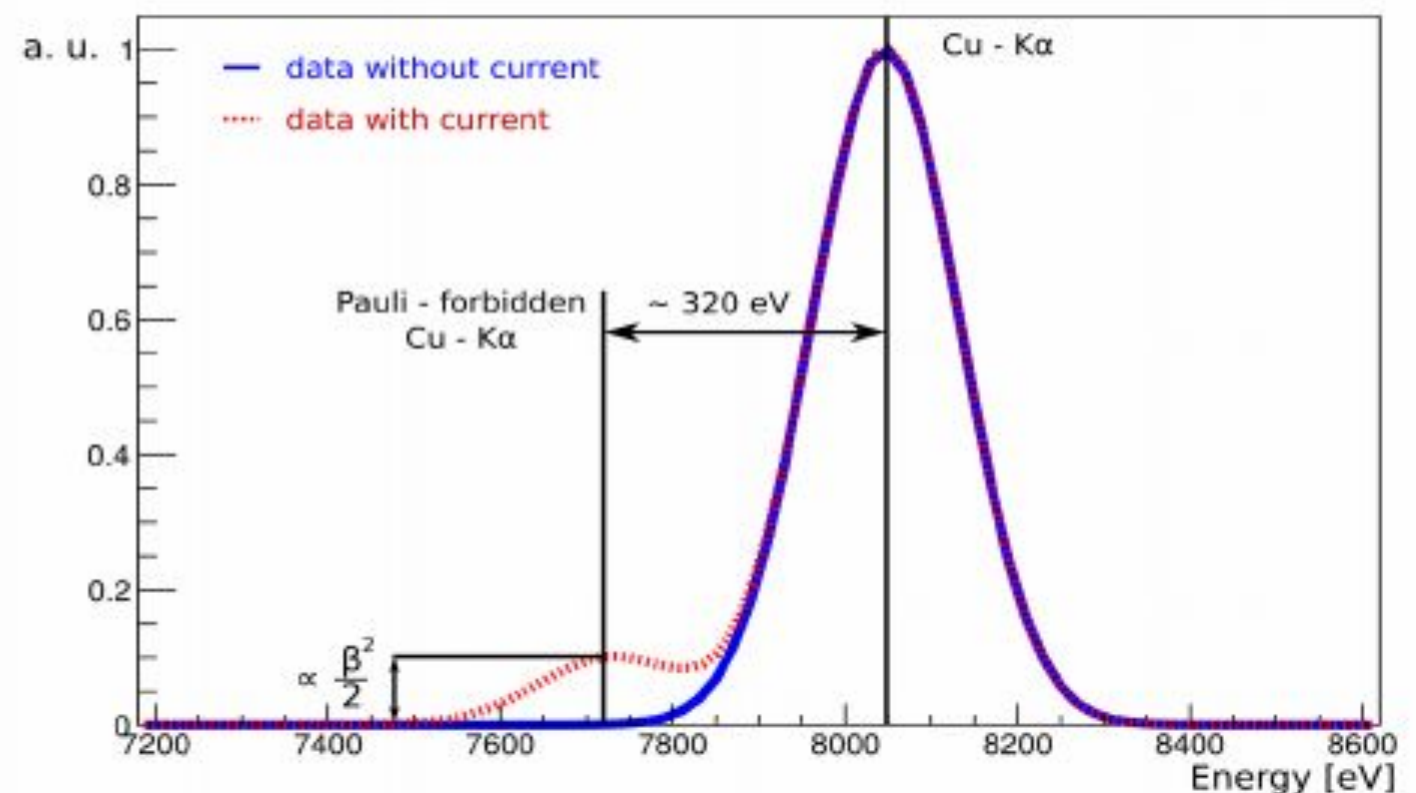
a) copper ultrapure cylindrical foil
b) surrounded by 16 Charge Coupled Devices
   (CCD) res. at 8 keV 320 eV (FWHM)
c) inside a vacuum chamber: CCDs cooled to
   168K by a cryogenic system
d) amplifiers + read out ADC boards.

subtracted spectrum
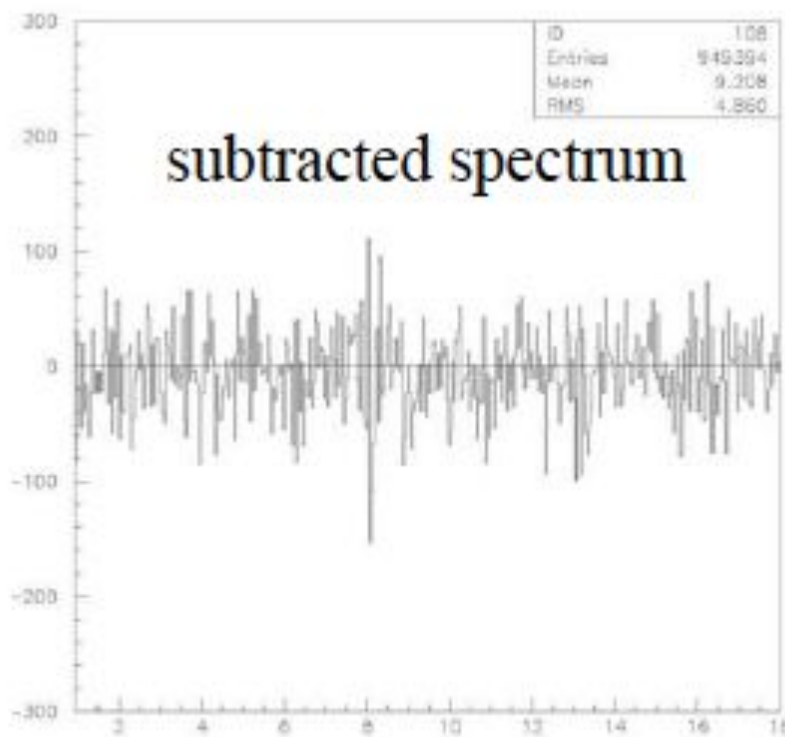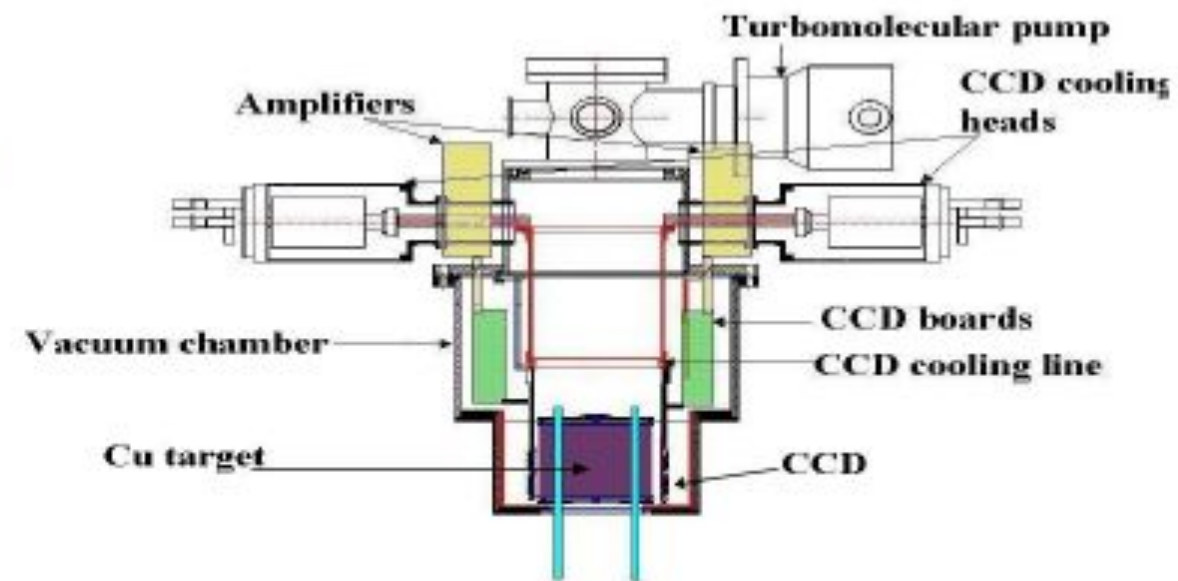
$$\beta^2/2 \leq 4.7 \times 10^{-29}$$

improved the limit obtained by Ramberg & Snow
by a factor ~ 400

(Foundation of Physics 41 (2011) 282+ other papers)

GOAL OF VIP-2 :   improve the VIP result of 2 orders of magnitude

VIP-2 major upgrade

a) **Silicon Drift Detectors (SDDs)** → higher resolution (190 eV FWHM at 8.0 keV), faster (triggerable) detectors. 4 arrays of 2 x 4 SDDs 8mm x 8mm each, liquid argon closed circuit cooling - 160 °C

b) **2 strip shaped Cu targets** (25 μm x 7 cm x 2 cm) more compact target → higher acceptance, thinner → higher efficiency
DC current supply to Cu bars

Cu strips cooled by a closed Fryka chiller circuit → **higher current** (100 A) @ 20 °C of Cu target implies 1 °K heating in SDDs
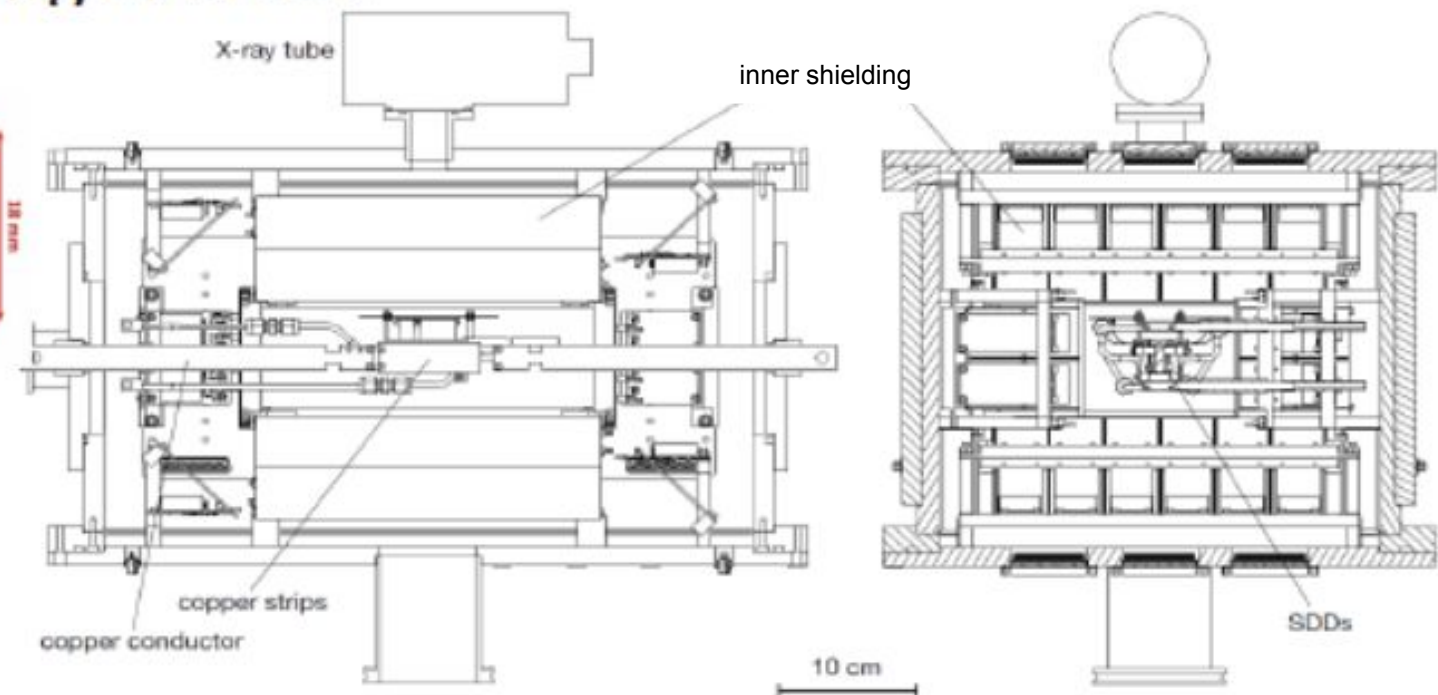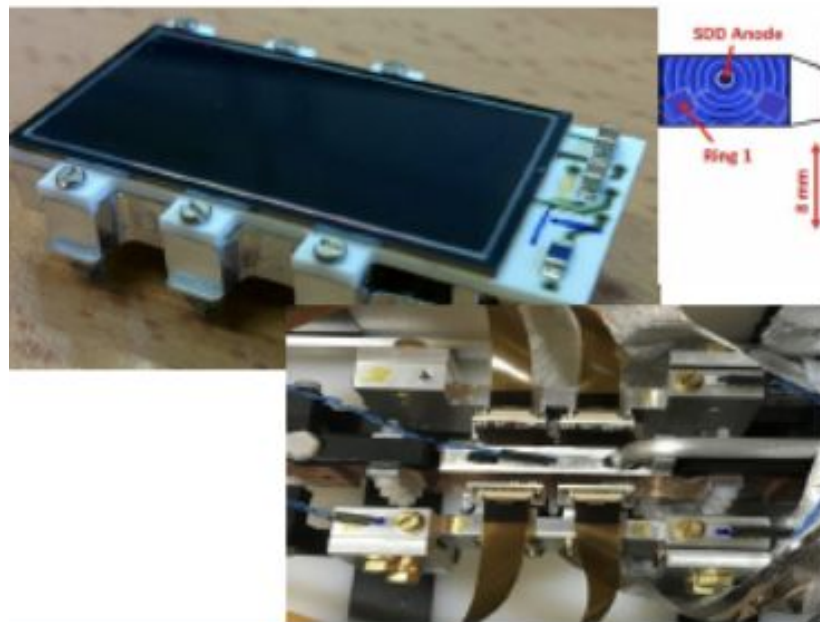
Presa dati continuativa 2019 - 2021

Period	Files	Current
May 2019	07/05/2019->14/05/2019	0A
May-June 2019	14/05/2019->12/06/2019	150A
June-July 2019	12/06/2019->10/07/2019	0A
July 2019	10/07/2019->29/07/2019	180A
August 2019	31/07/2019->04/09/2019	0A
September 2019	20/09/2019->01/10/2019	180A
October-November 2019	01/10/2019->05/11/2019	0A
November-December 2019	05/11/2019->19/12/2019	180A
December January 2020	19/12/2019->21/01/2020	0A
January February March 2020	21/01/2020->18/03/2020	180A
March May 2020	18/03/2020->04/05/2020	0A
May 2020	05/05/2020->07/07/2020	180A
July September 2020	09/07/2020->03/09/2020	0A
September 2020	03/09/2020->16/09/2020	180A
September October 2020	18/09/2020->06/10/2020	180A
October December 2020	06/10/2020->16/12/2020	Moduled
December January 2021	17/12/2020->08/01/2021	0A
January March 2021	08/01/2021->11/03/2021	180A
March May 2021	12/03/2021->11/05/2021	0A

after maintenance activity performed during the first phase of shack reorganization, the data taking restarted (fine Luglio-10 Agosto 2021) (0A). Then system shut down to allow the shack renovation activity by LNGS staff, which was concluded July 2022. End of July 2022 VIP-2 was transported and mounted at LNGS.

$$t^{wc} = 27110263 \text{ s} = 314 \text{ days}$$
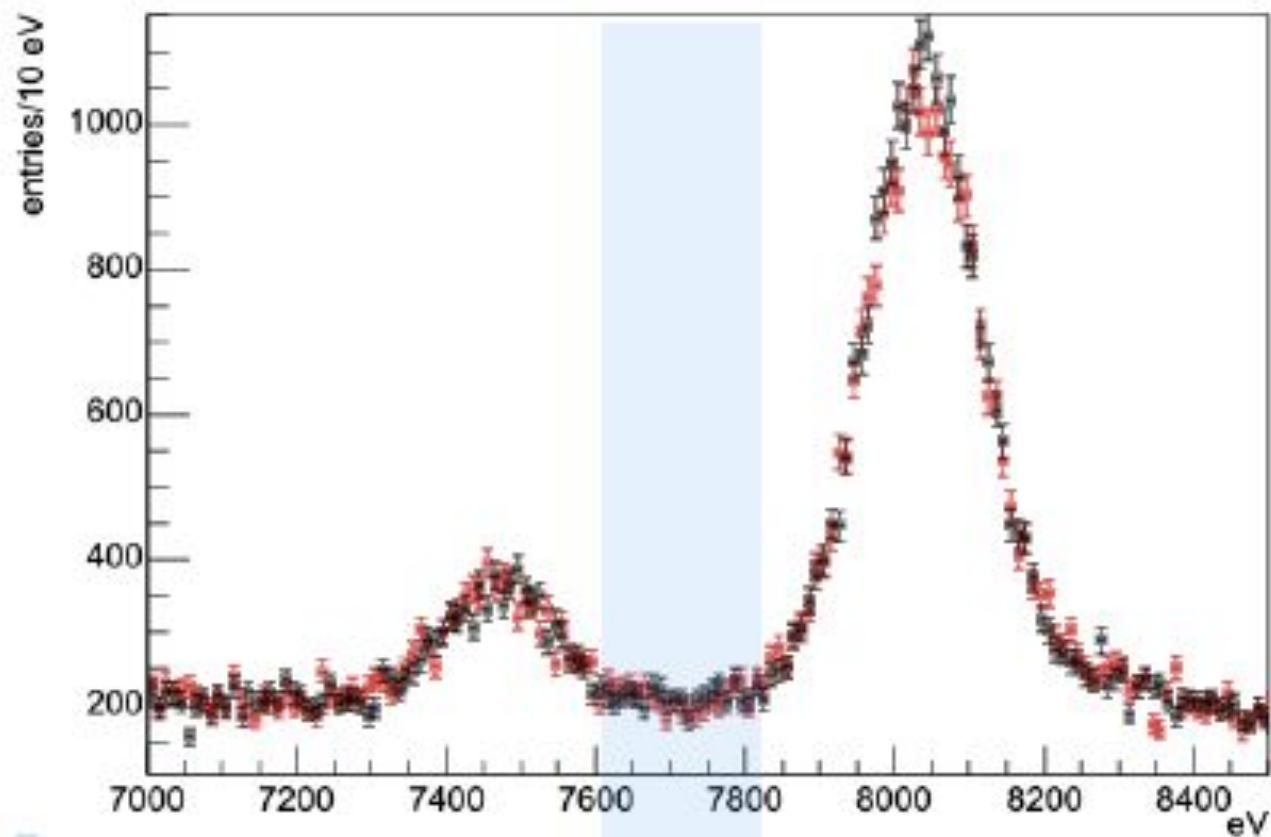
$$t^{woc} = 26916404 \text{ s} = 311 \text{ days}$$
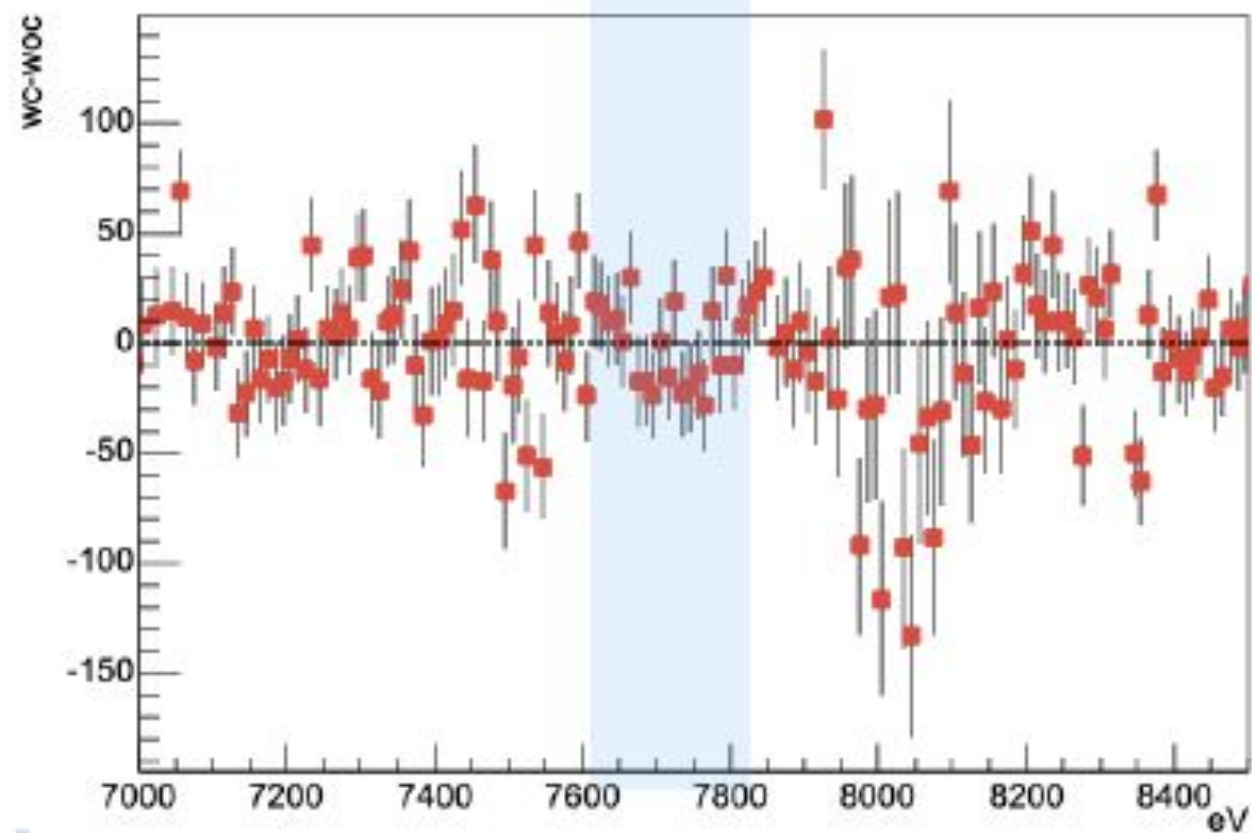
$$t^{wc}/t^{woc} = 1.0072022(6)$$

Statistical model

Statistical model improved to account for uncertainties on the parameters of the signal and background shapes, and scale factor of the current on/off spectra:

- **the two spectra are simultaneously analysed by constructing the joint likelihood:**

$$\mathcal{L} = \text{Poiss}(Data^{wc}|f^{wc}(\boldsymbol{\theta})) \times \text{Poiss}(Data^{woc}|f^{woc}(\boldsymbol{\theta}) \times \text{SCALE})$$
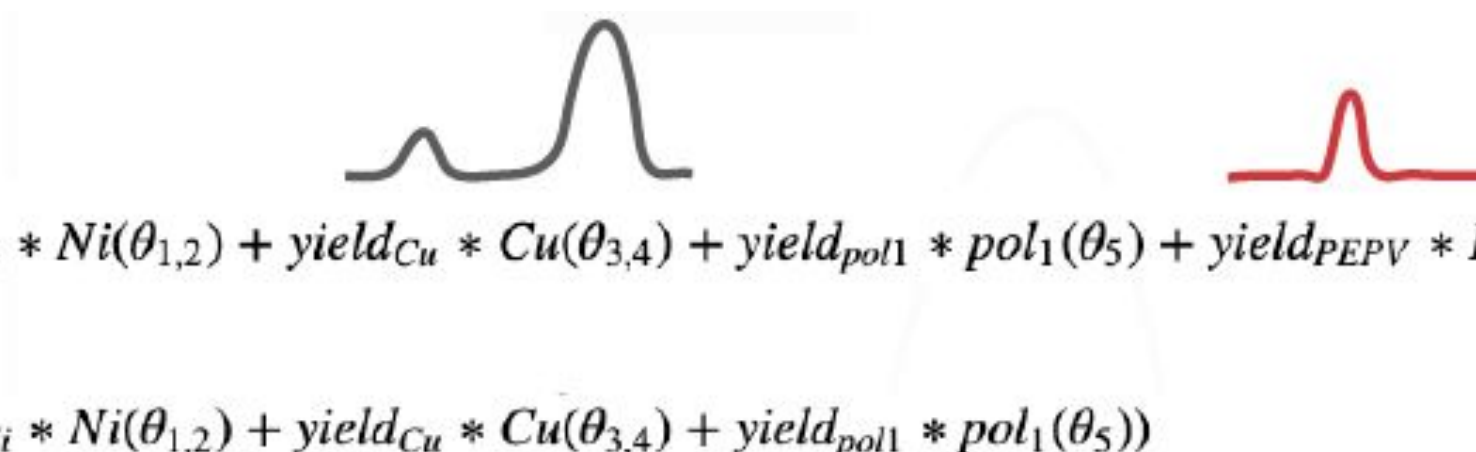
$$f^{wc}(\boldsymbol{\theta}) = yield_{Ni} * Ni(\theta_{1,2}) + yield_{Cu} * Cu(\theta_{3,4}) + yield_{pol1} * pol_1(\theta_5) + yield_{PEPV} * PEPV(\theta_4)$$

$$f^{woc}(\boldsymbol{\theta}) = (yield_{Ni} * Ni(\theta_{1,2}) + yield_{Cu} * Cu(\theta_{3,4}) + yield_{pol1} * pol_1(\theta_5))$$

where θ is the vector of parameters of the signal and bkg shapes

- **The posterior *pdf* is obtained based on the Bayes theorem:**

$$P(S, B, s, \theta_S, \theta_B|\text{data}_{wc}, \text{data}_{woc}) = \frac{\mathcal{L}}{N} P_0(S) \cdot P_0(B) \cdot P_0(s) \cdot P_0(\theta_S) \cdot P_0(\theta_B)$$

SCALE has a gaussian prior at t_{wc} / t_{woc}

SHAPE par. - have flat priors, except gaussians for transitions positions and *B*

Analysis Strategy

With current
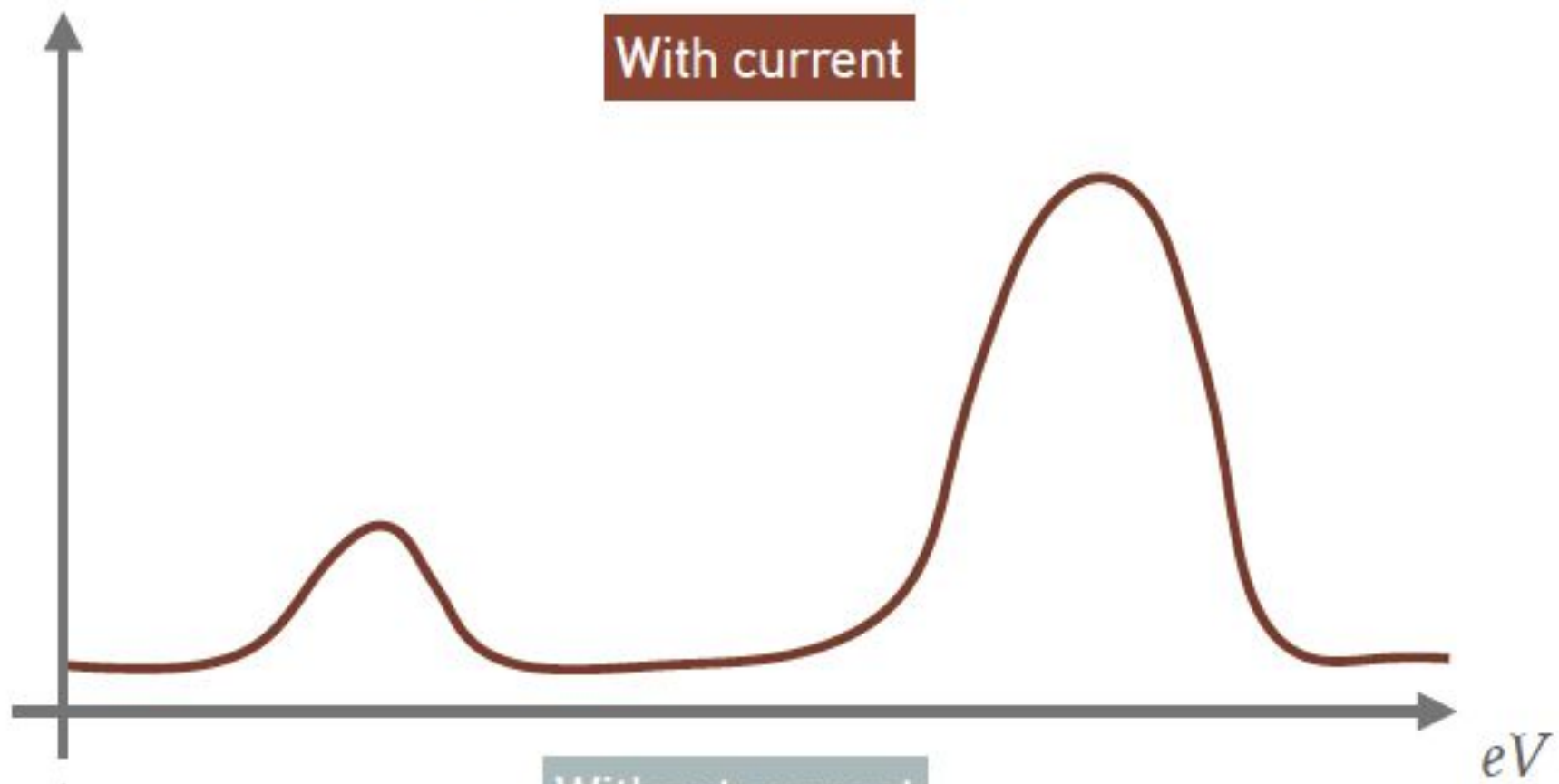
Without current
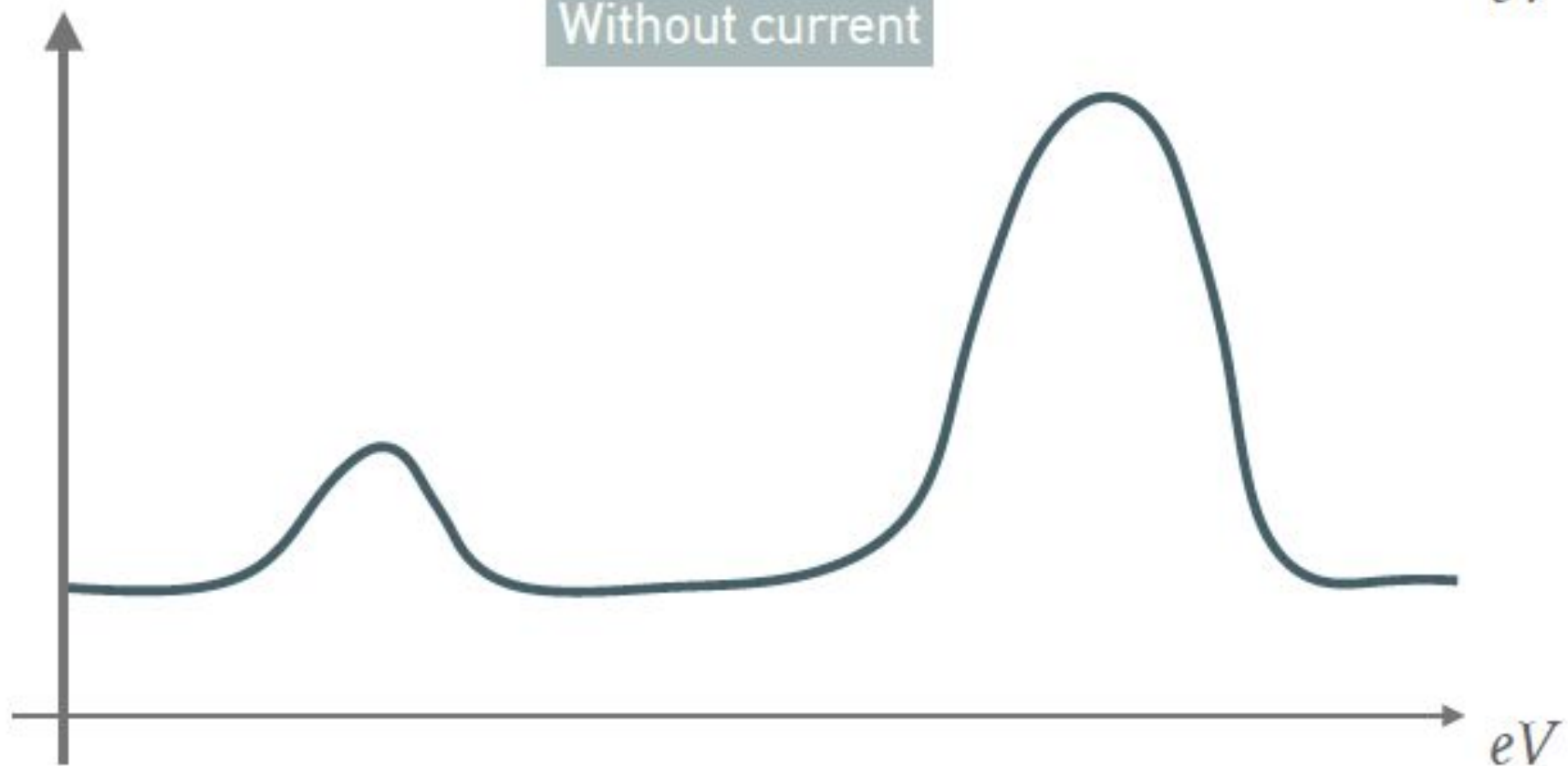
8 params

= polynomial(1) + Gaussian Ni + Gaussian Cu
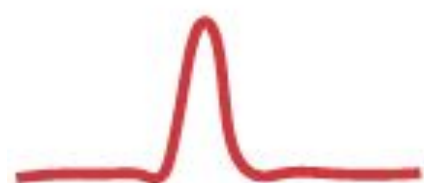
1 param

= **Gaussian PEPV**

With current

eV

With current

Without current

$x\ t^{wc}/t^{woc}$

eV

eV
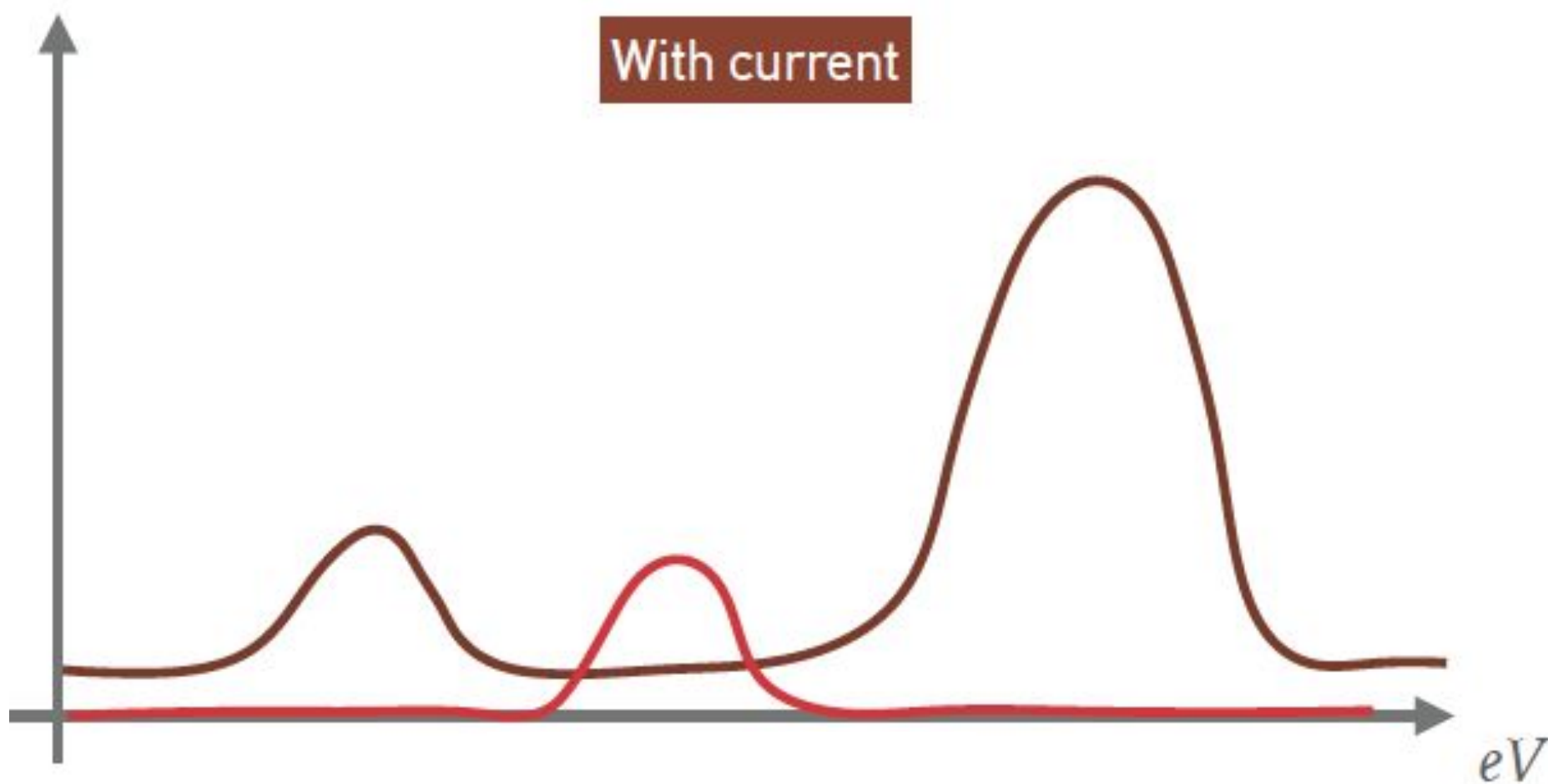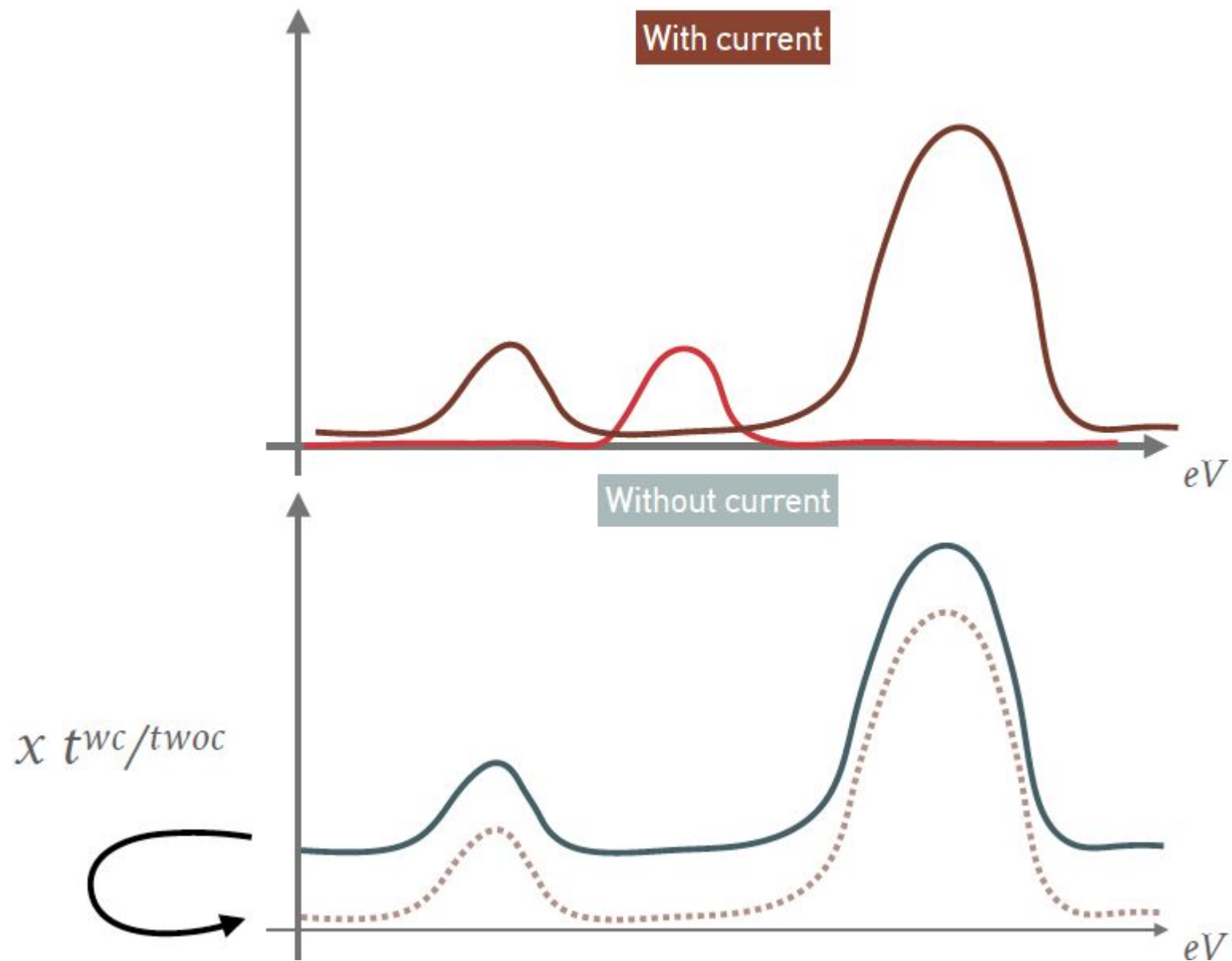
8 params

= polynomial(1) + Gaussian Ni + Gaussian Cu

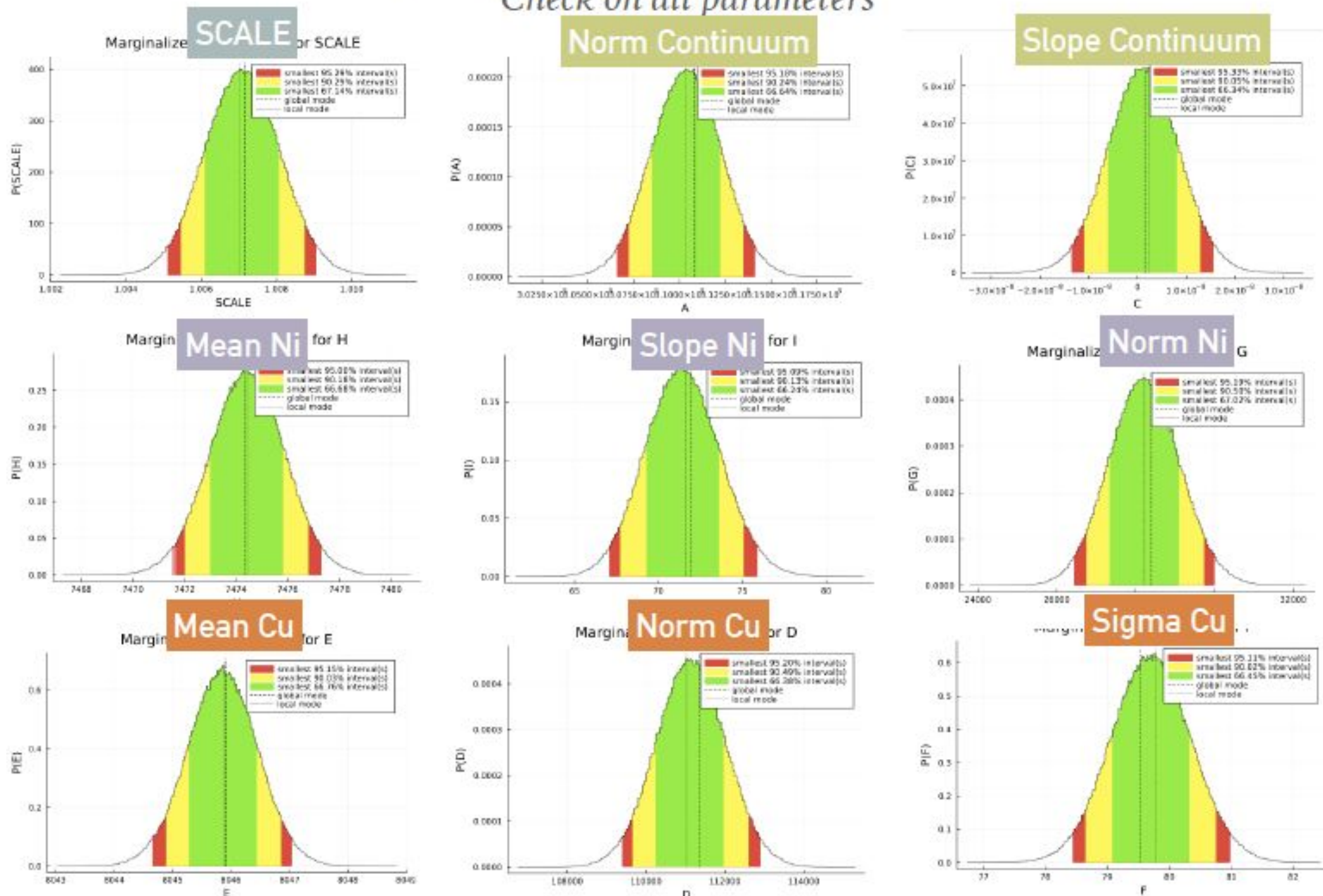1 param

= Gaussian PEPV

= SCALE = Gaussian(t^{wc}/t^{woc})

$$p(\theta_i | \mathcal{D}, M) = \int p(\boldsymbol{\theta} | \mathcal{D}, M) \prod_{i \neq j} d\theta_j$$

Marginalized Probability density

calculated by means of adaptive Metropolis-Hastings MCMC

Check on all parameters

Marginalized Probability density

$$p(\theta_i | \mathcal{D}, M) = \int p(\boldsymbol{\theta} | \mathcal{D}, M) \prod_{i \neq j} d\theta_j.$$

With current

Without current

calculated by means of adaptive Metropolis-Hastings MCMC

Marginalized Distribution for S
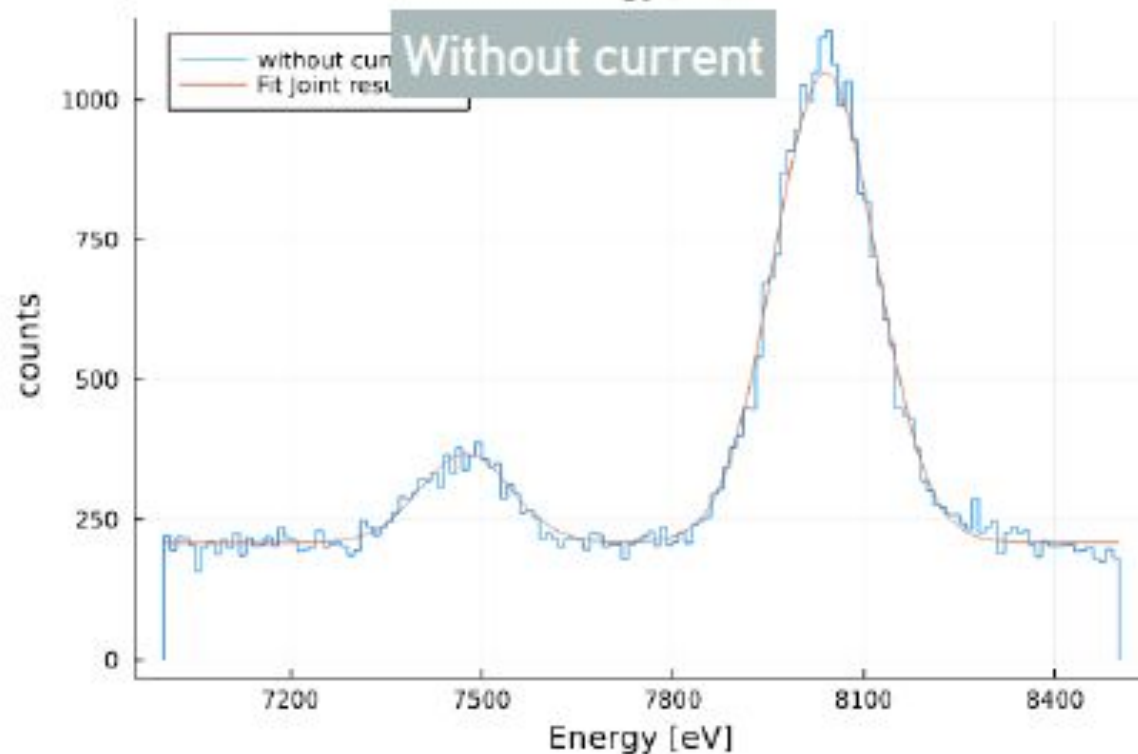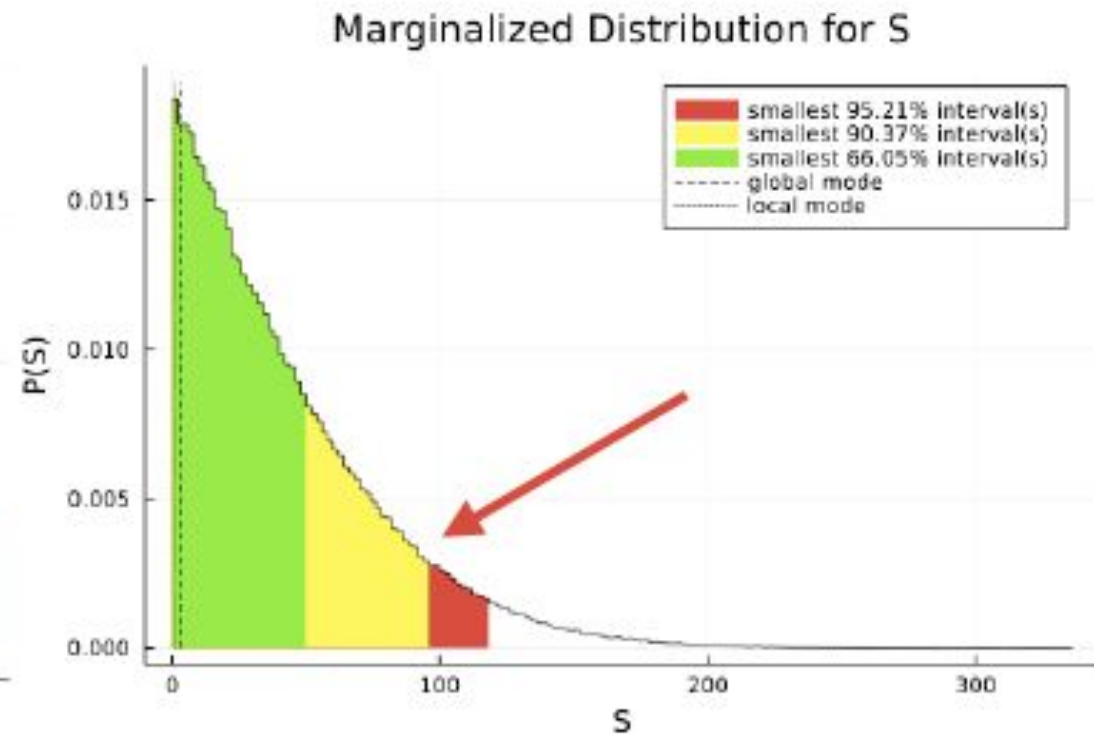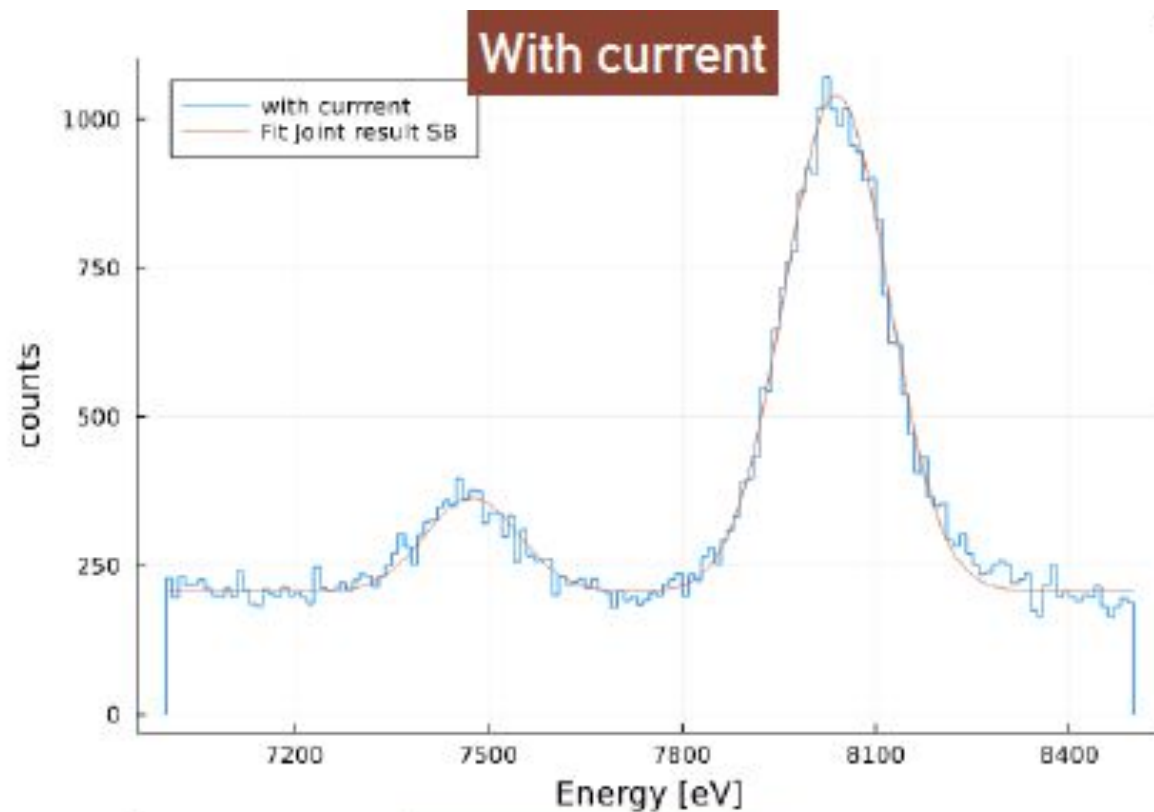
90% Upper Limit on Signal: 93

Scan the PEP violation probability as a function of Z (i.e. of Energy)

Okun, L.:

"The special place enjoyed by the Pauli principle in modern theoretical physics does not mean that this principle does not require further and exhaustive experimental tests. On the contrary, it is specifically the fundamental nature of the Pauli principle which would make such tests, over the entire periodic table, of special interest"
L. Possible violation of the Pauli principle in atoms. JETP Lett.
1987, 46, 529532

"High sensitivity Pauli Exclusion Principle tests by the VIP experiment: status and perspectives"

Paper on the preparation of VIP-3 experiment IN PRINT in APPA.

Proved increment of a factor 2 in efficiency at 20 keV keeping fixed E resolution (with respect present technological limits for 450um) -> scan of $\beta^2/2$ for electrons in higher Z materials (Ag, Sn and Pd);
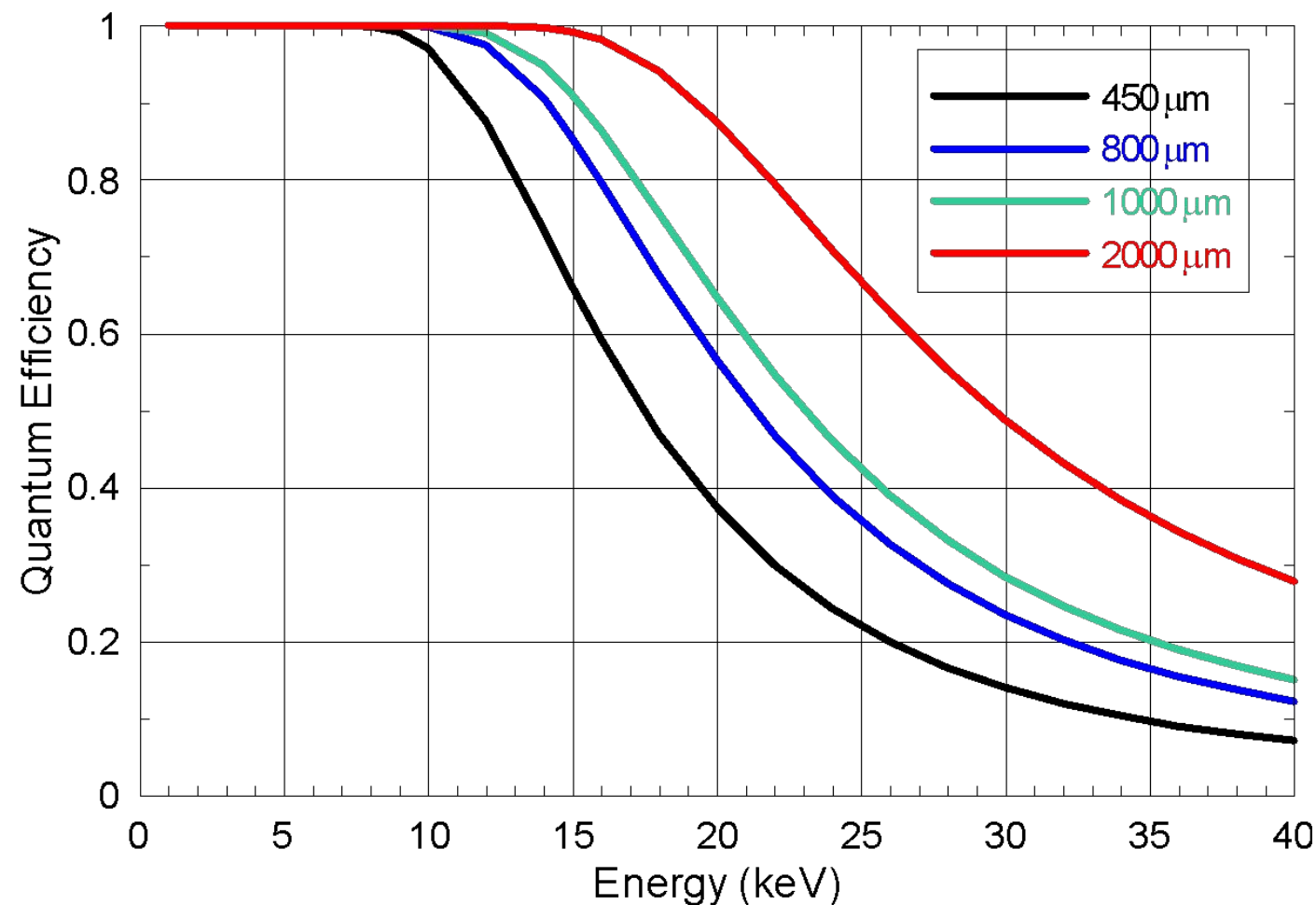
new SDD detectors architecture: geometry of 2x4 SDDs units, each of 8x8 mm^2, with a new improved readout electronics and ceramics. Production and development in collaboration with FBK & Politecnico di Milano.

Updates on 1mm SDD production run:

The run has been stopped after the first lithography steps due to a major stop of the FBK clean room for construction works (new clean room).

N. Zorzi (FBK): laboratorio ripartito ad inizio marzo 2022, ma il run e' rimasto bloccato fino a metà maggio per la mancata fornitura del precursore gassoso necessario per gli impianti di boro… la generale difficoltà nel reperimento di materie prime a livello mondiale sta comunque generando una incertezza sui tempi di consegna… Il run KAONNIS … ha comunque raggiunto ad oggi circa il 30% del flusso di processo previsto… si stima che il run potra' essere completato per meta' dicembre.

Design of the new board for the SDD array:

o   A meeting of the collaboration to discuss design guidelines for the new board has been held in Frascati in Dec. 2021.

o   Modifications are necessary to cope with the new dimensions of the array and the new 'focusing electrode' on the back side. Preferences have been expressed towards a 'conservative' design aimed to populate the experiment with single arrays more than the '2-SDD stacked' design. **Design evaluations are ongoing accordingly**.

New materials beside alumina, are also under considerations.

New SDD run for VIP (and Kaonnis)

- Pixel dimensions: 7.9 mm × 7.9 mm

- Extended width of last drift ring (improve collection at the border of the active area)

- Increased number of GRs (control lateral depletion in thick sensors)

- Total chip dimensions: 35.6 mm × 19.8 mm

  -> ~ 2 mm wider than previous chip
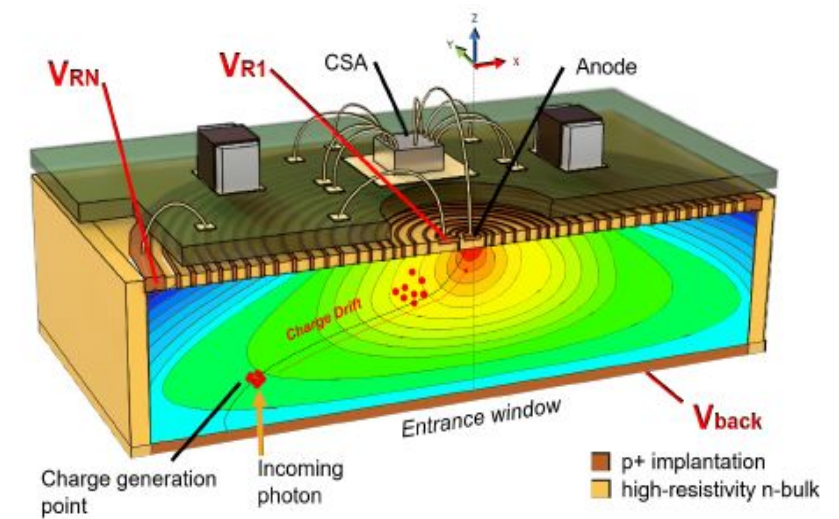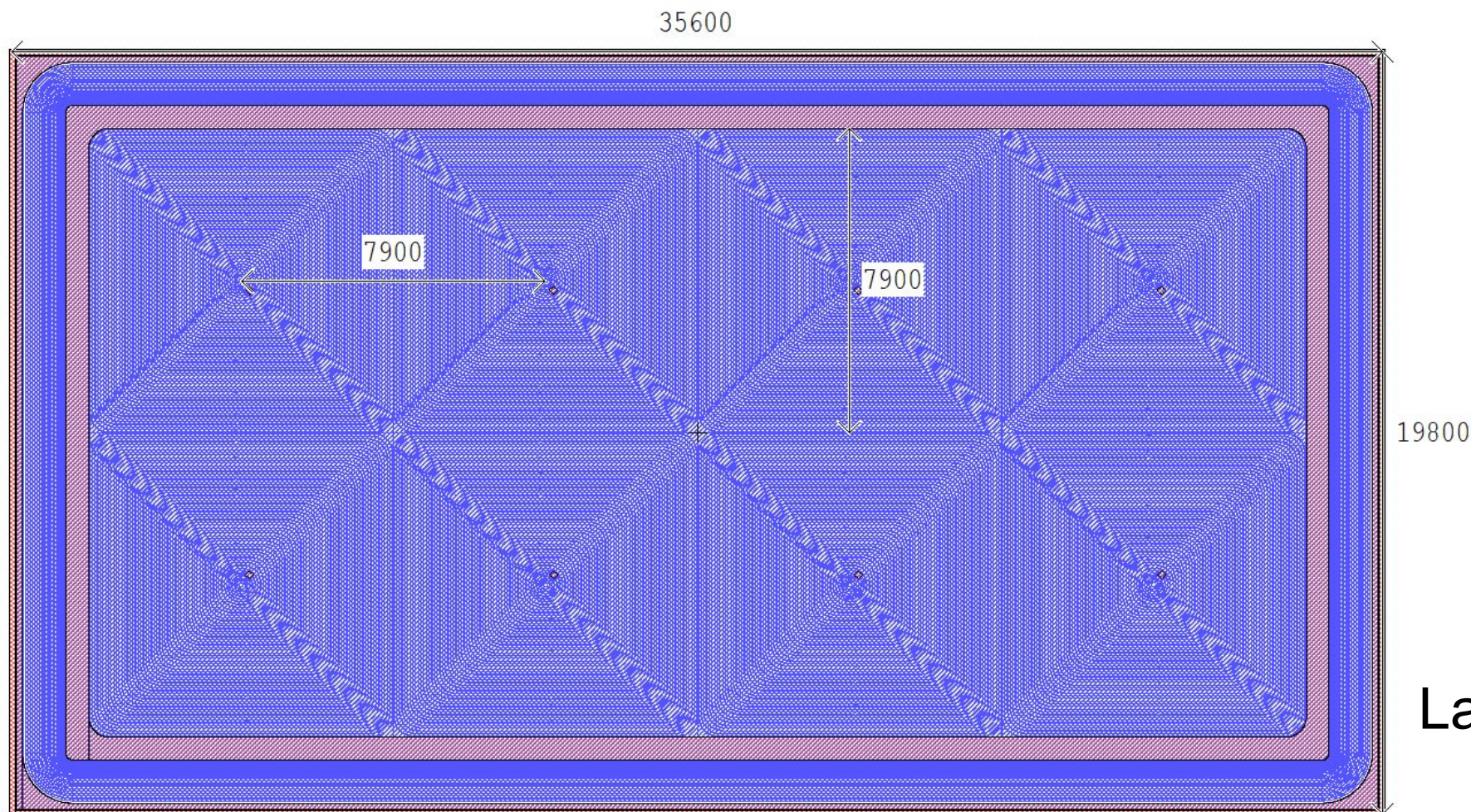
Layout of the main SDD array – Anode side

New SDD run for VIP (and Kaonnis)

- Introduced focusing electrode on the window (reduce charge sharing)

- Single connection to polarize all the pixel windows

- Single connection to polarize focusing electrode

- Improved robustness of bonding pads
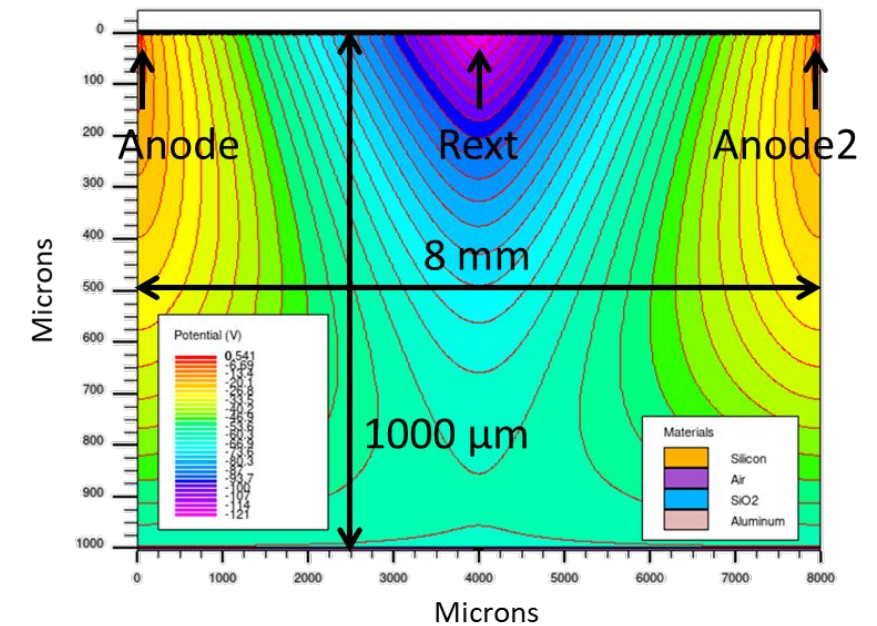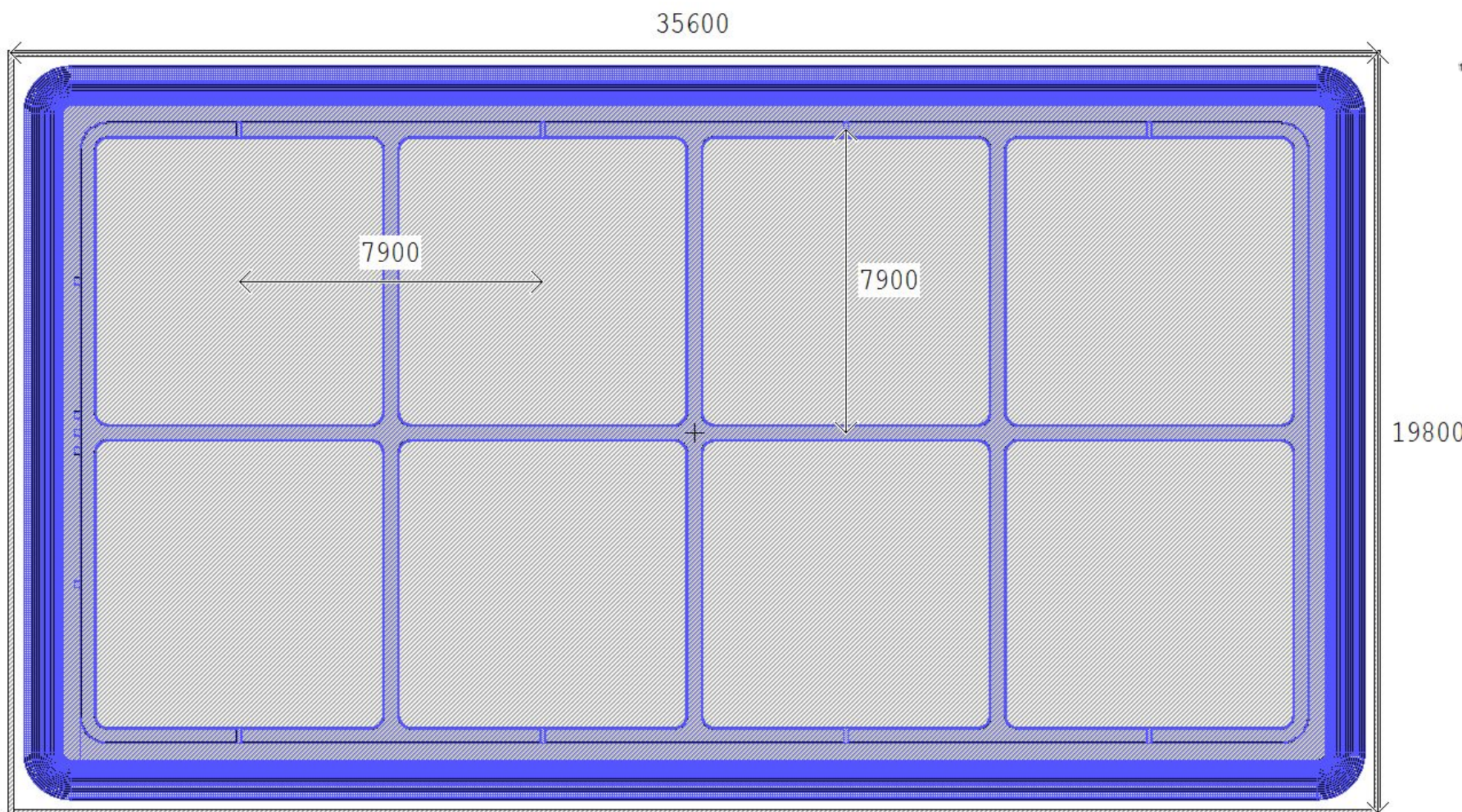
Layout of the main SDD array – Window side

Realization of a new vacuum chamber dedicated to the VIP-3 experiment:

- optimized to arrange the new compact SDD detectors (detectors+front end electronic), target and cooling system.
- the increased number of active channels with respect to the present VIP-2 apparatus (64 instead of 32, to increase the geometrical efficiency), requires new dedicated SDDs - target arrangement, new cold head to satisfy the increased power request of the new system, new vacuum flange connectors (more pins) to bring the signals out to the DAQ, the vacuum tight electrical feedthrough dedicated to the circulating current in the target will be improved (electrical stability and thermal dissipation) allowing to safety operate up to 400A.

VIP SETUP WITH "CROSS VACUUM CHAMBER"

Isometric view
Scale: 1:5
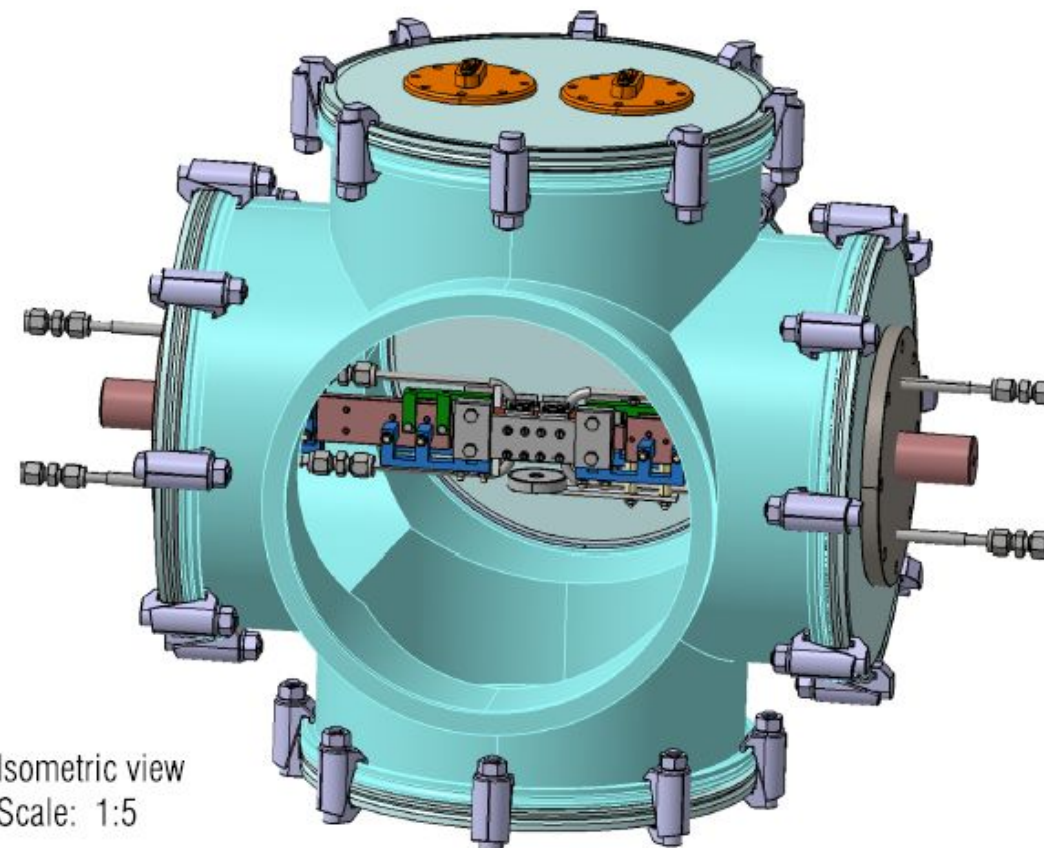
- **Realization of the new thermal contact** between the cold-finger and SDDs detectors made in pure copper (minimize natural copper radio-contamination).

- **Realization of a new target cooling system** made in pure copper (10 times higher thermal conductivity): 1) reduce the detectors working temperature (improving the energy and timing resolution) 2) increase the applicable maximum current circulating in the target (new power supply 400A).

- Layout of the inner part of the compact SDD detectors system:

- **Layout of the inner part of the compact SDD detectors system:**

VIP – compact SDD and target cooling design

Cold head

Cooling adapter

SDD cooling block

target cooling

SDD cooling bar
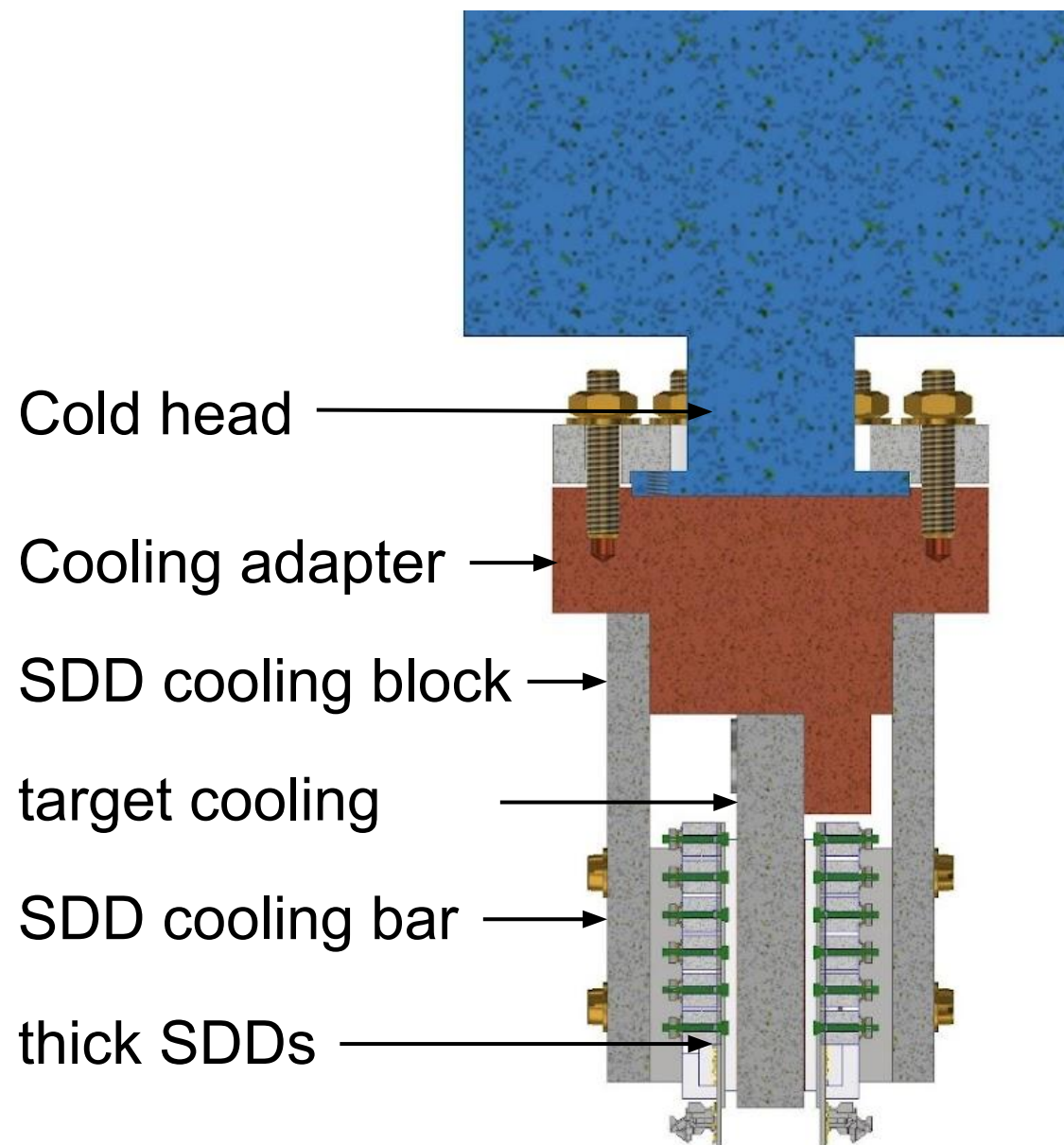
thick SDDs

Total 8 thick SDD units
- 64 SDD cells
- each cell 64 mm^2
- active area 41 cm^2

- **Layout of the inner part of the compact SDD detectors system:**

VIP – compact SDD and target cooling design
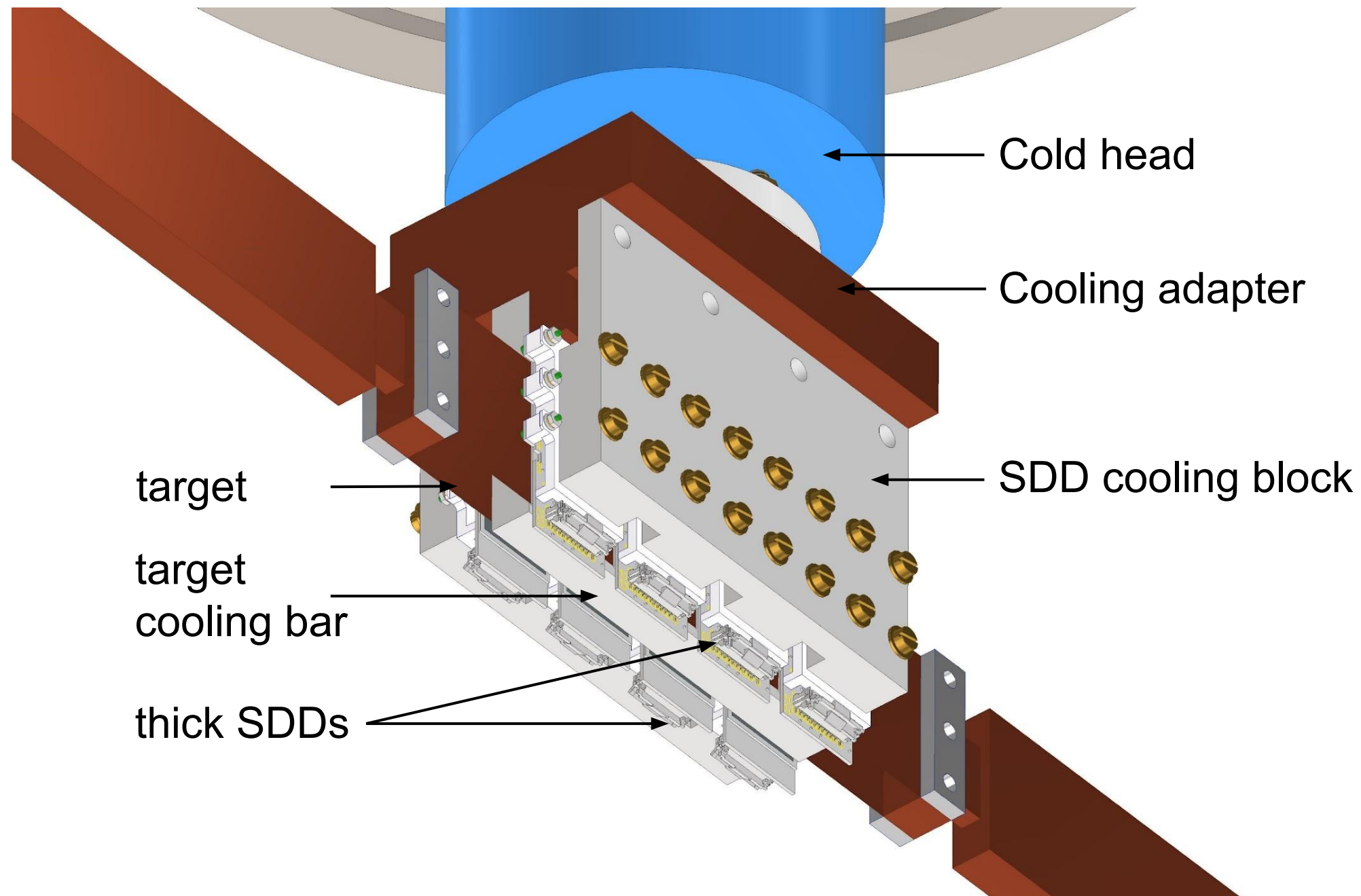
GATOR facility at LNGS

The Gator Facility

- Low-background germanium counting facility for high-sensitivity γ-ray spectrometry

- Located at the Gran Sasso underground laboratory in Italy (LNGS) at a depth of 3600 m water equivalent

- Core: p-type coaxial high-purity germanium (HPGe) detector with 2.2 kg sensitive mass and a relative efficiency of 100.5%

- Sample chamber volume: 25×25×33 cm^3

- Currently used for material radioassay for rare-event search experiments in astroparticle physic (XENON, LEGEND,...)
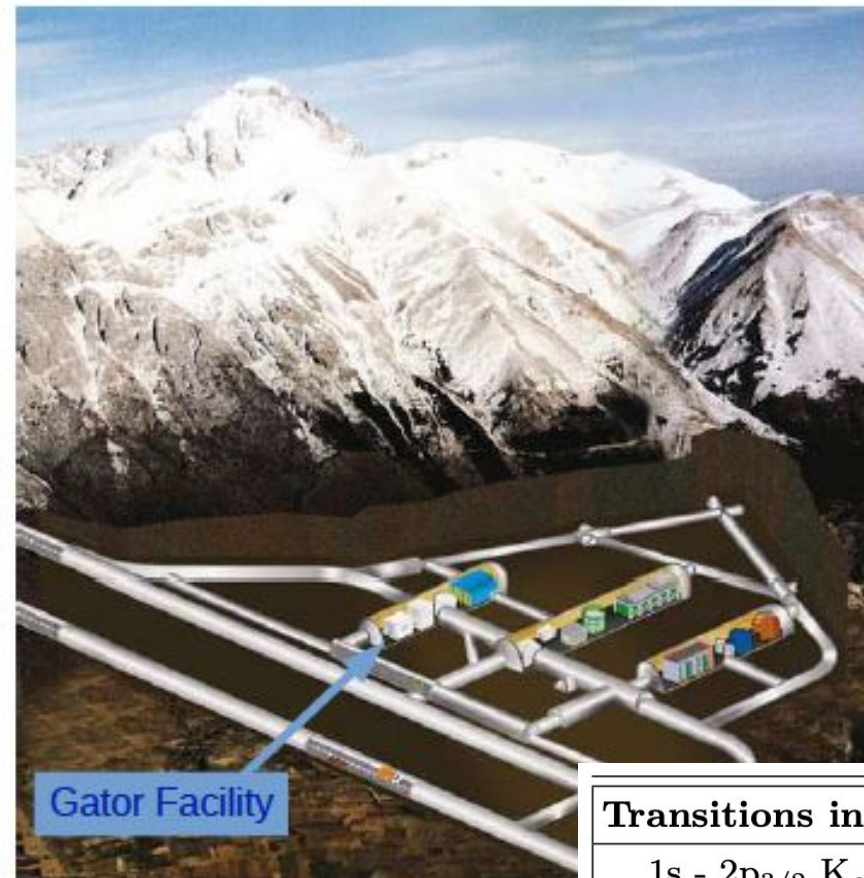
Gator Facility

Transitions in Pb	allow. (keV)	forb. (keV)
1s - 2p$_{3/2}$ K$_{\alpha 1}$	74.961	73.713
1s - 2p$_{1/2}$ K$_{\alpha 2}$	72.798	71.652
1s - 3p$_{3/2}$ K$_{\beta 1}$	84.939	83.856
1s - 4p$_{1/2(3/2)}$ K$_{\beta 2}$	87.320	86.418
1s - 3p$_{1/2}$ K$_{\beta 3}$	84.450	83.385

- measurement of $\beta^2/2$ in Pb (Z = 82) respecting MG superselection, at energies not accessible with SDD detectors

- implications of the measurement for CPT deformation induced PEP violation & for the generalized Collapse Models (dissipative and non-Markovian), in which the expected spontaneous radiation rate critically depends on the charged emitters configuration (cancellation effects), are under study.

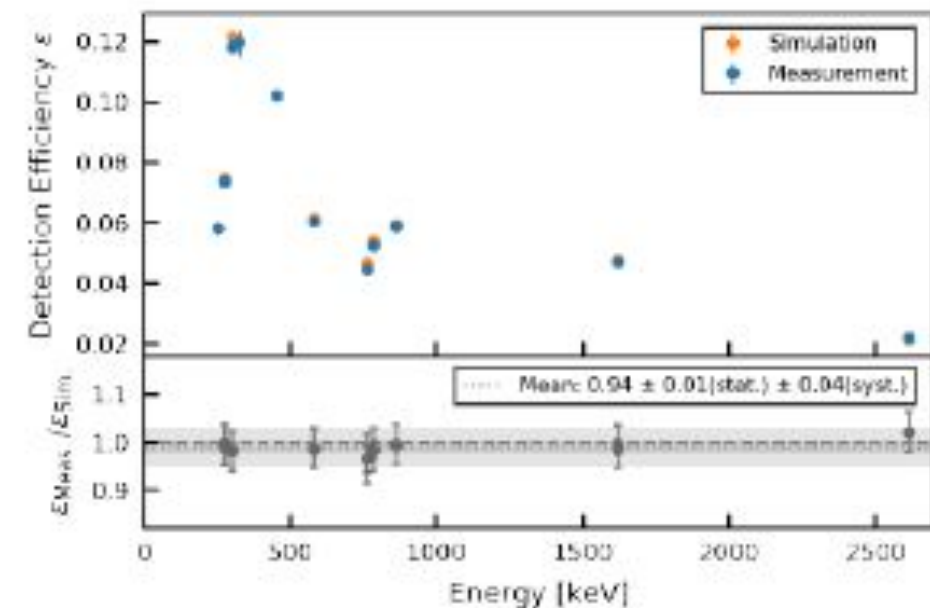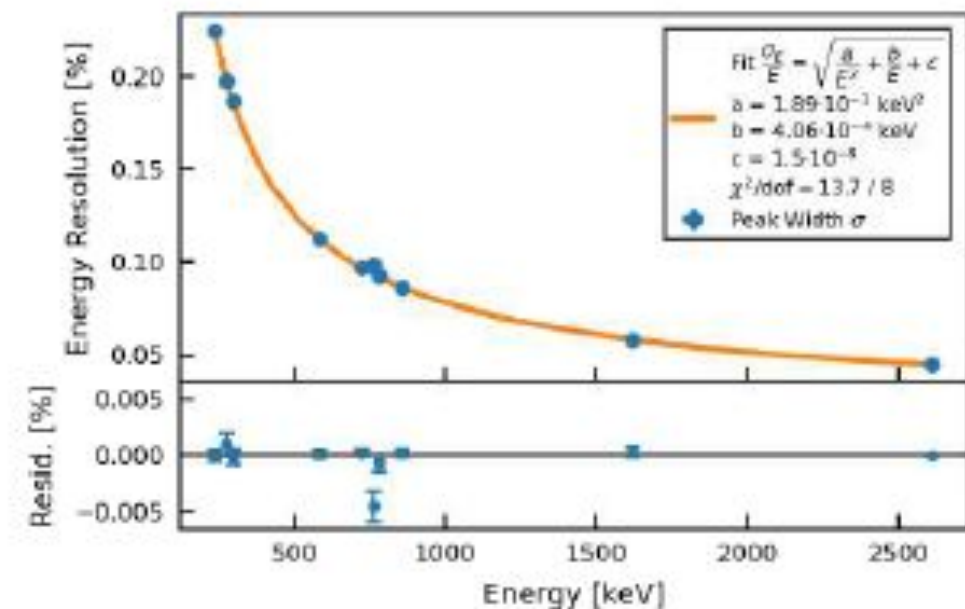# GATOR detector cooling & shielding

The Gator Detector
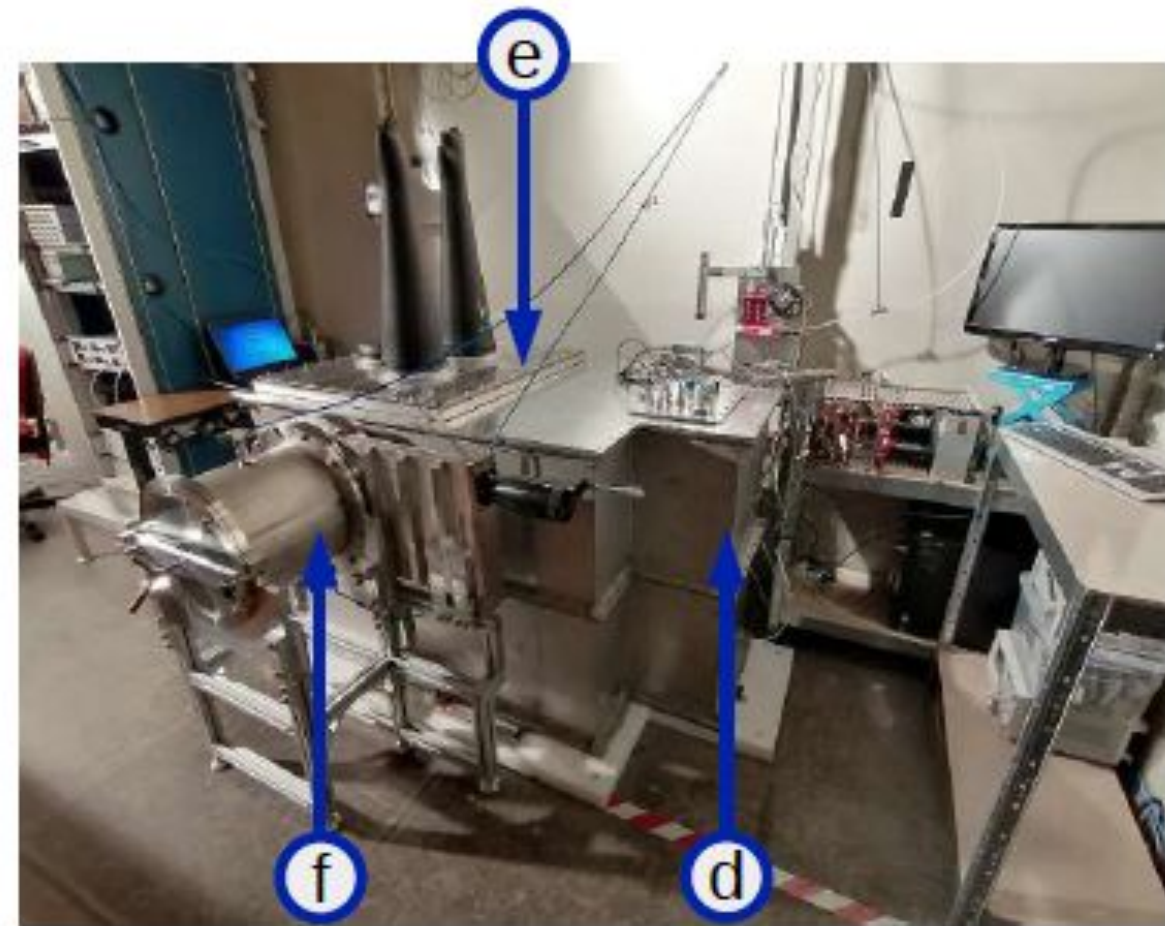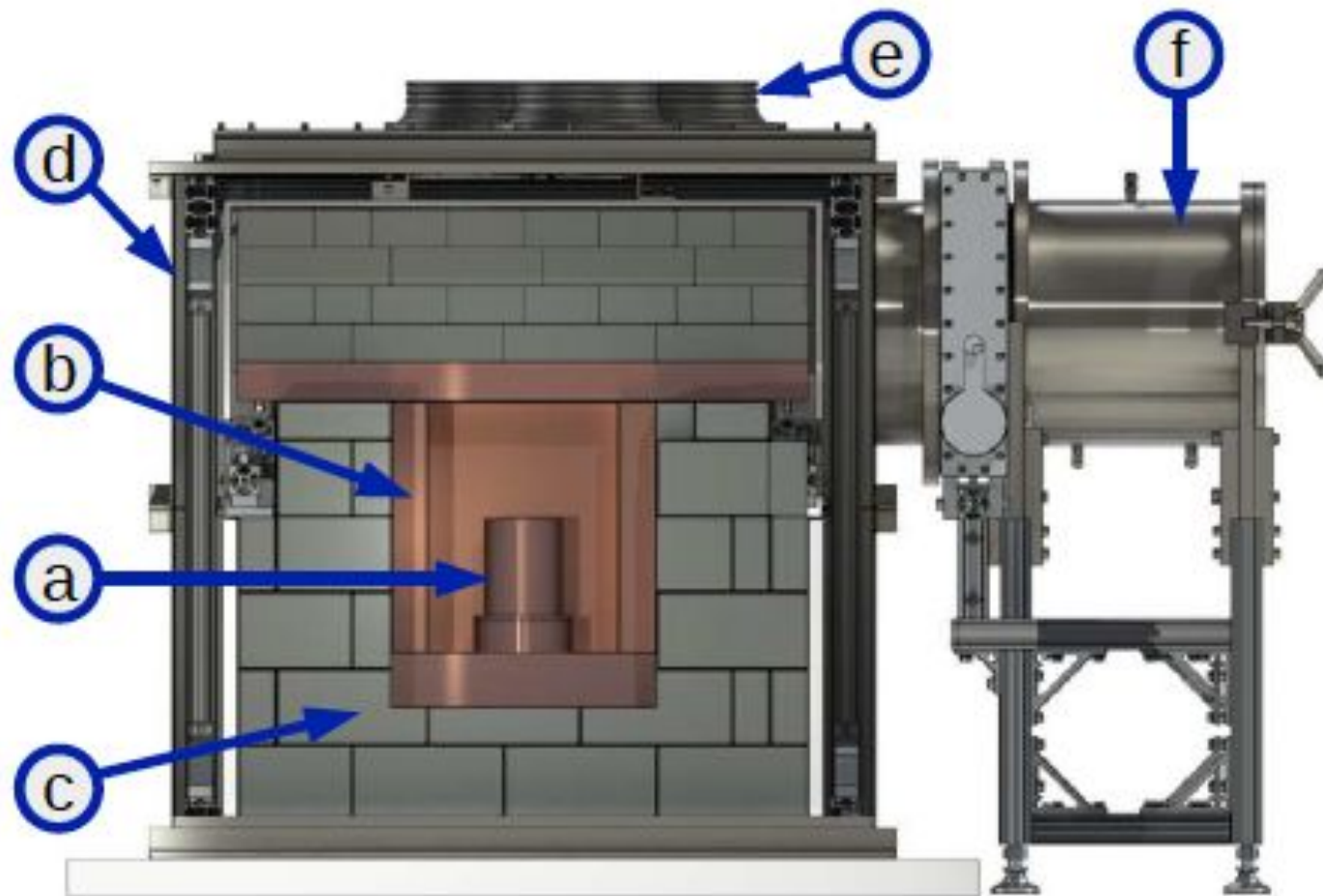
(a) HPGe detector inside Cu-OFE cryostat (cooled with LN_2 via copper coldfinger), (b) OFHC Cu cavity, (c) lead shield, polyethylene sheet, (d) airtight stainless steel enclosure (purged with GN_2), (e) glove ports, (f) sample load lock

Energy Range and Resolution

- Covered MCA energy range: approx. 10 − 2700 keV

- Analysis range: approx. 35 − 2700 keV (noise-dominated for E ≲ 35 keV)

- Regular calibrations of the detector with radioactive sources (e.g. ^{228}Th) or high-activity samples

  - FWHM at 74.96 keV (1s−2p$_{3/2}$ K$_{\alpha 1}$ transition in Pb): ~ 1.1 keV

  - Verification of simulated efficiencies and consistent activities related lines

GATOR detector + environmental bkg

- Main contributions:
  - detector & shielding materials
  - environmental radon

- Integrated background rate in the energy region
  - 65-90 keV: (4.4 ± 0.3) d^{-1}kg^{-1}
  - 100-2700 keV: (82.0 ± 0.7) d^{-1}kg^{-1}

- Temporally stable within runs (χ^2/ndf ≈ 1)
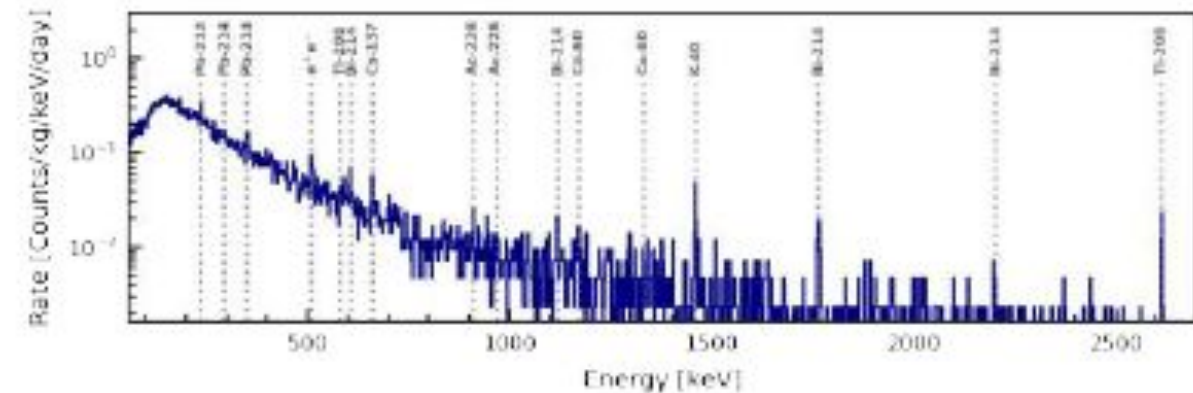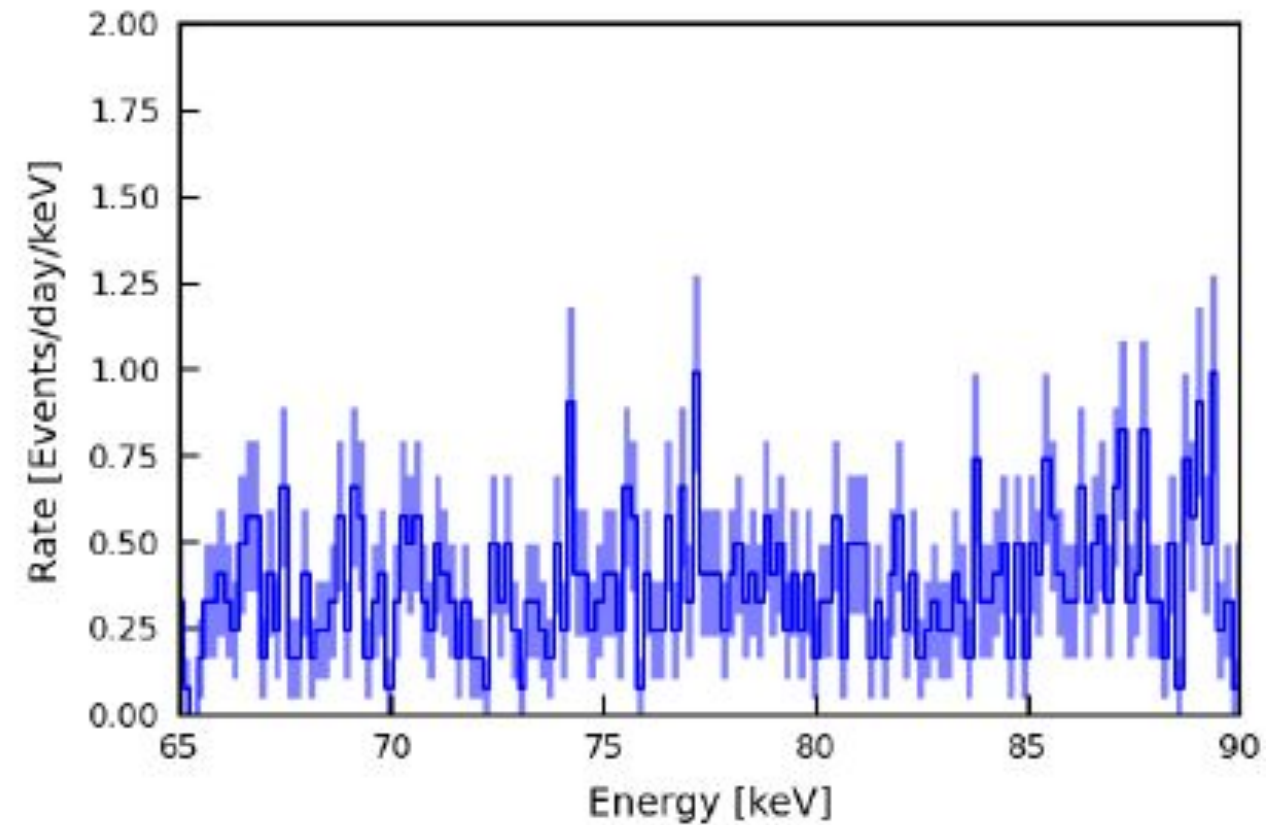
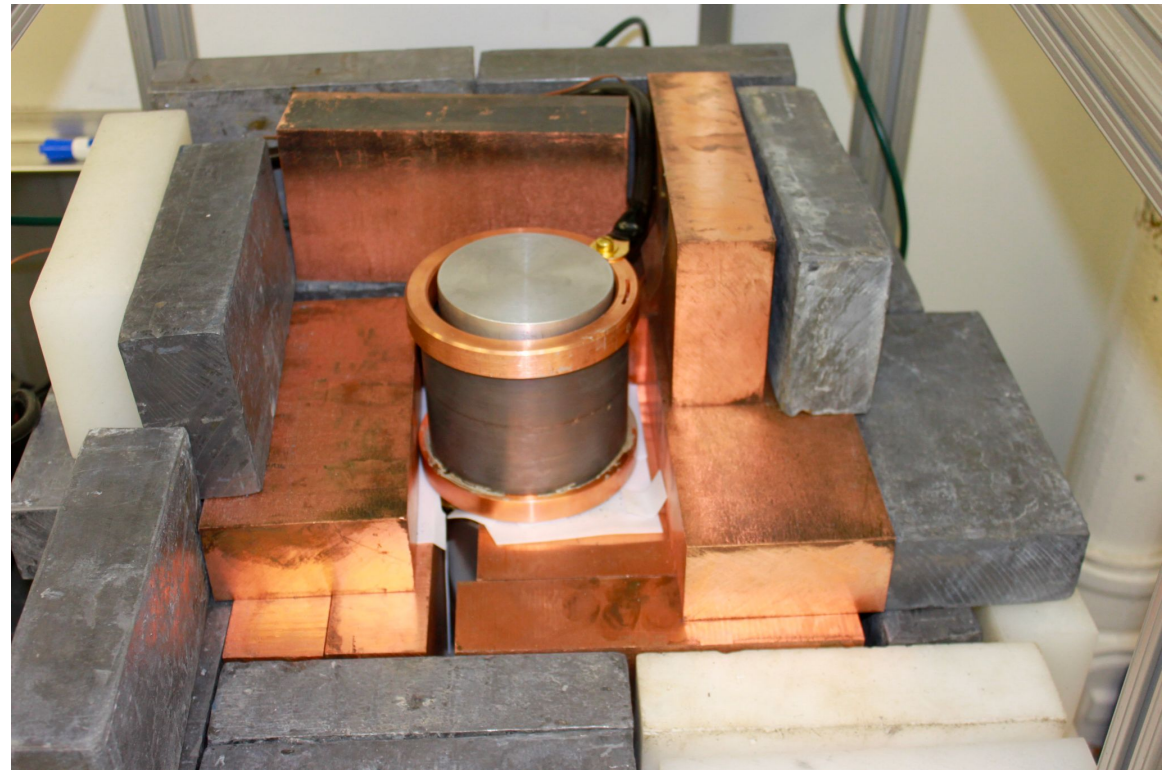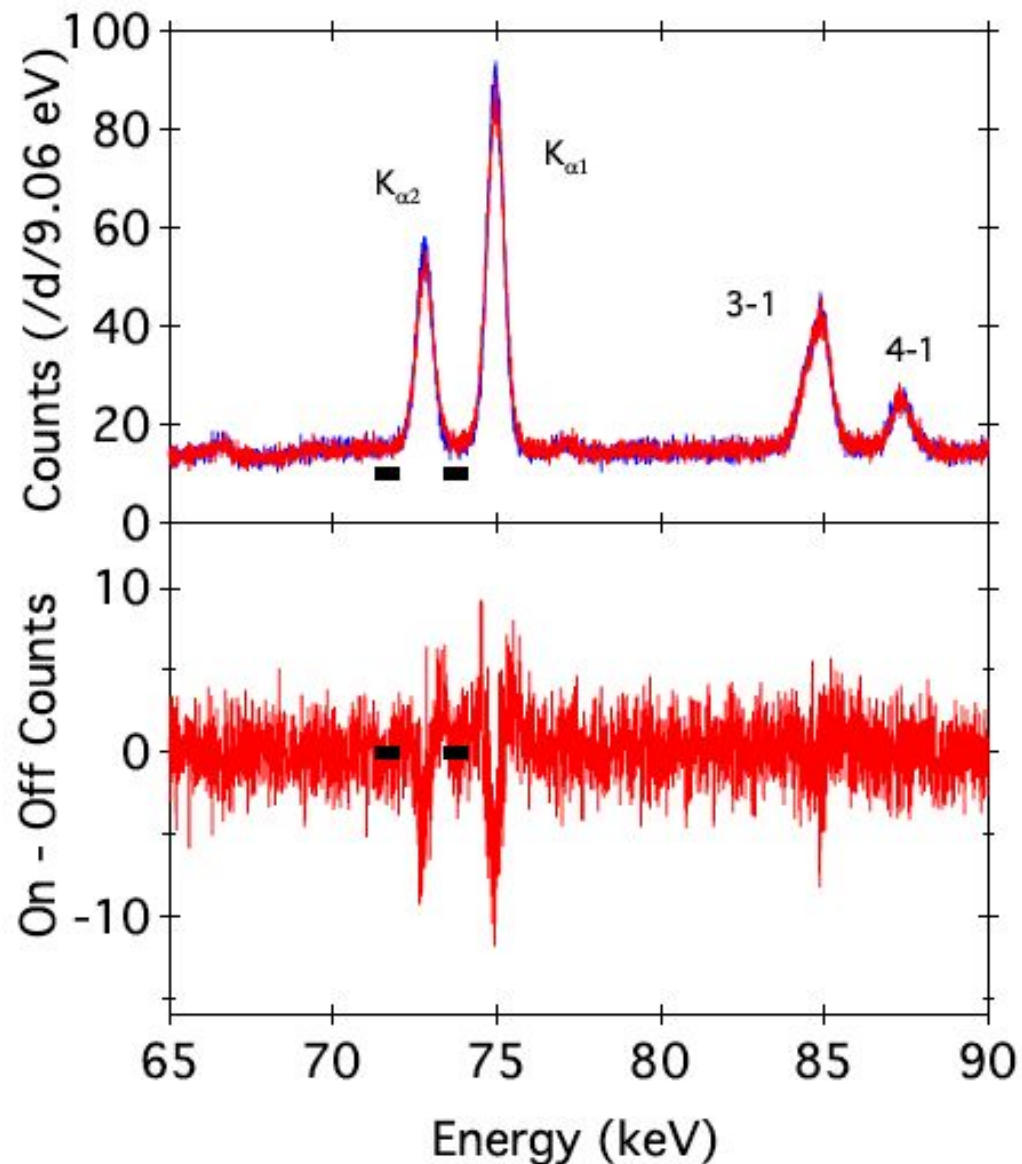**test measurement** in preparation **to be performed within 2022 for**:

- **background determination with Pb target**
- **low-energy calibration optimization**

Exploratory measurement performed above ground

- **point-contact Ge detector**
- **Pb target**
- **110 A circulating current**

obtained limit:
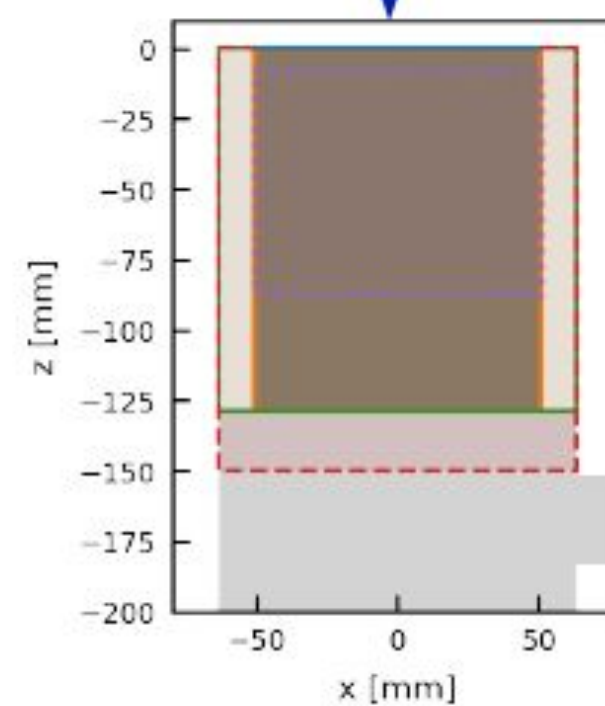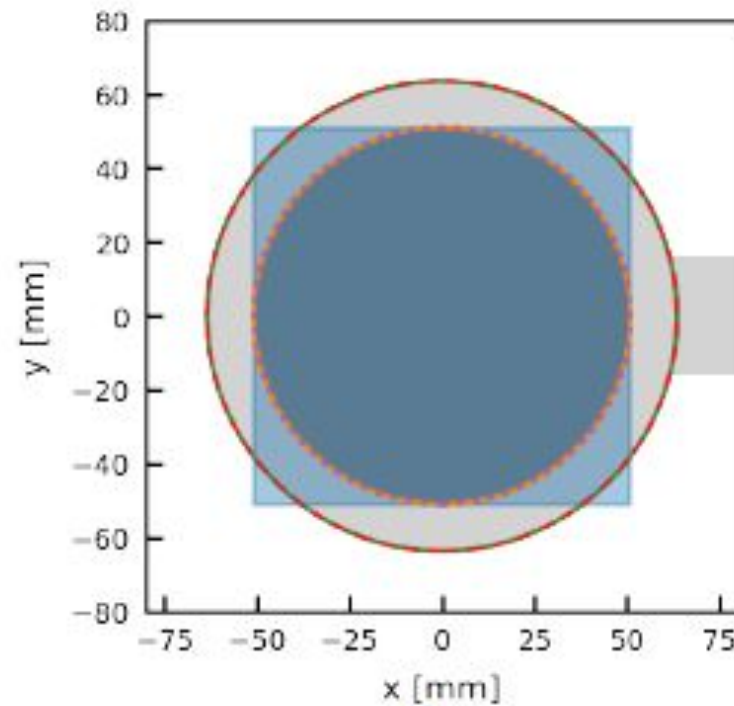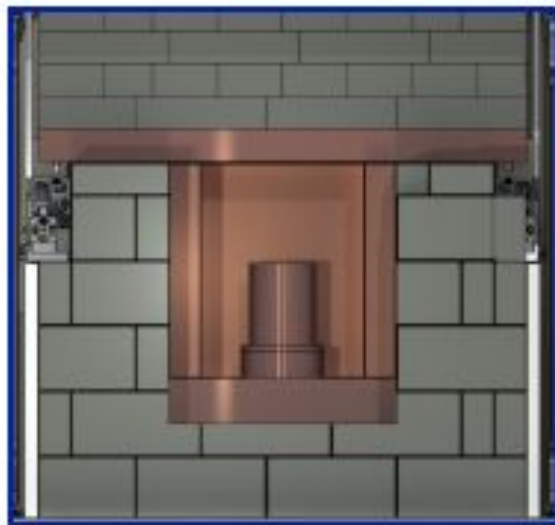
$$\beta^2/2 < 1.5 \cdot 10^{-27}$$

expected improvement from the

VIP - GATOR collaboration

dedicated measurement 2 o.m. at least

MC simulations
for the optimization of the target geometry

Investigated Geometries Pb Conductor

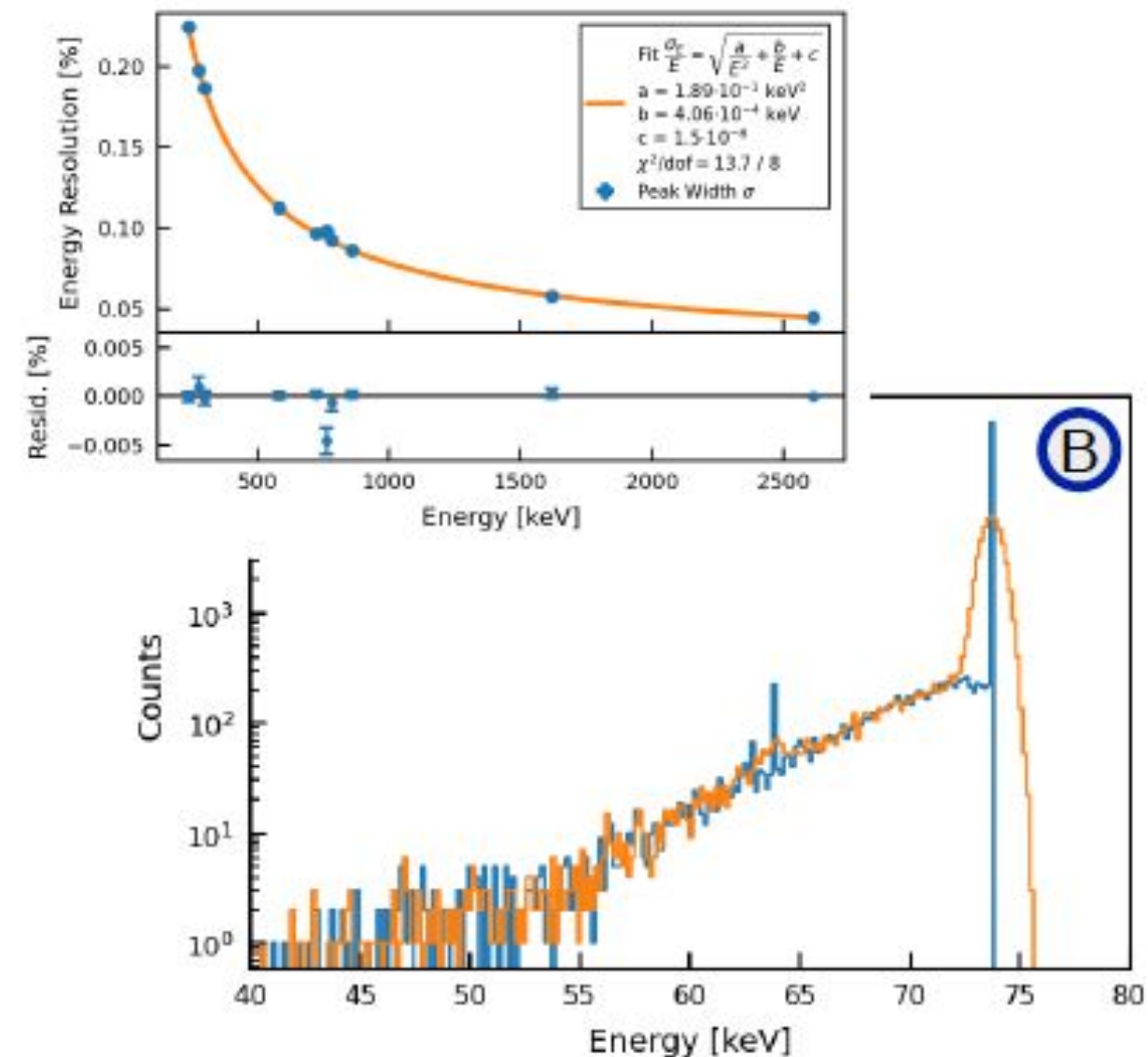## Geant4 Simulations

- Geant4 simulations with framework for sample efficiency simulations*

- Number of simulated gammas: $10^7 - 10^8$ (depending on thickness)

- Gamma energy: 73.713 keV (energy of PEP violating Pb $K_{\alpha 1}$)

- Reduced length (0.1 μm) and energy (250 eV) cuts in *PhysicsList*
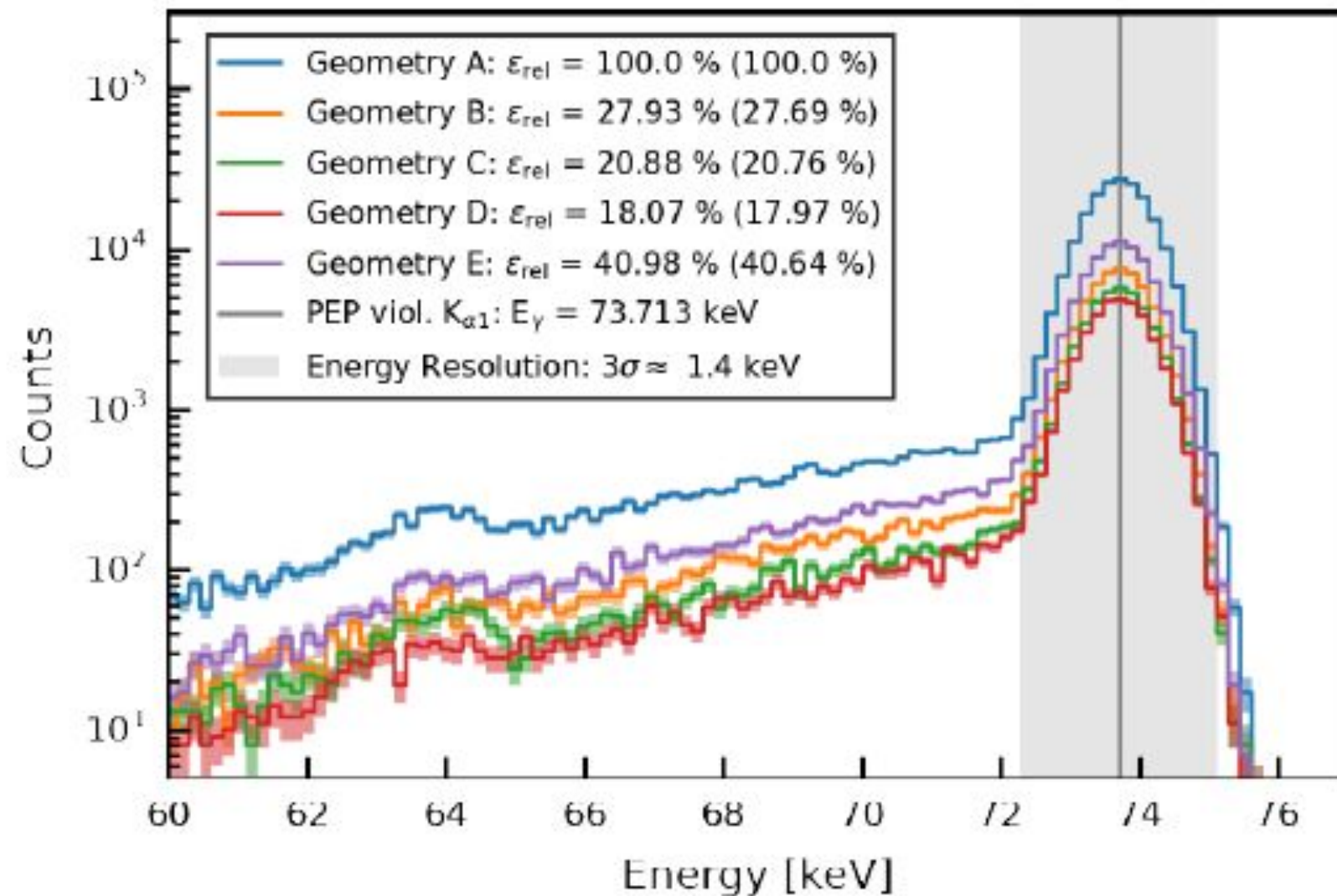
- Energy-resolution smearing, binning according to Gator MCA

Impact Geometry (Thickness 25µm)

- Detection efficiency:

  Counts in $E_\gamma \pm 3\sigma$ /
  Total simulated γs

- Gross counts; in brackets
 net counts, i.e. Compton
  subtracted ($\pm$ [3σ, 6σ])

- Plate on top (A) highest
  detection efficiency,
  cylinder along sens. volume
  (E) factor ~2.5 lower

Legend:
- Geometry A: ε_{rel} = 100.0 % (100.0 %)
- Geometry B: ε_{rel} = 27.93 % (27.69 %)
- Geometry C: ε_{rel} = 20.88 % (20.76 %)
- Geometry D: ε_{rel} = 18.07 % (17.97 %)
- Geometry E: ε_{rel} = 40.98 % (40.64 %)
- PEP viol. $K_{\alpha 1}$: E_γ = 73.713 keV
- Energy Resolution: $3\sigma \approx$ 1.4 keV

Figure of Merit for Geometry

- For same current density j, the integral charge q and hence the number of eventual X-rays scales with the volume

  → Scale efficiencies for given thickness (here 25 µm) with conductor area facing the detector for figure or merit

- Maximum deviation FOM ~ 10 %
  → Select most convenient geometry*

- Other impacts from geometry, e.g. induced B-field, resistance ($R \sim L/A$), and power dissipation resulting in heat-up, weight / required holder,… need to be considered as well
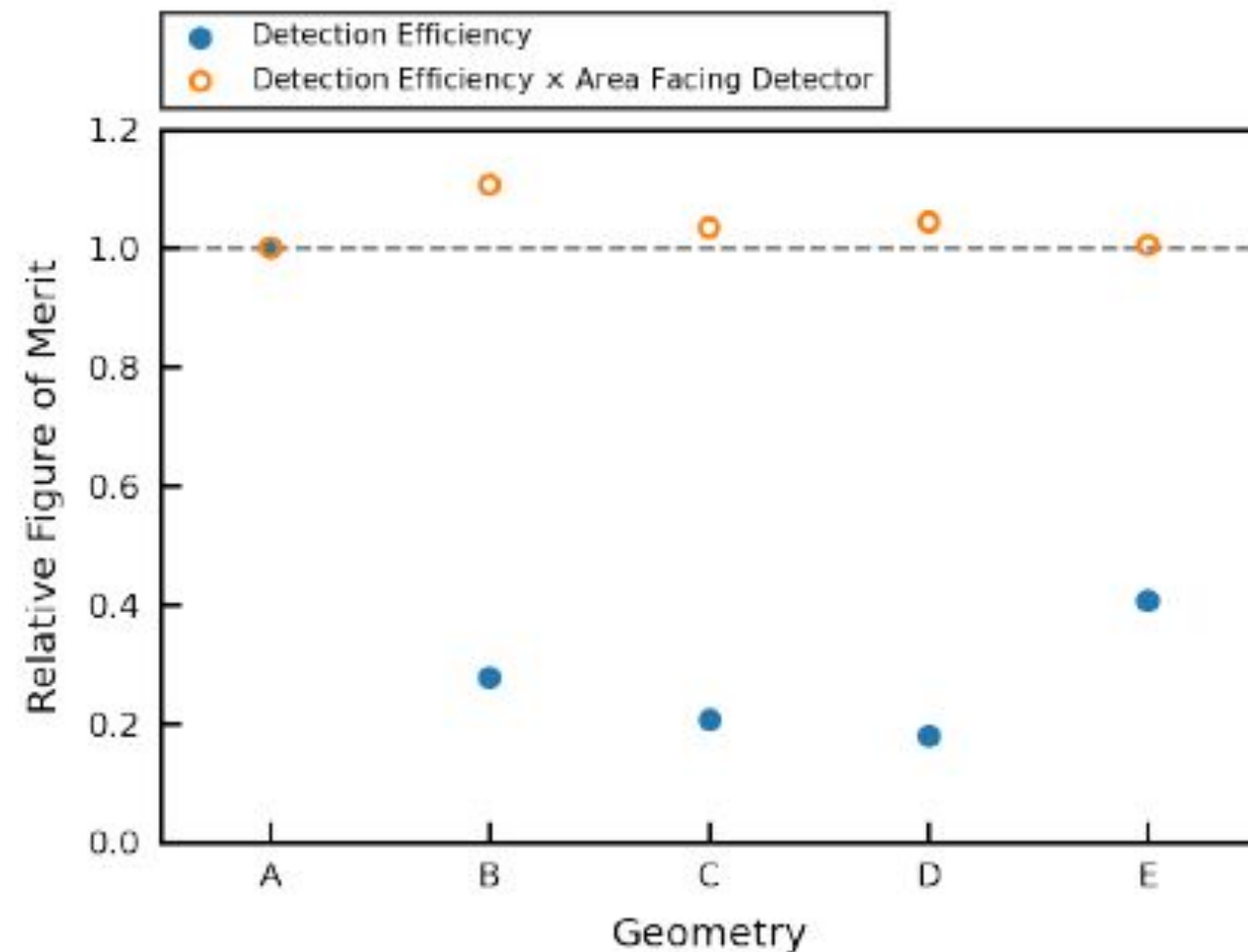
Detection efficiency simulation

Impact Thickness (Cylindrical Geometry D)
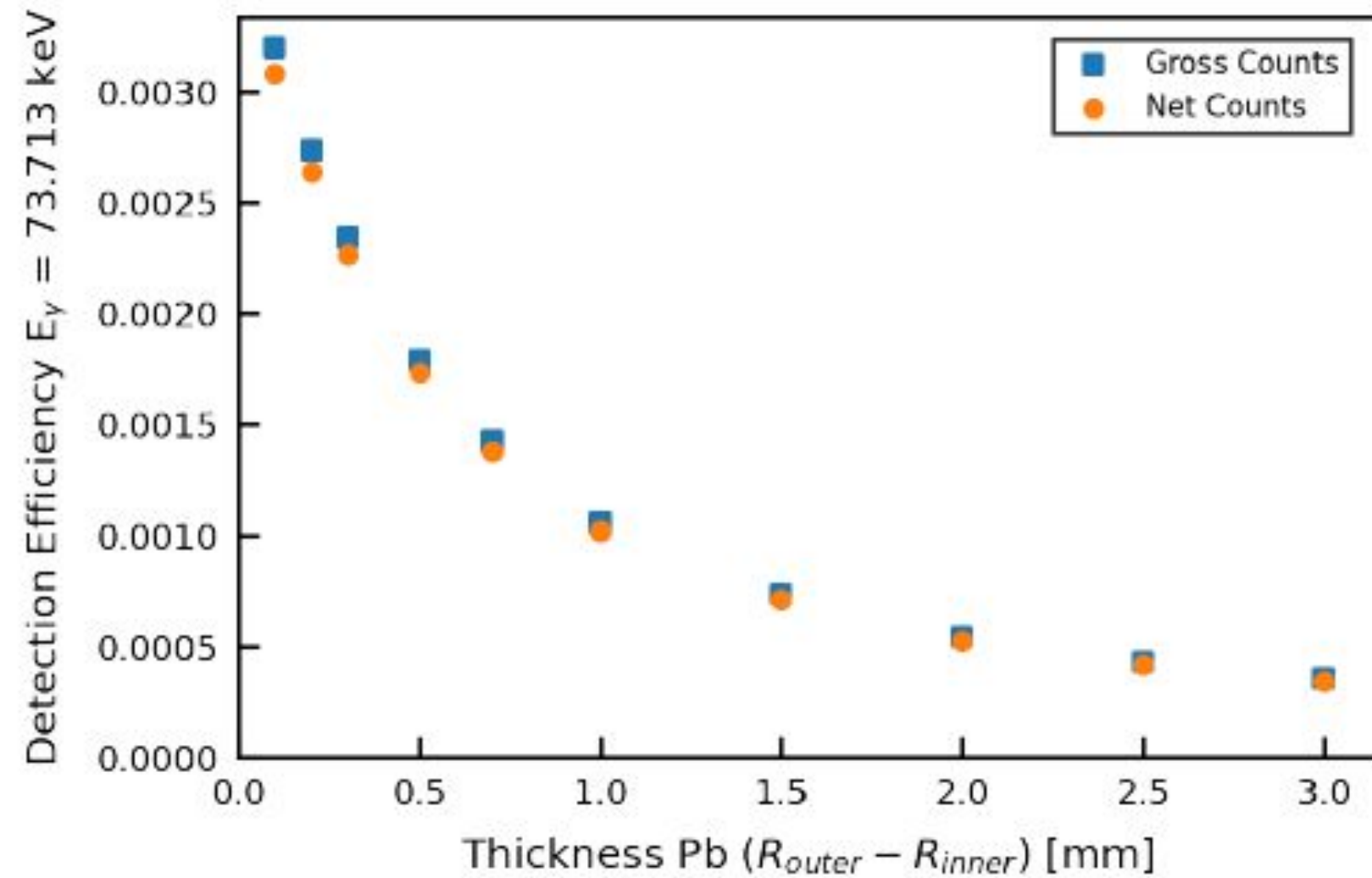
preliminary simulations of power dissipation

- Challenge: Power dissipation from current will result in heat-up

- Assuming homogeneous conductivity:

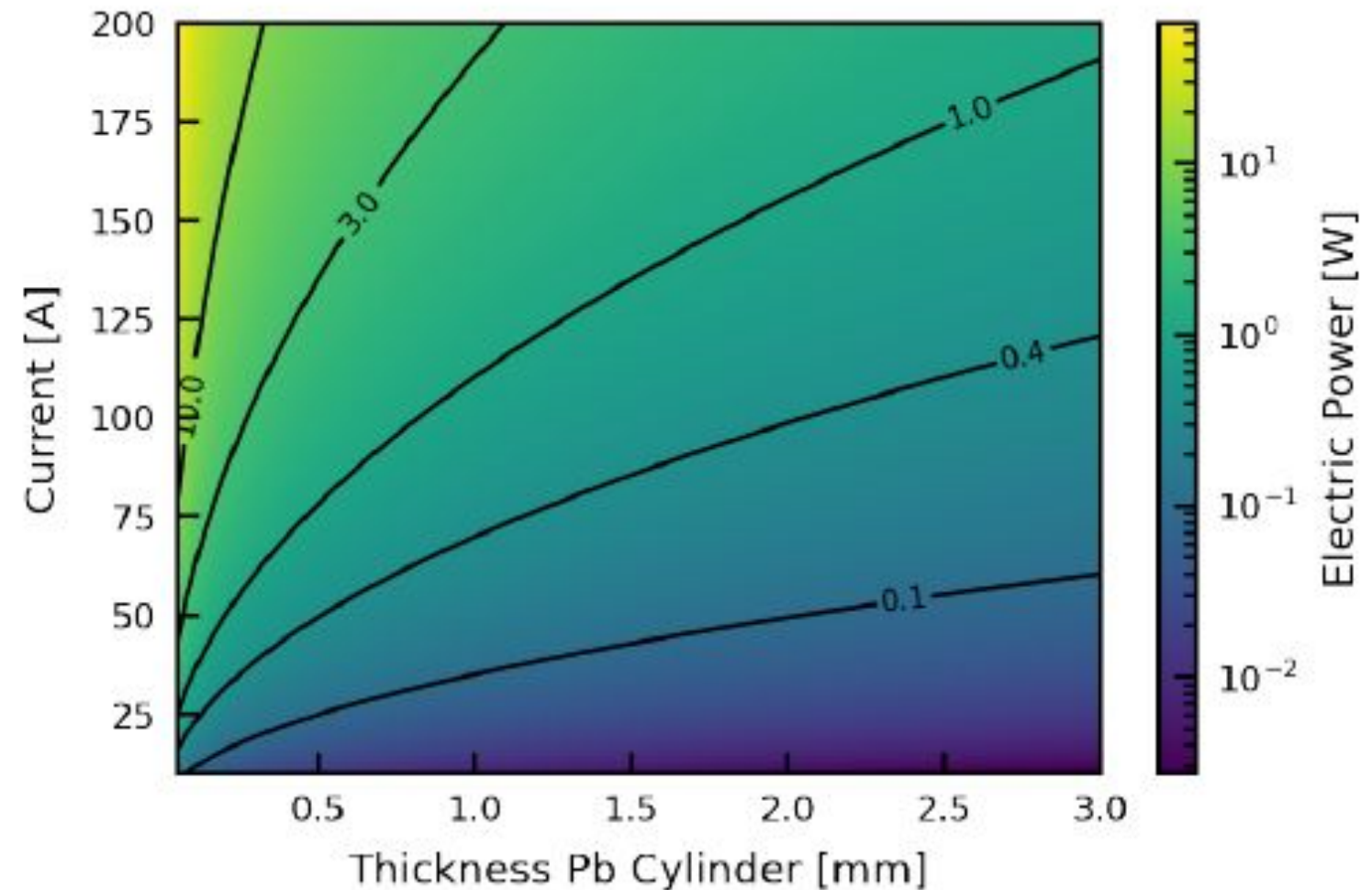$$P = R \cdot I^2 = \frac{\rho \cdot l}{A} \cdot I^2$$

$$\rho_{Pb}(T = 20\,°C) = 2.2 \cdot 10^{-7}\,\Omega m \ ^*$$

- For cylindrical geometry D:

$$l = 0.15\,m$$
$$A \approx 2\pi \cdot r_{inner} \cdot d$$
$$\approx 0.4\,m \cdot d$$

for current along cylinder axis, results in previous meeting for assumption of circular current

with I = 400 A **expected improvement** w.r. to *Found.Phys.* 42 (2012) 1015-1030

on $\beta^2/2$ of a **factor at least 10^2**

target cooling system "VIP-like" (chiller) needed to counteract heating.
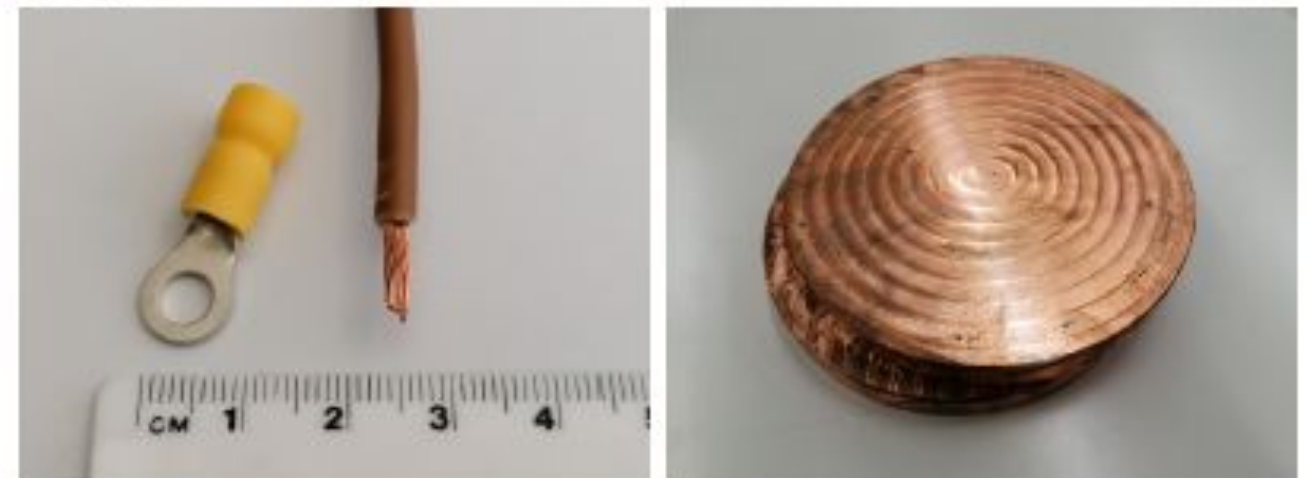
Test measurement 2022

Preparation of a test setup is ongoing for a 2 months test measurement within 2022 for:

- **background determination**
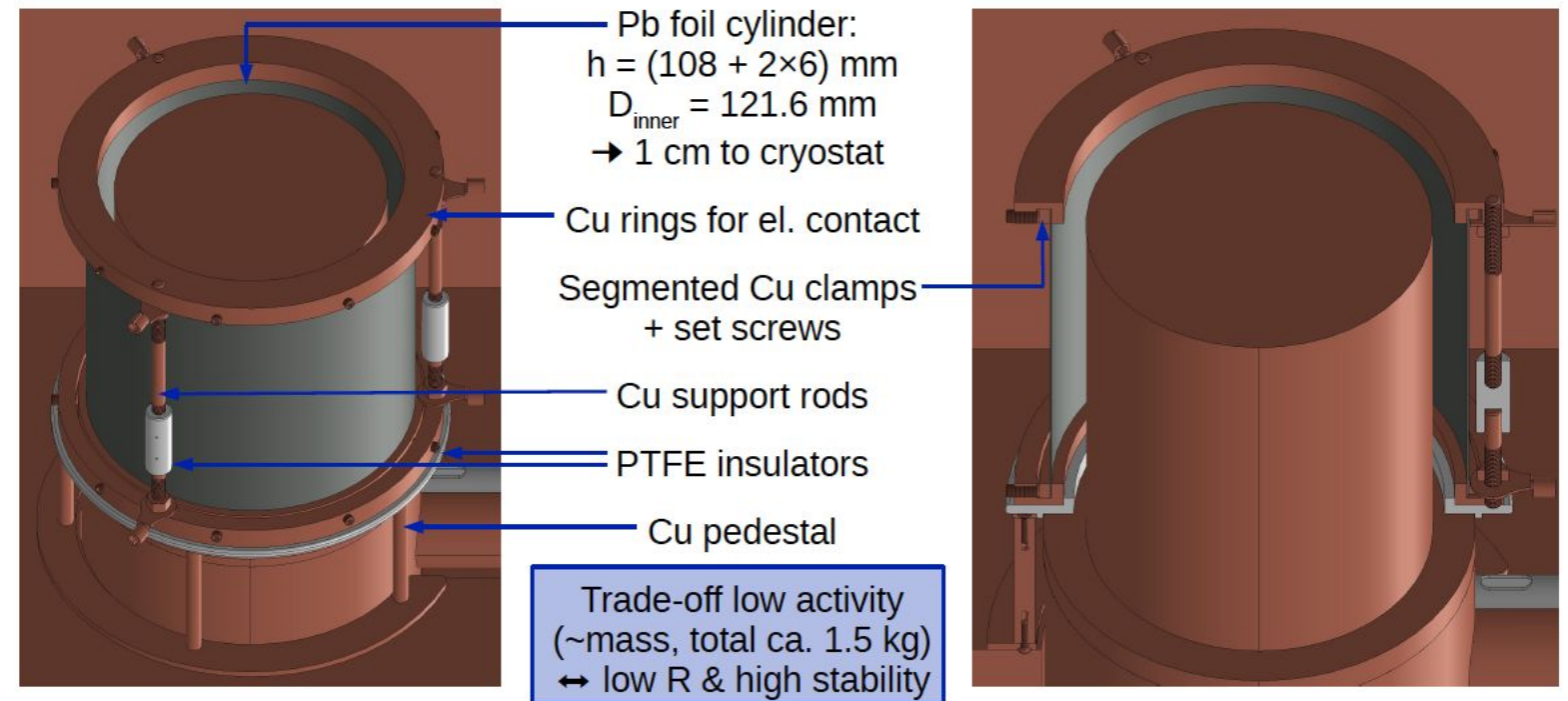- **low-energy calibration optimization**

Next steps:

- **estimation heat-up under various environments**
- **test different cabling + connectors, design of multiple cables system for minimal power dissipation at maximal flexibility with high current**

Design of HPGe + target cylindrical geometry

Pb foil cylinder:
$h = (108 + 2 \times 6)$ mm
$D_{inner} = 121.6$ mm
→ 1 cm to cryostat

Cu rings for el. contact

Segmented Cu clamps
+ set screws

Cu support rods

PTFE insulators

Cu pedestal

Trade-off low activity
(~mass, total ca. 1.5 kg)
↔ low R & high stability

large contribution to power dissipation from cables due to reduced space between shielding and cryostat cold finger -> water cooling system needed
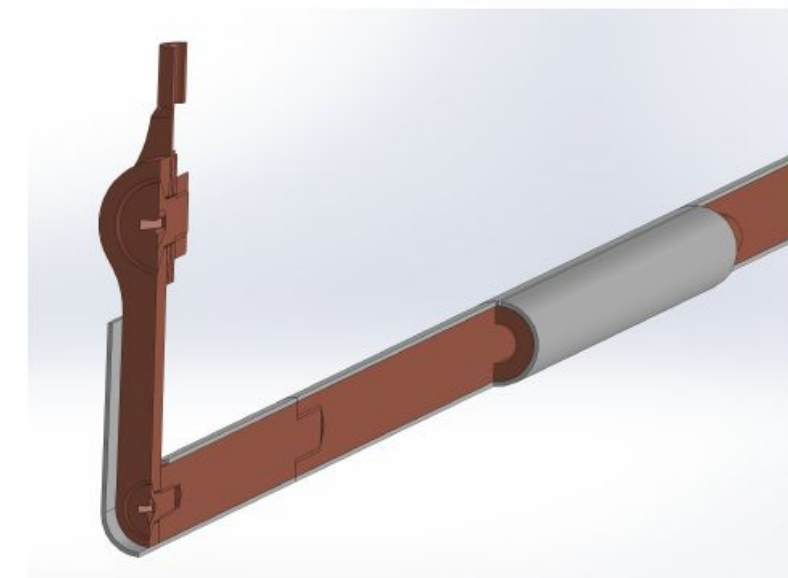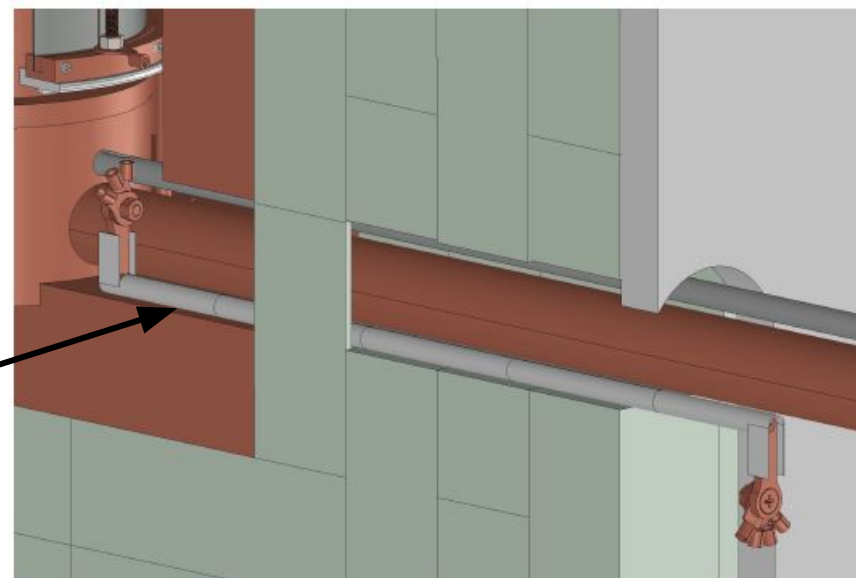
- **design of feed-through flange ongoing**
- **design of cabling-connectors ongoing**
- **design of the target cooling system ongoing**

VIP-2 Closed systems results

PEP violation in quantum gravity

Quantum gravity models can embed PEP violating transitions

**PEP is a consequence of the spin statistics theorem based on:
Lorentz/Poincaré and CPT symmetries; locality; unitarity and causality. Deeply related to the very same nature of space and time**

$\downarrow$

Non-commutativity of space-time is common to several quantum gravity frameworks (e.g. *k*-Poincarè, θ-Poincarè)

$\downarrow$

non-commutativity induces a deformation of the Lorentz symmetry and of the locality → naturally encodes the violation of PEP not constrained by MG

**PEP violation is suppressed with δ^2 (*E*, Λ)
E is the characteristic transition energy, Λ is the scale of the space-time non-commutativity emergence.**

A. P. Balachandran, G. Mangano, A. Pinzul and S. Vaidya, Int. J. Mod. Phys. A 21 (2006) 3111

A.P. Balachandran, T.R. Govindarajan, G. Mangano, A. Pinzul, B.A. Qureshi and S. Vaidya, Phys. Rev. D 75 (2007)

A. Addazi, P. Belli, R. Bernabei and A. Marciano, Chin. Phys. C 42 (2018) no.9

testing PEP violation in quantum gravity

Theoretical prediction *Int.J.Mod.Phys.A* 35 (2020) 32, 2042003

specific calculation of atomic levels transitions probabilities for θ-Poincaré

$$W \simeq W_0 \phi_{PEPV}\,, \qquad \phi_{\mathrm{PEPV}} = \delta^2 \simeq \frac{D}{2}\frac{E_N}{\Lambda}\frac{\Delta E}{\Lambda} \qquad \phi_{\mathrm{PEPV}} = \delta^2 \simeq \frac{C}{2}\frac{\bar{E}_1}{\Lambda}\frac{\bar{E}_2}{\Lambda}$$

for non-vanishing (vanishing) electric like components of the θμν tensor.

Connection with quon algebra (in the case of quon fields however the q factor does not show any energy dependence):

$$q(E) = -1 + 2\delta^2(E)$$

An experimental bound on the probability that PEP may be violated in atomic transition processes, straightforwardly translates into a bound on the new physics scale Λ, consistently with the choice of the θ0i components.

Experimental Setup

High purity Ge detector measurement:

- high purity co-axial p-type germanium detector (HPGe),
  diameter of 8.0 cm, length of 8.0 cm, surrounded by an inactive layer of
  lithium-doped germanium of 0.075 mm.
- The target material is composed of three cylindrical sections of radio-pure
  Roman lead, completely surrounding the detector.
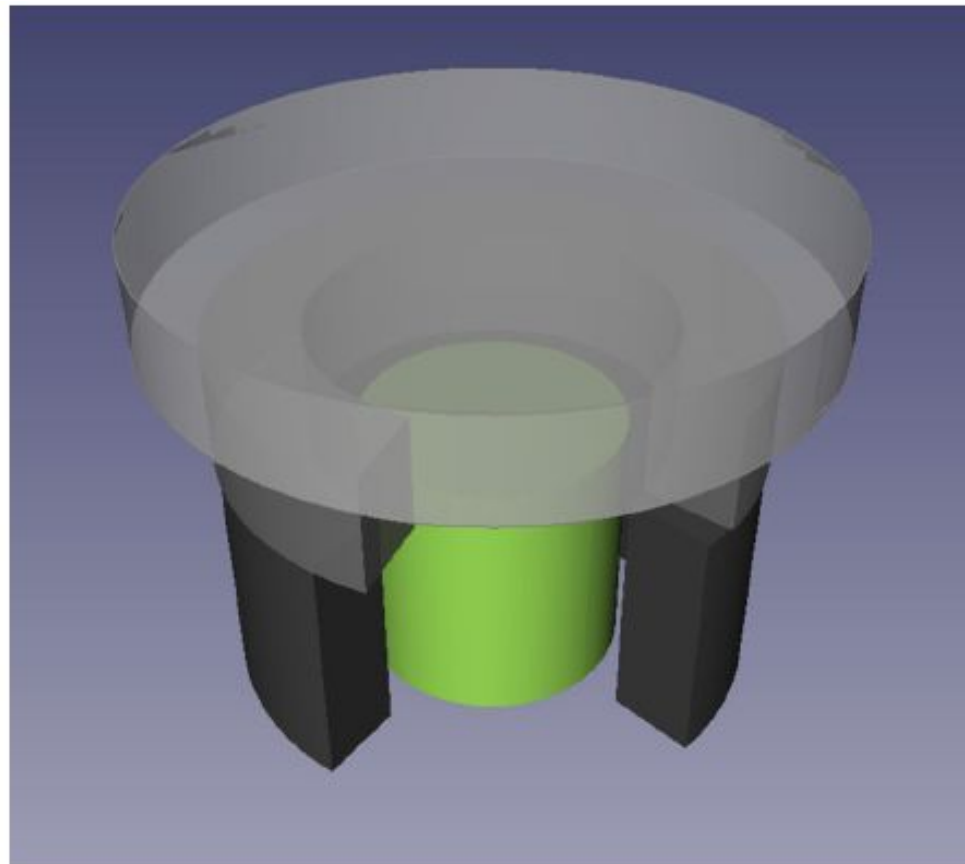
Fig. 1 Schematic representation of the Ge crystal (in green) and the
surrounding lead target cylindrical sections (in grey)

Experimental Setup

- Passive shielding: inner - electrolytic copper, outer - lead

- 10B-polyethylene plates reduce the neutron flux towards the detector

- shield + cryostat enclosed in air tight steel housing flushed with nitrogen to avoid contact with external air (and thus radon).
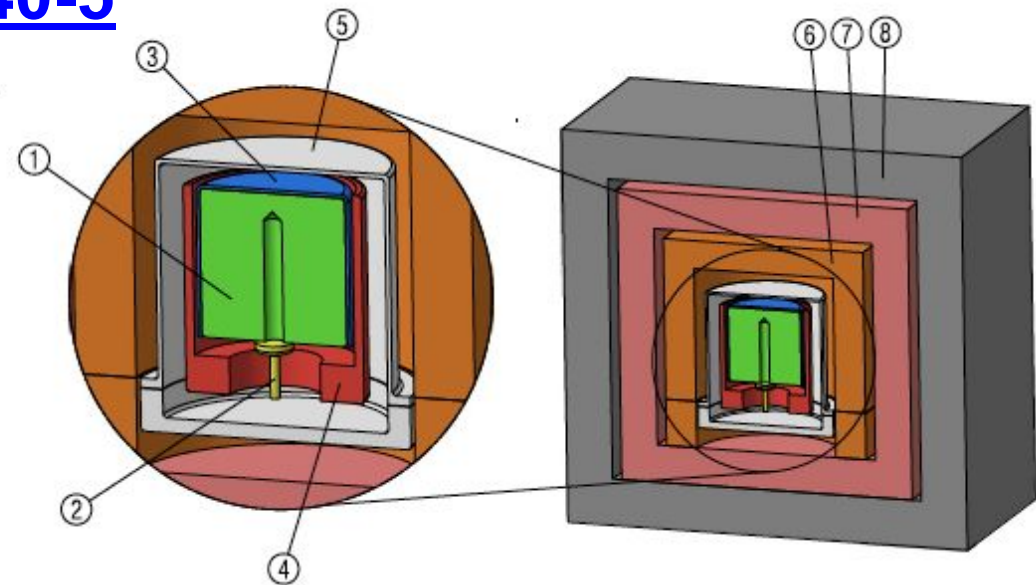
K. Piscicchia et al., Eur. Phys. J. C (2020) 80: 508
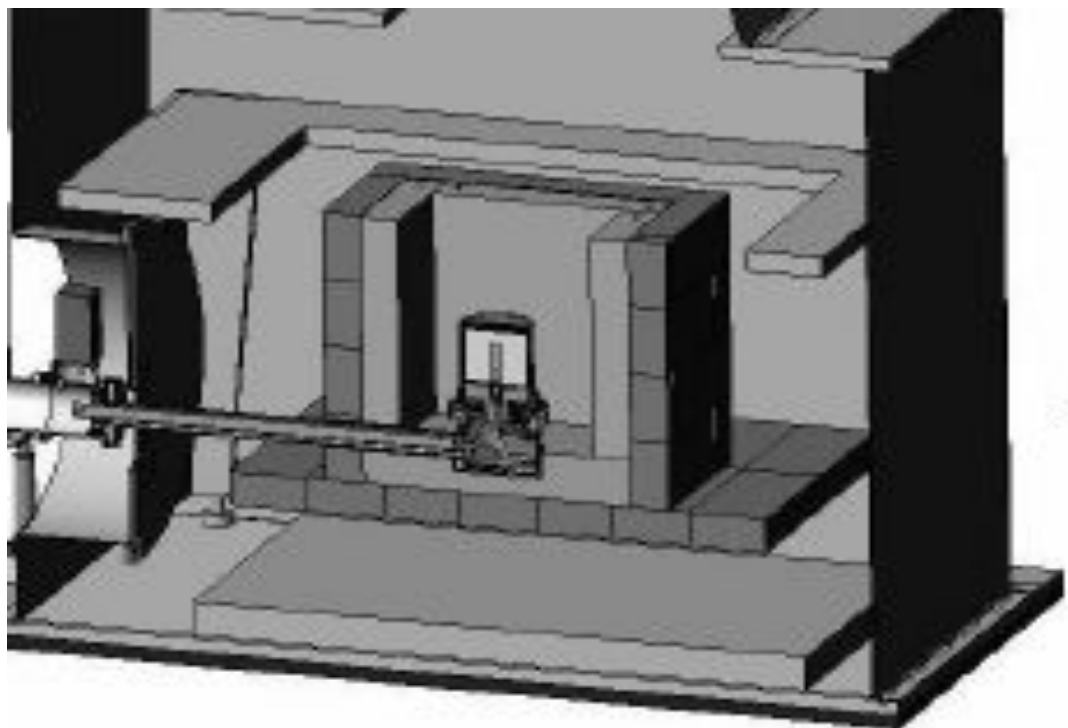https://doi.org/10.1140/epjc/s10052-020-8040-5

Figure 1: *Schematic representation of the experimental setup: 1 - Ge crystal, 2 - Electric contact, 3 - Plastic insulator, 4 - Copper cup, 5 - Copper end-cup, 6 - Copper block and plate, 7 - Inner Copper shield, 8 - Lead shield.*

Statistical model

- The *pdf* of the expected number of total signal counts *S* given the measured distribution is:
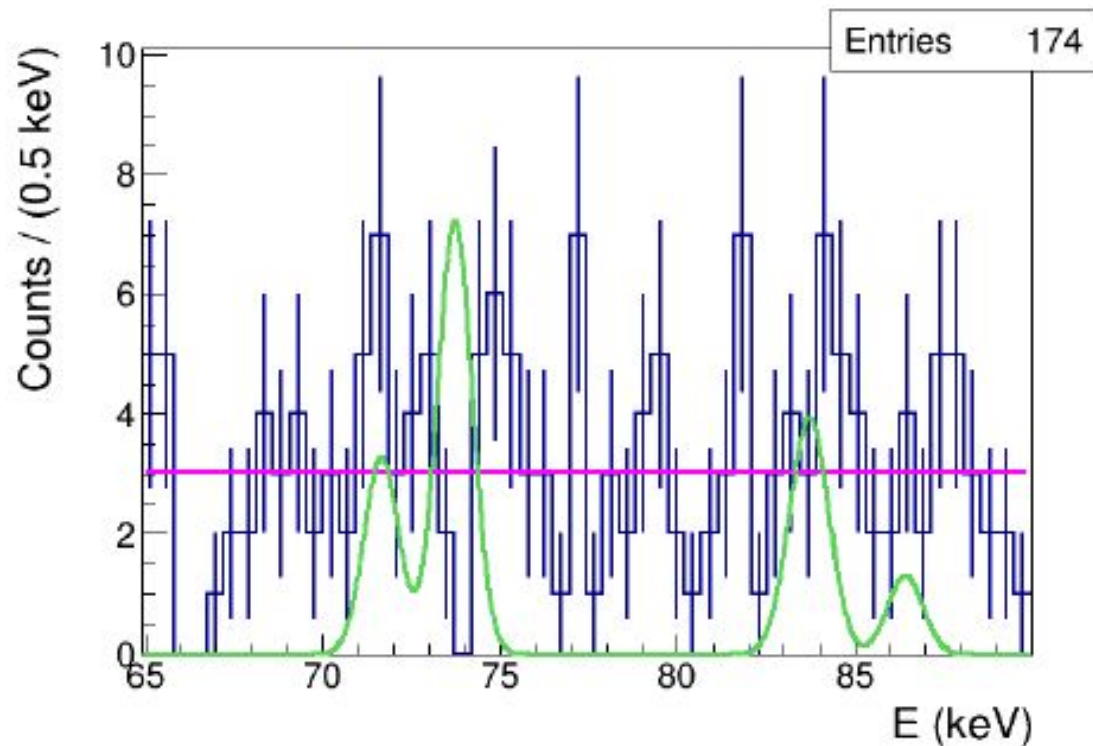
$$P(S|data) = \int_0^\infty \int_{\mathcal{D}_\mathbf{p}} P(S, B|data, \mathbf{p}) \, d^m\mathbf{p} \, dB$$

$$P(S, B|data, \mathbf{p}) =$$

$$= \frac{P(data|S, B, \mathbf{p}) \cdot f(\mathbf{p}) \cdot P_0(S) \cdot P_0(B)}{\int P(data|S, B, \mathbf{p}) \cdot f(\mathbf{p}) \cdot P_0(S) \cdot P_0(B) \, d^m\mathbf{p} \, dS \, dB}$$
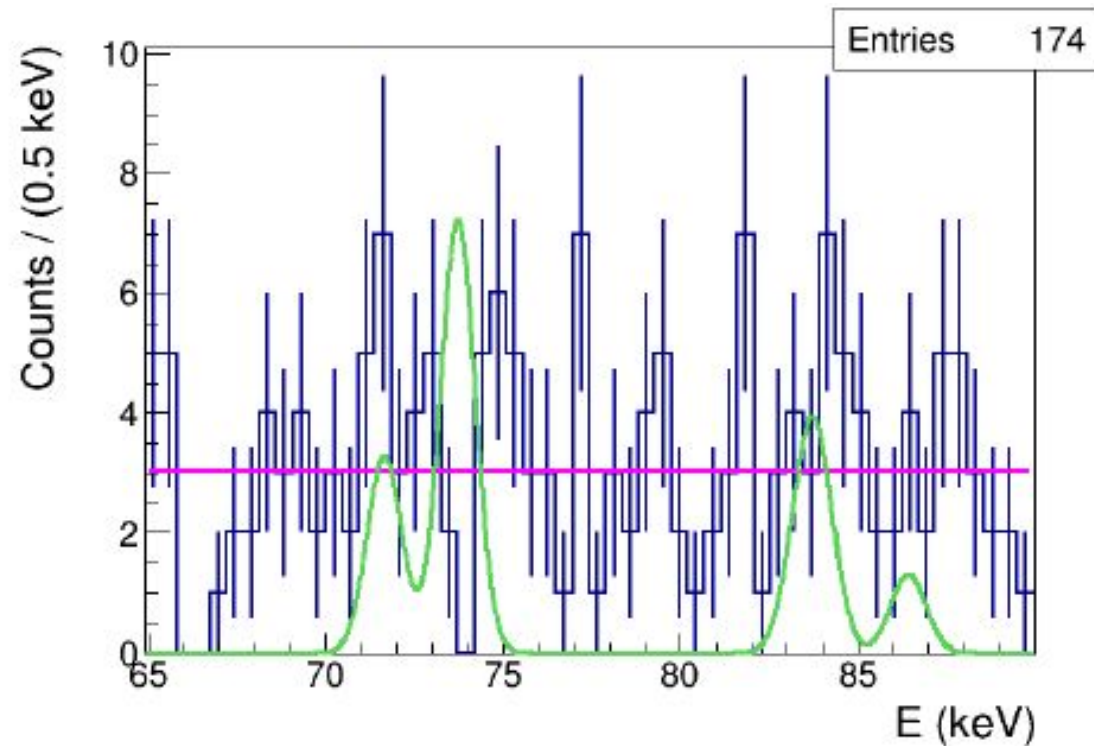

FIG. 1. The measured X-ray spectrum, in the region of the K_α and K_β standard and violating transitions in Pb, is shown in blue; the magenta line represents the fit of the background distribution. The green line corresponds to the shape of the expected signal distribution (with arbitrary normalization) for the A_3 analysis and the M_3 parametrization.

The prior for S consistent with existing limits [Found. Phys. 42, 1015-1030 (2012)].

- the likelihood is weighted on the joint *pdf* of the experimental parameters

$$P(data|S, B, \mathbf{p}) = \prod_{i=1}^{N} \frac{\lambda_i(S, B, \mathbf{p})^{n_i} e^{-\lambda_i(S, B, \mathbf{p})}}{n_i!}$$

$$\lambda_i(S, B) = B \cdot \int_{\Delta E_i} f_B(E, \alpha) \, dE +$$

$$+ S \cdot \int_{\Delta E_i} f_S(E, \sigma) \, dE = B \cdot c_{Bi} + S \cdot c_{Si}$$

Statistical model

- **First analysis which accounts for the predicted energy dependence** of the PEP violation probability. Expected rate of Kalpha1 transitions:

$$\Gamma_{K_{\alpha 1}} = \frac{\delta^2(E_{K_{\alpha 1}})}{\tau_{K_{\alpha 1}}} \cdot \frac{BR_{K_{\alpha 1}}}{BR_{K_{\alpha 1}} + BR_{K_{\alpha 2}}} \cdot 6 \cdot N_{atom} \cdot \epsilon(E_{K_{\alpha 1}}).$$

FIG. 1. The measured X-ray spectrum, in the region of the K_α and K_β standard and violating transitions in Pb, is shown in blue; the magenta line represents the fit of the background distribution. The green line corresponds to the shape of the expected signal distribution (with arbitrary normalization) for the A_3 analysis and the M_3 parametrization.

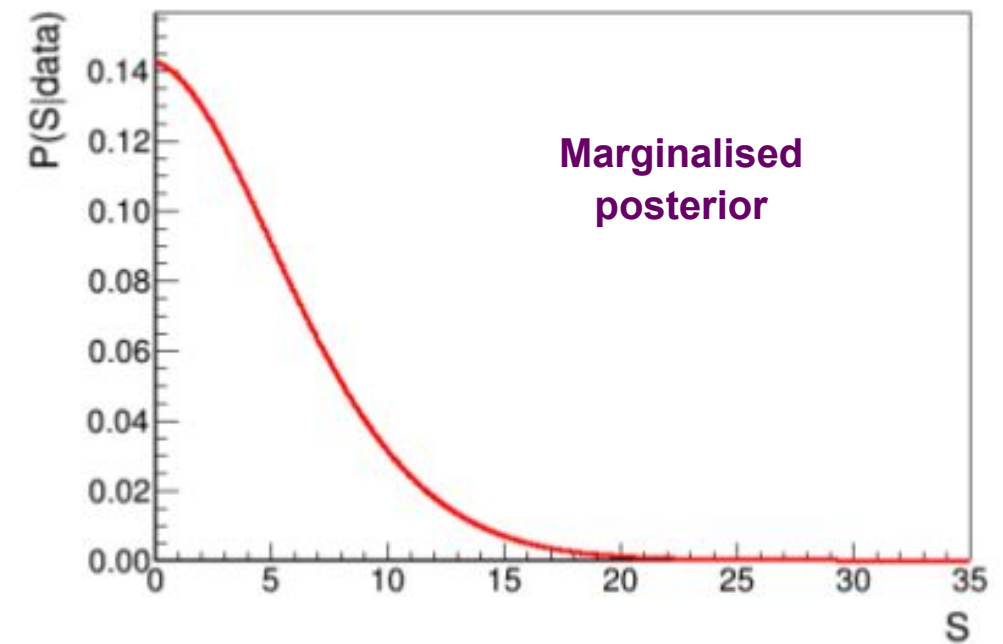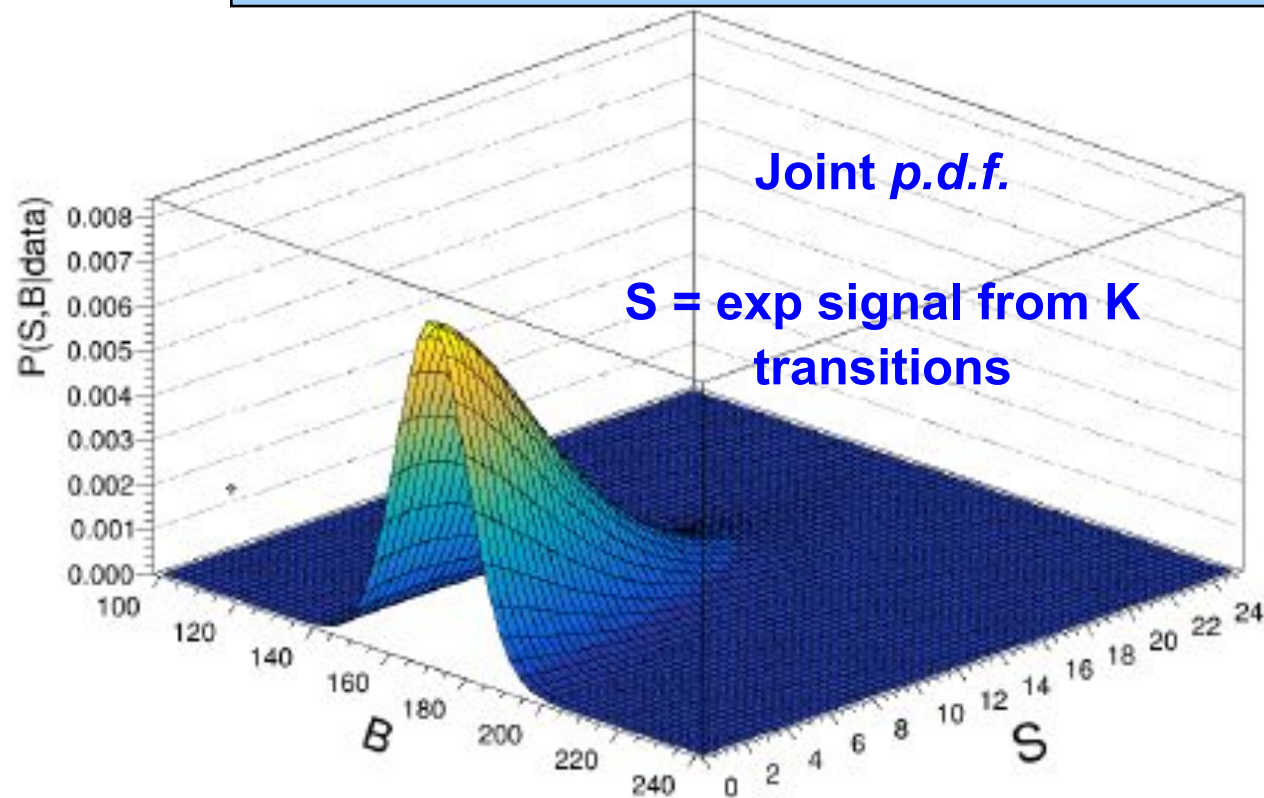- **probability to observe n transitions in the time t:**

$$P(n;t) = \frac{(\Gamma_{K_{\alpha 1}} t)^n e^{-\Gamma_{K_{\alpha 1}} t}}{n!},$$

$$f_S(E, k) = \frac{1}{N} \cdot \sum_{K=1}^{N_K} \Gamma_K \frac{1}{\sqrt{2\pi\sigma_K^2}} \cdot e^{-\frac{(E-E_K)^2}{2\sigma_K^2}}$$

- **upper limit on the non-commutativity scale:**

$$\mu = \sum_{K=1}^{N_K} \mu_K = \frac{\aleph}{\Lambda^k} < \bar{S}$$

Results

Joint *p.d.f.*

S = exp signal from K transitions

Marginalised posterior

From which an upper limit on the
non-commutativity scale is obtained (90% Probability):

θ_{0i}	$\bar{S}$	lower limit on Λ (Planck scales)
$\theta_{0i} = 0$	13.2990	$6.9 \cdot 10^{-2}$
$\theta_{0i} \neq 0$	18.1515	$2.6 \cdot 10^{2}$

accepted PRL: "Strongest atomic physics bounds on Non-Commutative Quantum Gravity Models"

Novel theoretical perspectives

New collaboration ongoing with Prof. Nick Mavromatos

exciting new scenarios -> **"**If CPT is ill-defined one may also encounter violations of the spin-statistics theorem, with possible consequences for the Pauli Exclusion Principle**"**

Models & Searches of CPT Violation: a personal, very partial, list

Nick E. Mavromatos[*]

Spin-Statistics, Quantum Decoherence and CPT Violation: models, consequences and searches

by Prof. Nikolaos Mavromatos (King's College London)

VIP-2 Closed systems activity 2021/2022

BEGe detector activity 2021/2022

- In order to improve on this limit → improve on efficiency → use Ge as active material.

- Difficulty: HPGe below 20 keV high background due to electronic noise,

- solution BEGe + Pulse Shape analysis: rejection of electronic noise, disentangle multi vs single hits events (photons from Ge vs photons from outside)

Experimental apparatus realized, 3 months data taking run July-September 2021

signals from preamplifier were directly fed in the 50 ohm impedance input of the CAEN FADC Mod DT5743 to preserve the signal integrity. The 12bit resolution and 3.2Gs/s sampling rate allowed to successfully reconstruct the shape of the incoming signals.
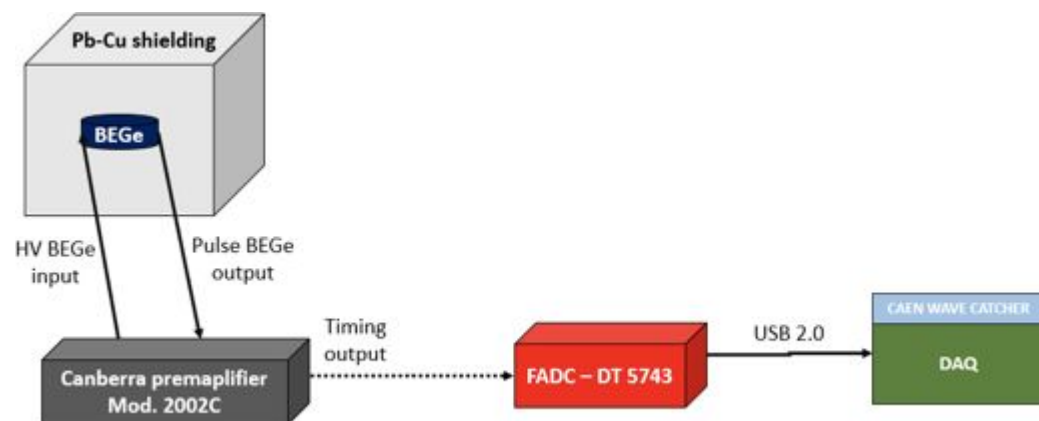
Block diagram of BEGe experimental apparatus

Connection of the Front-End electronic to the BEGe's Canberra preamplifier (Mod. 2002C), behind the liquid N2 dewar
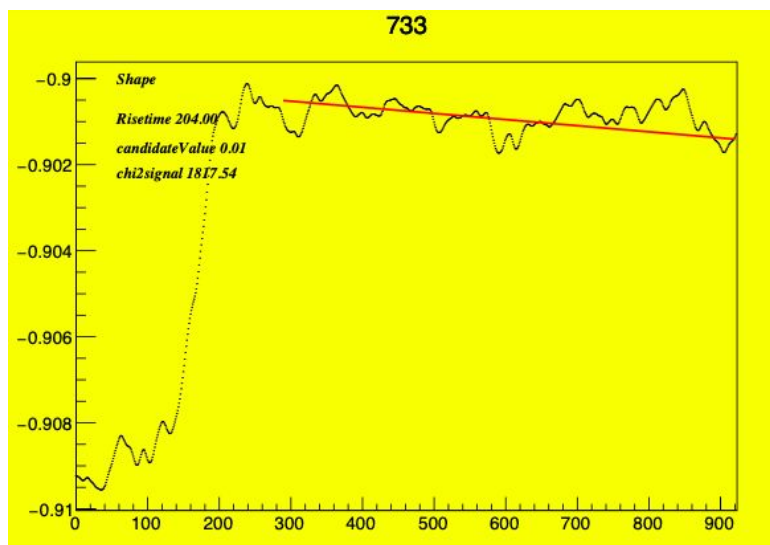
BEGe detector activity 2021/2022

- **Dedicated pulse shape discrimination agorithm**, **amplitude and shape based, REALIZED**
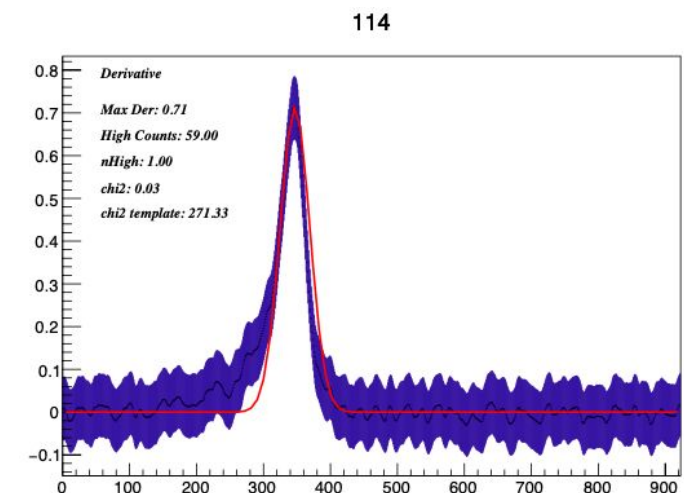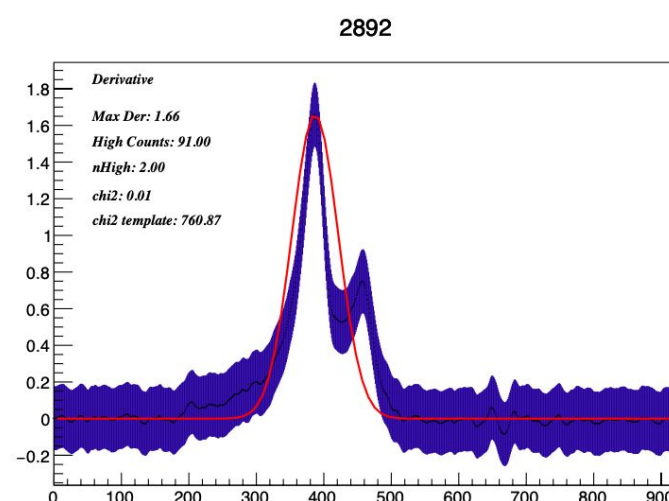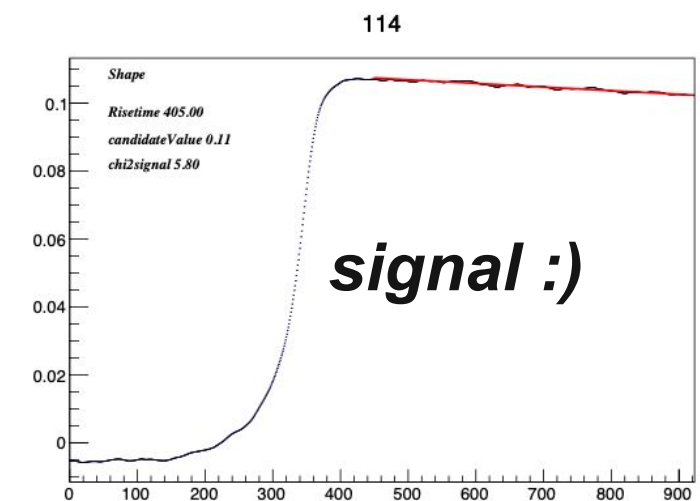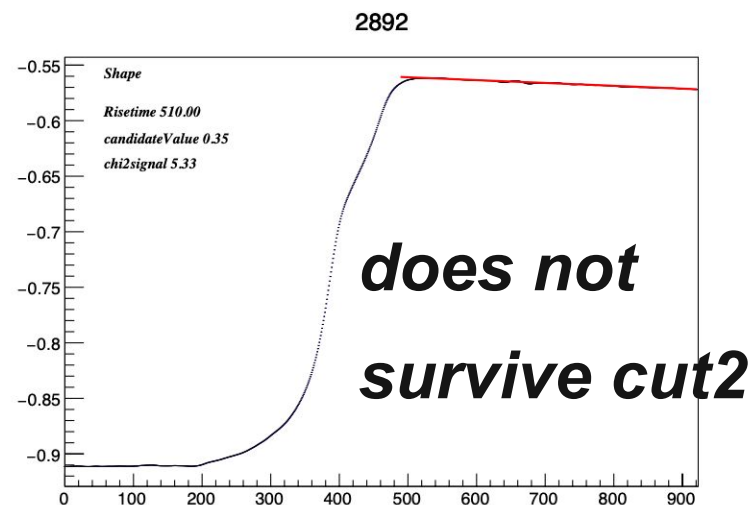
three steps selection:
1) comparison of the fluctuations mean values at pulse beginning and end,
2) χ^2 discrimination with respect to a linear behaviour at pulse end,
3) pulse derivative selection based on both width and discrimination (using err. func. template)
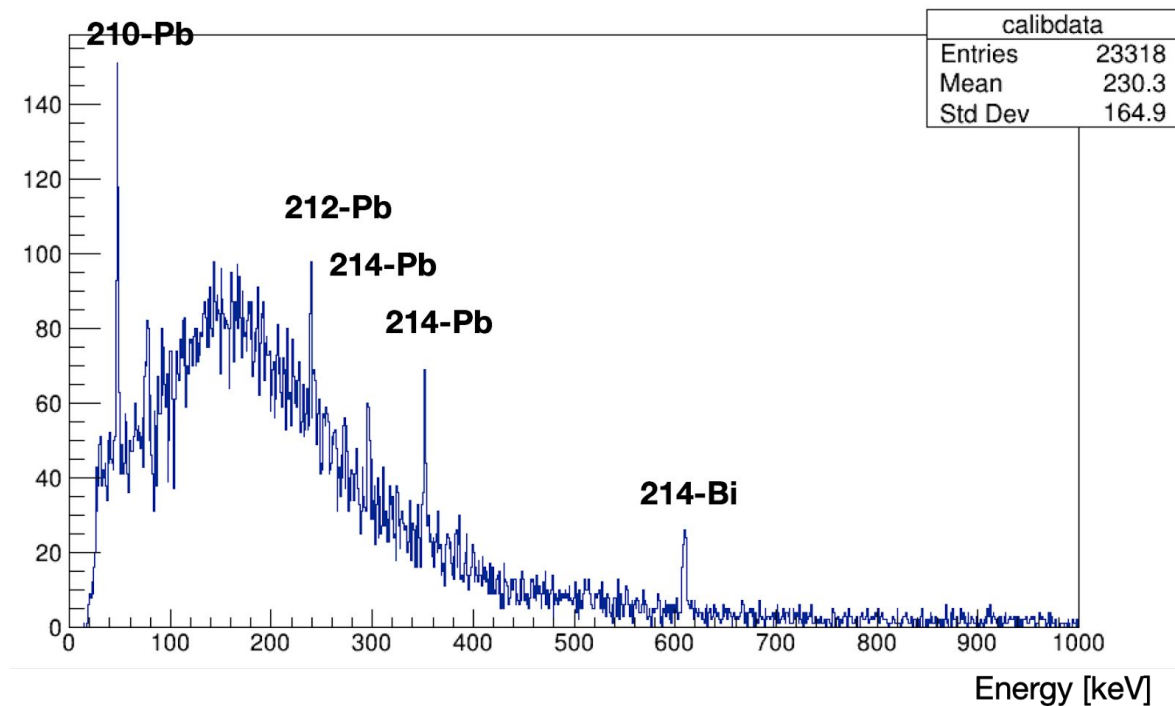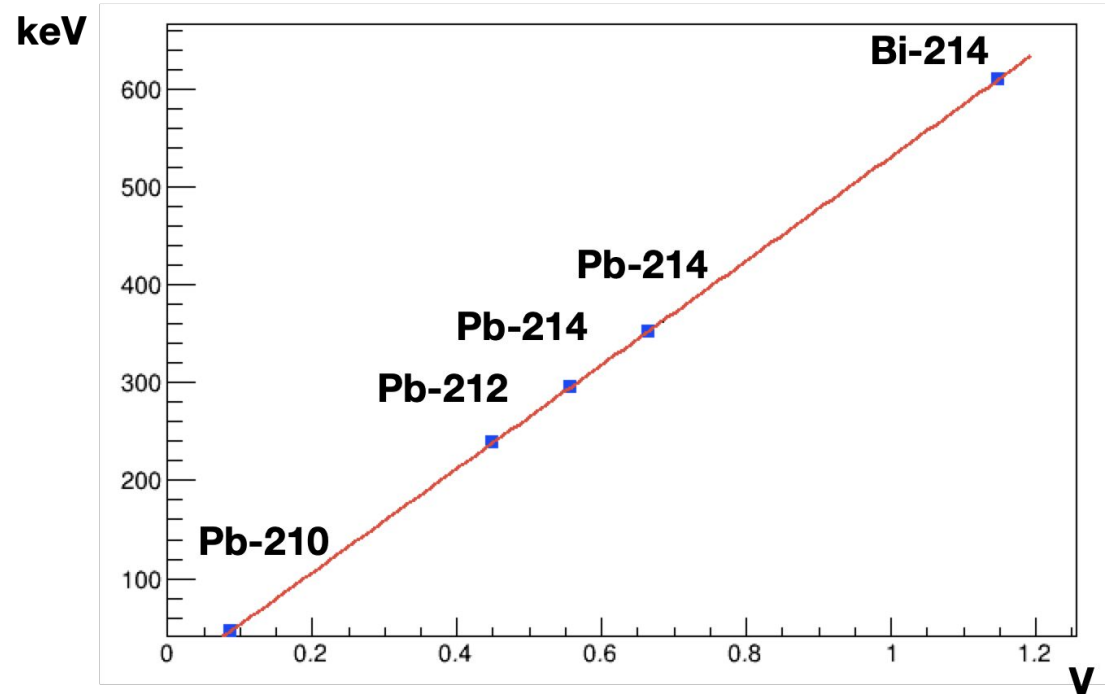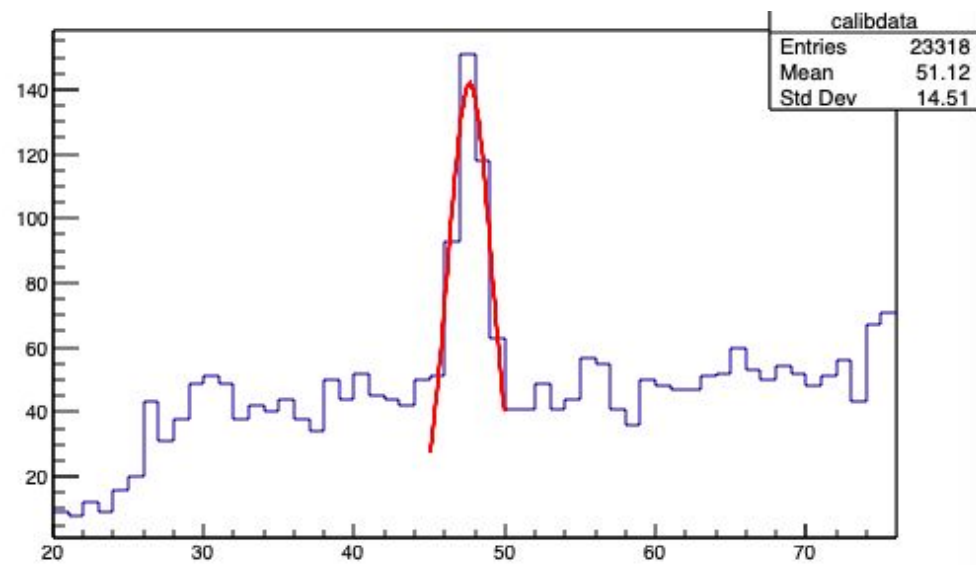
EXAMPLE:

survives cut1 but not cut2

does not survive cut2

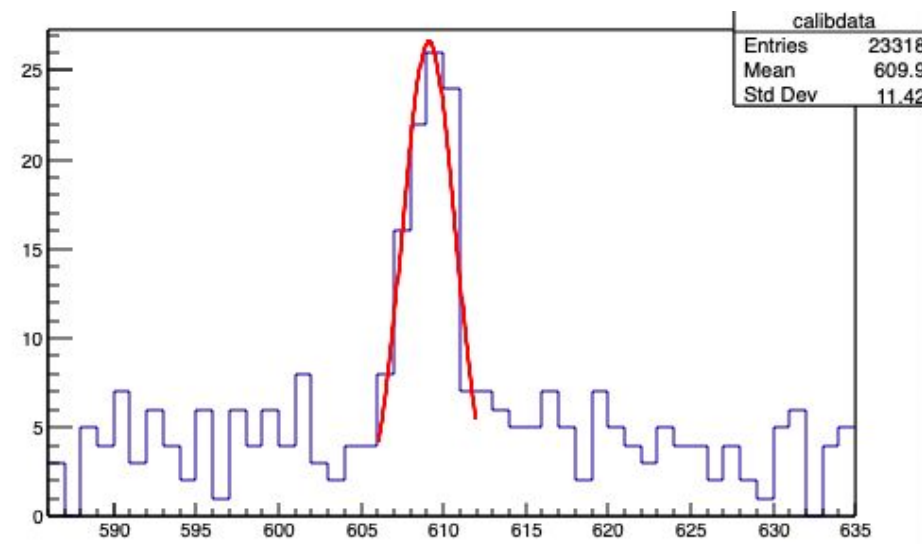*signal :)*

BEGe detector activity 2021/2022

- **Acquired energy spectrum (3 months data taking July-September 2021) for the selected events CALIBRATED**

- **Energy resolution and lower-threshold**

sigma @ 50 keV: ~1.5 keV

sigma @ 610 keV: ~1.6 keV

BEGe detector activity 2021/2022

The analysis of the 2021 data revealed an intrinsic lower energy threshold of about 20 keV, due to electronic noise at low-voltages and an intrinsic noise of the digitizer at 4 mV.

A typical example: for a 18 mV signal amplitude a peak-to-peak noise of 4 mV is evident
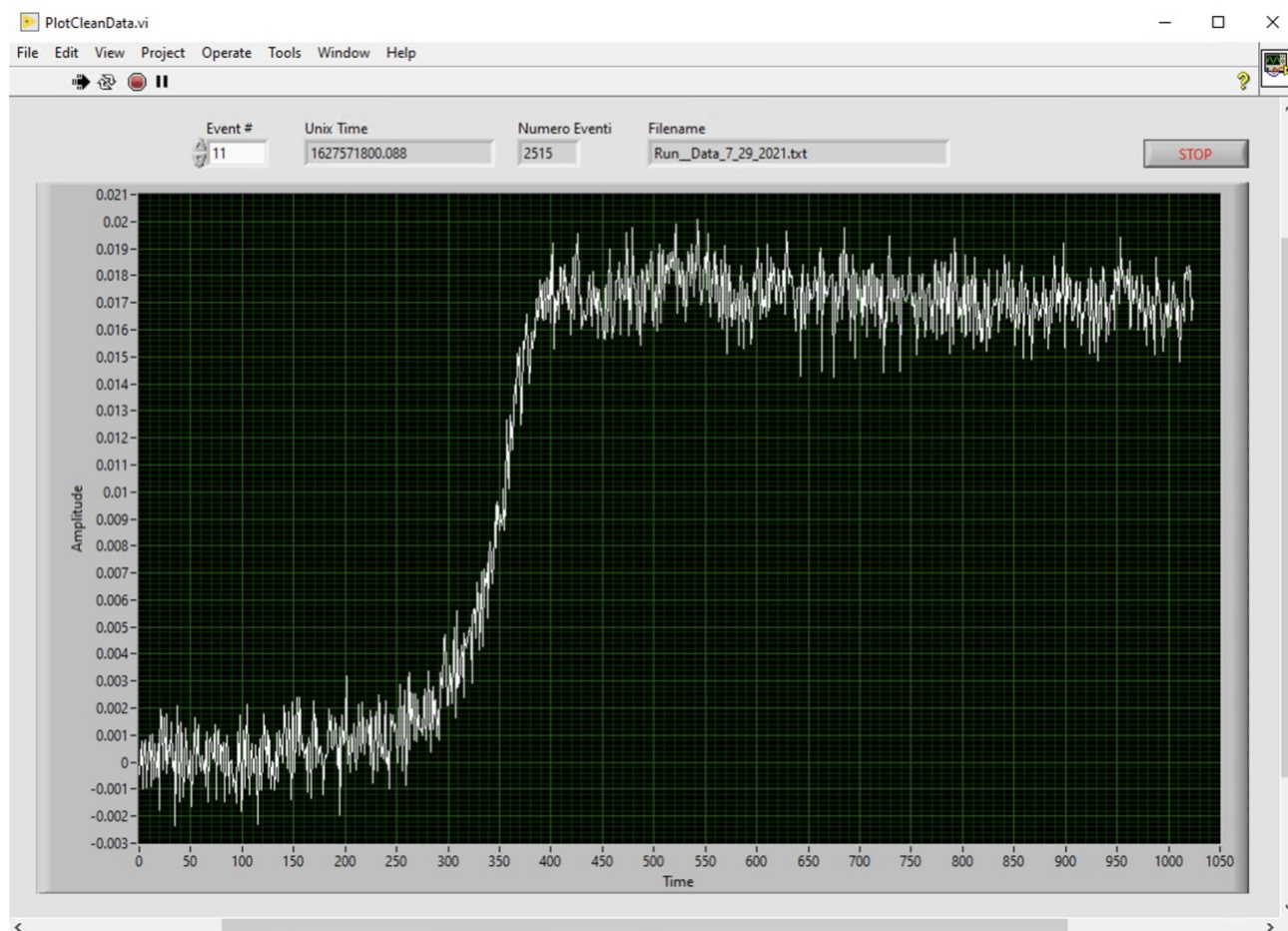

The goal of the experiment is to reach a lower energy threshold of 6-7 keV, corresponding to 4-5 mV (to measure eventual signal of PEP violating Kalpha transitions in Ge), the experimental apparatus was then further improved:

- **Flash-ADC-Computer USB connection replaced with optical fibre interface, to reduce electronic noise at low voltages,**
- **wide band low noise amplifier (for the moment on loan) introduced, with a gain of a factor 10 in tension. An extremely-low noise power supply was realized for the digitizer and for the amplifier.**

BEGe detector activity 2021/2022

-   A new data taking started in 8 Feb 2022 (presently ongoing), goal: increase the amplitude of the BEGe signals corresponding to photons of few keV -> push the low energy limit to the desired limit of few keV
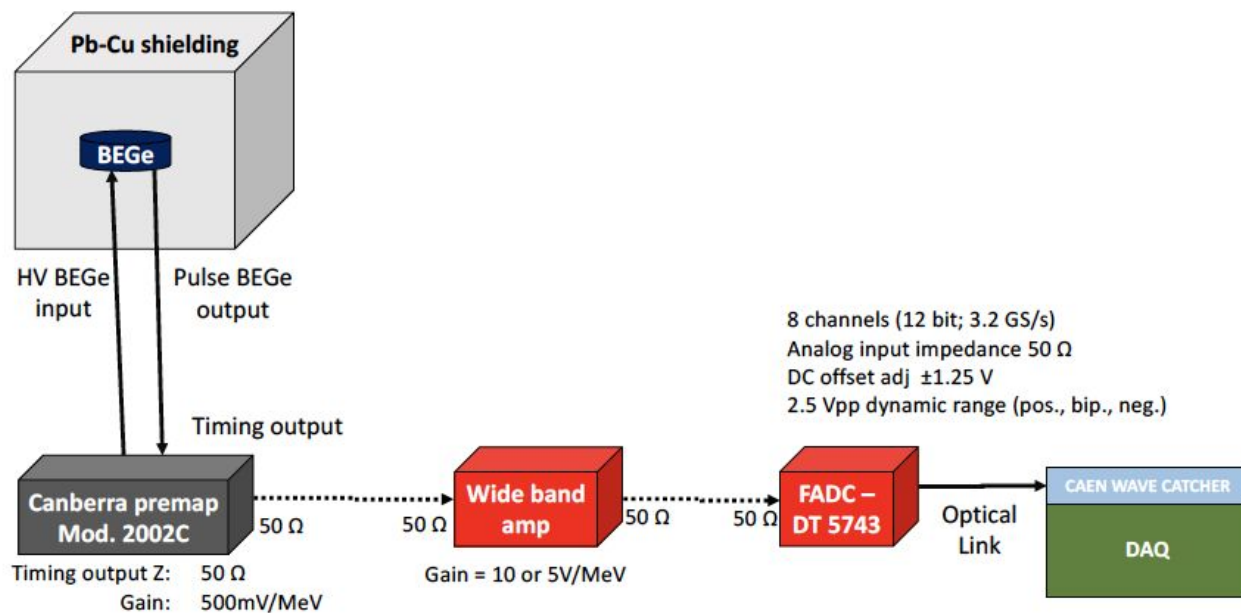
-   Typical event from the 2022 data set, with amplitude comparable to the previous figure (signal shape is changed due to the shaping time introduced by the amplifier). The peak-to-peak noise is now reduced to the level of about 0.5 mV, thus demonstrating the capability of the new setup to disentangle signals of 4-5 mV amplitude.